

# Functional Characterization of Hexokinase Isoforms in Tobacco (*Nicotiana tabacum*)

Dissertation

zur Erlangung des  
Doktorgrades der Naturwissenschaften (Dr. rer. nat.)

Der

Naturwissenschaftlichen Fakultät I  
Biowissenschaften, Institut für Biologie  
der Martin-Luther-Universität  
Halle-Wittenberg,

vorgelegt

von Herrn Young-Min Kim  
geb. am 18.01.1979 in Lünen

Datum der Verteidigung: 27.02.2014

Gutachter:

1. Prof. Dr. Nicolaus von Wirén (IPK Gatersleben)
2. Prof. Dr. Thomas Roitsch (University of Copenhagen)
3. Dr. Hardy Rolletschek (IPK Gatersleben)

Sangerhausen, den 17.11. 2013

for my wife Kasia

*für meine Frau Kasia*

*„Nur wenige wissen, wie viel man wissen muss, um zu wissen,  
wie wenig man weiß.“*

Werner Heisenberg (\*05.12.1901; †01.02.1976)

## **Danksagung**

Der praktische Teil der vorliegenden Arbeit wurde am Leibniz-Institut für Pflanzengenetik und Kulturpflanzenforschung (IPK, Gatersleben) in der Arbeitsgruppe Molekulare Pflanzenphysiologie (MPP) unter Dr. Mohammad-Reza Hajirezaei begonnen und in der neu formierten Arbeitsgruppe Molekulare Pflanzenernährung (MPE) unter Prof. Nicolaus von Wirén fortgesetzt und abgeschlossen. Dieses Projekt wurde gefördert von der Deutschen Forschungsgemeinschaft (DFG), wofür ich mich an dieser Stelle persönlich bedanken möchte. Hiermit möchte ich allen ganz herzlich danken, die mich bei der Bearbeitung dieser Arbeit unterstützt haben. Insbesondere gilt mein Dank natürlich meinem Betreuer Mo, der mich erst mit diesem Projekt betraut hat. Zudem muss ich mich vielfach für die zahlreiche technische Hilfe bei der Regeneration und Analyse transgener Pflanzen durch Andrea Knospe, Heike Nierig, Melanie Ruff und Wally Wendt bedanken, ohne die ich das praktische Pensum nie geschafft hätte. Für den enormen Beitrag bei den Hefeexperimenten muss ich mich ganz herzlich bei Julia Verena Köber bedanken. Des Weiteren noch vielen Dank für die technische Unterstützung an Dr. Michael Melzer und Dr. Twan Rutten (AG Strukturelle Zellbiologie) sowie Dr. Nico Heinzl (AG Heterosis).

Auch die Hilfe meiner wissenschaftlichen Kollegen der Gruppe MPP bzw. MPE hat, sowohl innerhalb als auch außerhalb des Labors, wesentlich zum Fortschritt dieser Arbeit beigetragen. Ihnen sei an dieser Stelle herzlichst gedankt.

Ein großes Dankeschön den Mitarbeitern aus dem Gewächshaus, Brigitte Braun und Waltraut Wackermann sowie Enk Geyer, die sich immer äußerst fürsorglich um meine Pflanzen gekümmert haben und stets ein offenes Ohr für meine Sorgen hatten.

Ich bedanke mich vielmals bei Prof. Nicolaus von Wirén für Ihre hilfreichen Anregungen bei diesem Projekt und der schriftlichen Verfassung meiner Arbeit sowie den Willen, diese zu begutachten. An dieser Stelle auch vielen lieben Dank an Prof. Thomas Roitsch, für die freundliche Bereiterklärung diese Arbeit ebenfalls zu begutachten.

*Last but not least* gilt mein unendlicher Dank meiner Frau, der ich auch diese Arbeit widme. Ohne ihre unermüdliche Unterstützung und Geduld hätte ich diese Arbeit niemals soweit voran bringen können und mit Sicherheit schon lange das Handtuch geworfen.

Ich hoffe, dass ich alle Beteiligten in genügendem Umfang für ihre Hilfe gewürdigt habe.



<b>1</b>	<b>Introduction</b>	<b>12</b>
1.1	Starch as primary product of photosynthesis in leaves	12
1.2	Sucrose – the major transport form for carbohydrates in plants	13
1.3	Hexokinase – Gateway of the glucose metabolism	14
1.4	Multiple HXK isoforms are common in planta	16
1.5	Cellular and intracellular localizations of HXK's	17
1.6	Hexokinase as glucose sensor	19
1.7	Using RNA interference pathways for the elucidation of gene functions	20
1.8	Characterization of HXK's in tobacco	21
1.9	Aim of this study	23
<b>2</b>	<b>Material &amp; Methods</b>	<b>25</b>
2.1	Plant material and growth conditions	25
2.1.1	Tobacco	25
2.1.2	<i>Arabidopsis</i>	25
2.2	Bacteria strains	25
2.3	Yeast strain	26
2.4	Vector construction	26
2.4.1	Tissue-specific localization	26
2.4.2	Yeast complementation	26
2.4.3	Overexpression of tobacco hexokinase 1	27
2.4.4	Silencing of tobacco hexokinase 1	27
2.5	Plant transformation	28
2.5.1	Tobacco	28
2.5.2	<i>Arabidopsis</i>	28
2.6	Yeast transformation	29
2.7	RNA isolation and quantitative real-time PCR	30
2.8	Northern Blot analysis	31
2.9	Western Blot analysis	31
2.10	Protoplast isolation	32
2.11	Glucose phosphorylation activity	32
2.12	Photosynthetic activity	33
2.13	Chlorophyll determination	33
2.14	Nitrogen and carbon determination	33

2.15	Soluble sugar and starch determination	33
2.16	Glucose repression assay	34
2.17	Metabolite profiling	35
<b>3</b>	<b>Results</b>	<b>36</b>
3.1	Phylogenetic analysis of tobacco HXK isoforms	36
3.2	Expression analysis in tobacco plants	37
3.2.1	Expression of the tobacco HXK isoforms in different plant organs	37
3.2.2	Diurnal rhythm of <i>NtHXK1</i> expression	38
3.3	Tissue specific localization	39
3.3.1	Localization of NtHXK1 promoter:GFP	40
3.3.2	Localization of NtHXK1 promoter:GUS	40
3.4	Functional expression of NtHXK1 in yeast	41
3.5	Generation of transgenic tobacco plants with constitutively decreased expression of <i>NtHXK1</i>	43
3.6	Analysis of transgenic lines with elevated or reduced <i>NtHXK1</i> expression	43
3.6.1	Protein detection using protein gel blot analysis	43
3.6.2	Gene expression analysis	44
3.6.3	Hexokinase activity assay	45
3.7	Expression of active NtHXK isoforms in a selected <i>NtHXK1</i> RNAi line	46
3.8	Physiological characterization of <i>NtHXK1</i> RNAi lines	46
3.8.1	Phenotypic analysis	46
3.8.2	Ultrastructural analysis of HXK1-deficient tobacco plants	48
3.8.3	Photosynthesis, chlorophyll content and respiration	49
3.8.4	Carbon-to-nitrogen ratio	51
3.8.5	Qualitative determination of starch in leaves	51
3.8.6	Determination of insoluble sugar level during a day cycle	53
3.8.7	Determination of sugar concentrations in leaves	54
3.8.8	Metabolite profiling	55
3.9	Complementation of the mutant <i>gin2-1</i> by <i>NtHXK1</i>	56

3.10	Plant growth under different light conditions	58
<b>4</b>	<b>Discussion</b>	<b>60</b>
4.1	<i>NtHXK1</i> is expressed in aerial organs especially during the night	60
4.2	Transgenic plants display elevated and suppressed <i>NtHXK1</i> expression	61
4.3	<i>Starch-excess</i> phenotype is triggered by silencing <i>NtHXK1</i>	62
4.4	NtHXK1 performs as glucose sensor	63
4.5	Pivotal role of NtHXK1 in the transition of starch to energy	64
4.6	The role of NtHXK1 in non-autotrophic cells	67
4.7	Final conclusion	67
<b>5</b>	<b>Summary</b>	<b>69</b>
<b>6</b>	<b>Zusammenfassung</b>	<b>70</b>
<b>7</b>	<b>References</b>	<b>72</b>
<b>8</b>	<b>Appendix</b>	<b>78</b>
<b>9</b>	<b>Publikationsliste des Autors</b>	<b>84</b>
<b>10</b>	<b>Curriculum vitae</b>	<b>85</b>
<b>11</b>	<b>Eidesstattliche Erklärung</b>	<b>87</b>

## Abbreviations

**2n**=diploid > n haploid number

**3PGA** 3-phosphoglyceric acid

**A645** absorption at 645 nm

**ADP** adenosine diphosphate

**AtHXK** *Arabidopsis* hexokinase (*A. thaliana*)

**ATP** adenosine tri-phosphate

**bp** base pair

**BSA** bovine serum albumin

**C** carbon

**Ca** calcium

**cDNA** complementary deoxyribonucleic acid

**cInv** cytosolic Invertase

**Cl** chloride

**cwInv** cell-wall bound invertase

**DNA** deoxyribonucleic acid

**dsRNA** double stranded RNA

**DW** dry weight

**Ery4P** erythrose-4-phosphate

**FK** fructokinase

**FW** fresh weight

**Fru** fructose

**gin** glucose insensitive

**GFP** green fluorescent protein

**GK** glucokinase

**Glc** glucose

**Glc6PDH** glucose-6-phosphate dehydrogenase

**GUS**  $\beta$ -glucuronidase

**h** Hour

**HCl** hydrochloric acid

**HKL** hexokinase-like

**HPLC** high pressure liquid chromatography

**HXK** hexokinase

**ICMS** Ion chromatography–mass spectrometry

**IRMS** isotope ratio mass spectrometry

**Inv** invertase

**IRGA** infra red gas analyzer  
**K** kalium  
**kDA** kilodalton (massunit)  
**l** litre  
**LCMS** liquid chromatography–mass spectrometry  
**Ler** Landsberg erecta (*Arabidopsis* ecotype)  
**LiAc** lithium acetate  
**m** meter  
**Mal** maltose  
**Man** mannitol  
**Mbp** mega basepairs  
**Mg** magnesium  
**min** minute  
**ml** milliliter  
**mM** millimolar  
**mRNA** messenger ribonucleic acid  
**MS** Murashige and Skoog (plant growth medium) or  
**MS** mass spectrometry  
**N** nitrogen  
**Na** sodium  
**NAD** nicotine amide dinucleotide  
**NADP** nicotine amide dinucleotide phosphate  
**NDP-** nucleoside diphosphate  
**nm** nanometer  
**nmol** nanomole  
**NtHXK** tobacco hexokinase (*Nicotiana tabacum*)  
**°C** centigrade  
**OD** optical density  
**OPPP** oxidative pentose phosphate pathway  
**ORF** open reading frame  
**OsHXK** rice hexokinase (*oryza sativa*)  
**P** phosphate  
**PEG** polyethylene glucol  
**PEP** phosphoenolpyruvic acid  
**PCR** polymerase chain reaction  
**PGI** phosphoglucoisomerase  
**PGM** phosphoglucomutase

**PPFD** photosynthetic photon flux density  
**Prom** promoter  
**qPCR** quantitative real-time PCR  
**Rib5P** ribose-5-phosphate  
**RNA** ribonucleic acid  
**RNAi** RNA interference  
**RISC** RNA-induced silencing complex  
**rpm** rounds per minute  
**rRNA** ribosomal RNA  
**RT-PCR** reverse transcription - polymerase chain reaction  
**s** seconds  
**SD** standard deviation  
**SE** standard Error  
**Sex** starch excess  
**siRNA** small interfering RNA  
**SDS** sodium dodecyl sulfate  
**SPS** sucrose-6-phosphate synthase  
**ssRNA** single stranded RNA  
**Suc** sucrose  
**SuSy** sucrose synthase  
**TCA** tricarboxylic acid cycle  
**Tre** trehalose  
**TSS** transcription start sequence  
**UDP** uridine diphosphate  
**UV** ultraviolet  
**µg** microgram  
**µl** microlitre  
**V** volume  
**vInv** vacuolar Invertase  
**WT** wildtype  
**w/v** mass concentration (mass/volume)

## List of Figures

<b>Figure 1:</b>	Simplified schematic representation of the carbon metabolism leading to Glc in photosynthetic cells	<b>13</b>
<b>Figure 2:</b>	Central role of HXK in the Glc metabolism of plants	<b>15</b>
<b>Figure 3:</b>	Phylogenetic tree taken from Karve <i>et al.</i> (2010) with corrections Indicated in red	<b>17</b>
<b>Figure 4:</b>	Radial phylogenetic tree with the HXK isoforms from Arabidopsis and tobacco	<b>18</b>
<b>Figure 5:</b>	Comparison of sequence homology of tobacco hexokinases	<b>21</b>
<b>Figure 6:</b>	Intracellular localization of NtHXK1	<b>23</b>
<b>Figure 7:</b>	Schematic representation of the overexpression (upper) and the silencing construct (lower) of NtHXK1 isoform of tobacco	<b>28</b>
<b>Figure 8:</b>	Phylogenetic tree of the HXK isoforms from tobacco, rice and Arabidopsis	<b>36</b>
<b>Figure 9:</b>	Expression analysis of hexokinases in different plant organs	<b>38</b>
<b>Figure 10:</b>	Time course of <i>NtHXK1</i> mRNA content in sink (A) and source (B) leaves determined by qRT-PCR	<b>39</b>
<b>Figure 11:</b>	Pollen of plants expressing NtHXK1 promoter::GFP constructs	<b>40</b>
<b>Figure 12:</b>	GUS activity in flower tissues of plants expressing a NtHXK1 promoter::GUS construct	<b>41</b>
<b>Figure 13:</b>	Growth complementation of the hexokinase-deficient yeast triple mutant YSH7.4-3C	<b>42</b>
<b>Figure 14:</b>	Detection of NtHXK1 protein by protein gel blot analysis	<b>44</b>
<b>Figure 15:</b>	Expression analysis of A) the <i>NtHXK1</i> overexpression lines and B) the <i>NtHXK1</i> RNAi lines	<b>45</b>
<b>Figure 16:</b>	Relative glucose phosphorylation activity in (A) <i>NtHXK1</i> overexpressing and (B) <i>NtHXK1</i> RNAi lines	<b>45</b>
<b>Figure 17:</b>	Quantitative RT-PCR for gene expression analyses of the catalytic active NtHXK isoforms	<b>46</b>
<b>Figure 18:</b>	Growth of untransformed wild type plants and three transgenic lines	<b>47</b>
<b>Figure 19:</b>	Close-ups of plants from A) wild type (7 weeks), B) line HXK1-19 (9-10 weeks) and C) line HXK1-24 (9-10 weeks)	<b>48</b>
<b>Figure 20:</b>	Light and transmission electron microscopy of leaf cross sections	<b>49</b>
<b>Figure 21:</b>	Photosynthetic activity, chlorophyll content and respiration rates in WT and the <i>NtHXK1</i> RNAi lines	<b>50</b>
<b>Figure 22:</b>	Carbon and nitrogen concentrations in leaves of WT, HXK1-19, HXK1-24 and HXK1-64 as determined by an elemental analyzer	<b>51</b>

<b>Figure 23:</b>	Visualization of starch in leaves of <i>NtHXK1</i> RNAi and wild type plants	<b>52</b>
<b>Figure 24:</b>	Changes in starch concentrations during the course of day	<b>53</b>
<b>Figure 25:</b>	Soluble sugars, glucose, fructose and maltose concentrations in fully expanded leaf samples of wild type and <i>NtHXK1</i> -silenced plants	<b>54</b>
<b>Figure 26:</b>	Complementation of the <i>Arabidopsis</i> glucose insensitive mutant <i>gin2-1</i> by tobacco HXK1	<b>58</b>
<b>Figure 27:</b>	Effect of silenced <i>NtHXK1</i> expression on plant growth at different light conditions	<b>59</b>
<b>Figure 28:</b>	Pathway of starch breakdown in photosynthetic cells at night	<b>66</b>

## List of Tables

<b>Table 1:</b>	List of identified cDNA sequences with corresponding accession numbers	<b>16</b>
<b>Table 2:</b>	Percent identity of hexokinase amino acid sequences from tobacco compared to rice and <i>Arabidopsis</i>	<b>37</b>
<b>Table 3:</b>	Metabolite levels in mature leaves of <i>NtHXK1</i> silenced and over-expressing tobacco plants	<b>56</b>



# 1 Introduction

## 1.1 Starch as a primary product of photosynthesis in leaves

Starch is an insoluble  $\alpha$ -glucan composed of 20-25% amylose and 75-80% amylopectin. Amylopectin and amylose form semicrystalline, insoluble granules with an internal lamellar structure. While amylose represents a simple  $\alpha$ -1,4-linked chain, amylopectin is additionally connected by  $\alpha$ -1,6-bonds at branch points. In higher plants, starch is synthesized in plastids of photosynthetic and non-photosynthetic cells and is undeniable the most important storage carbohydrate. In leaves of most plants, part of the carbon assimilated through photosynthesis is retained in the chloroplasts as transitory starch and not converted to sucrose (Suc) for export to sinks. This transitory starch is remobilized during the night to supply leaf respiration and to provide precursors for sucrose synthesis used for continuous export to sink organs (Stitt *et al.*, 2010). Degradation of starch primarily takes place by hydrolysis of the glucans to maltose (Mal) and to a lower extent to glucose (Glc), which can be exported from the chloroplast and metabolized in the cytosol (Fig. 1). Mutations affecting key degrading enzymes decrease starch breakdown lead to starch accumulation and the formation of “starch excess” (*sex*) phenotypes (reviewed by Zeeman *et al.*, 2010). Rates of starch biosynthesis and degradation are dependent on the environmental conditions, in particular day length (Zeeman *et al.*, 2007). The rate of degradation is regulated such that starch reserves are almost, but not entirely, depleted at the end of the night (Stitt *et al.*, 2010). Gibon *et al.* (2004) showed that the rates of starch synthesis and breakdown were precisely adjusted to the light regime but only in the short run. This indicates an involvement of different sensing mechanism coordinating starch catabolism with daytime or the light period.

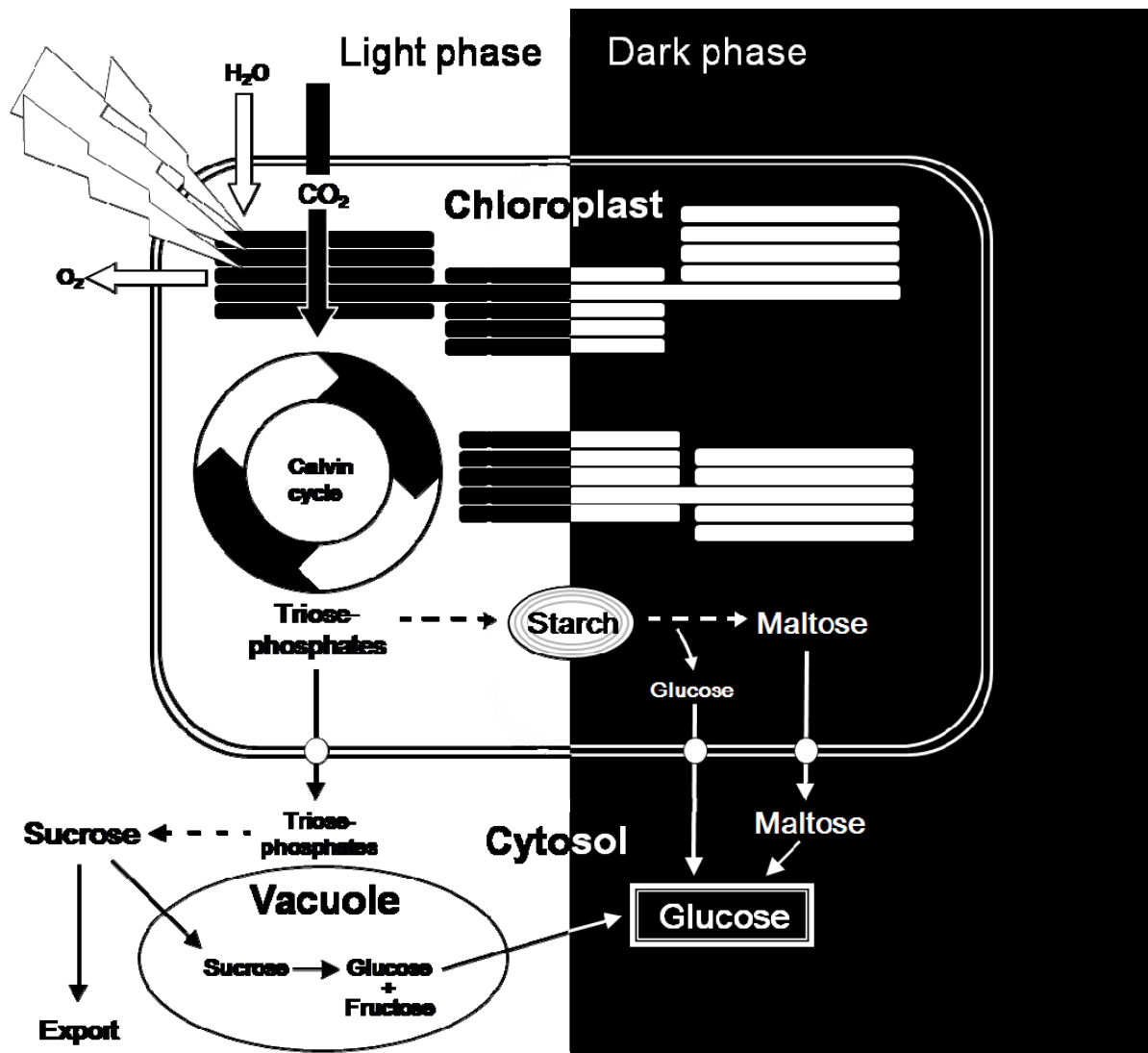


**Figure 1:** Simplified schematic representation of the carbon metabolism leading to Glc in photosynthetic cells; prepared according to models by Stitt *et al.* (2010)

## 1.2 Sucrose – the major transport form for carbohydrates in plants

Sucrose (Suc) is a disaccharide composed of glucose (Glc) and fructose (Fru) with a glycosidic link between C1 on the glucosyl subunit and C2 on the fructosyl unit at their reducing ends. It represents the primary transport form of reduced carbon in the majority of higher plants. It is synthesized in source leaves and transported via the phloem to sink tissues, where it is used for the heterotrophic metabolism, growth and synthesis of storage materials such as starch (Matic *et al.*, 2004). Its biosynthesis takes place in the cytoplasm of plant cells via the intermediates UDP-Glc and Fru-6-P catalyzed by Suc-6-P synthase (SPS). The monosaccharide precursors derive from photosynthetically produced triose phosphates (Fig. 1). In the sink leaves Suc is either cleaved in a reversible manner by sucrose synthase (SuSy) to Fru and UDP-Glc and/or irreversibly by invertases (Inv's) to Glc and Fru. Produced

glucose serves for the enzyme hexokinase (HXK) as substrate. Inv's can be cell-wall bound (cwInv), cytosolic (cInv) or vacuolar (vInv) whereas the general Inv activity is due to cwInv and vInv. Suc was also found to initiate signaling pathways leading to altered gene expression and physiological responses through the action of the respective receptor kinase (Wind *et al.*, 2010).

### 1.3 Hexokinase – Gateway of the glucose metabolism

The allosteric enzyme hexokinase (HXK) was first mentioned in a seminal paper by Otto Meyerhof in 1927 after it has been discovered in an extract from baker's yeast. In the 1940s its catalytic reaction was elucidated and summarized as:



In other words, HXK catalyzes the ATP-dependant phosphorylation of a hexose to hexose-6-phosphate, which, in case of Glc, is the first step of the Embden-Meyerhof-Parnas pathway, better known as glycolysis. An interest in plant HXK arose in 1952 and 1954 with increasing evidence for a functional glycolytic pathway present in plants. Around the same time, the discovery of the oxidative pentose phosphate pathway (OPPP) revealed another direction for the metabolism of glucose-6-phosphate (Glc6P), the main product of HXK (Claeysen and Rivoal, 2007). Additionally, Glc6P was found to supply another metabolic pathway, the NDP-glucose pathway, as well as the synthesis of trehalose (Tre) via trehalose-6-phosphate (Tre6P).

In summary, Glc6P acts as a precursor for cell wall biosynthesis and secondary metabolism, it provides the building block for starch biosynthesis, for the generation of reducing equivalents (NADPH) used in reductive biosynthesis reactions within the cells and for the production of ribose-5-phosphate (Rib5P), required in the synthesis of nucleotides and nucleic acids. Glc6P further fuels the production of erythrose-4-phosphate (Ery4P), needed in the synthesis of aromatic amino acids, synthesis of fatty and amino acids, formation of the high-energy compounds ATP and NADH (during glycolysis and respiration) and synthesis of Tre (Fig.2). HXK is present in all living organisms and is able to phosphorylate several hexoses including D-glucose (Glc), D-fructose (Fru), D-mannose (Man) and glucosamine at variable affinity (Schnarrenberger, 1990). So far, glucokinases (GKs) that exclusively phosphorylate glucose have not yet been found in eukaryotes (Dai *et al.*, 2002; Granot, 2008) whereas fructokinases (FKs) have been identified in plants, which share no obvious sequence homology with HXK

(Dai *et al.*, 2002). Bacterial HXK's have a molecular weight of approximately 50 kDa, whereas HXK's in multicellular organisms are often around 100 kDa and consist of two halves (N and C terminal). This suggests an evolutionary origin by duplication and fusion of a 50 kD ancestral HXK closely related to those of microorganisms (Cardenas *et al.*, 1998). Recently, the interest in HXK has been renewed with the discovery of sugar sensing and signaling mediated by HXK in plants (Moore *et al.*, 2003). Furthermore, HXK has been found to occur in multiple isoforms in a variety of plant species, raising the question: What is the physiological relevance of multiple HXK isoforms and which function does each isoform need to accomplish (Claeyssen and Rivoal, 2007)?

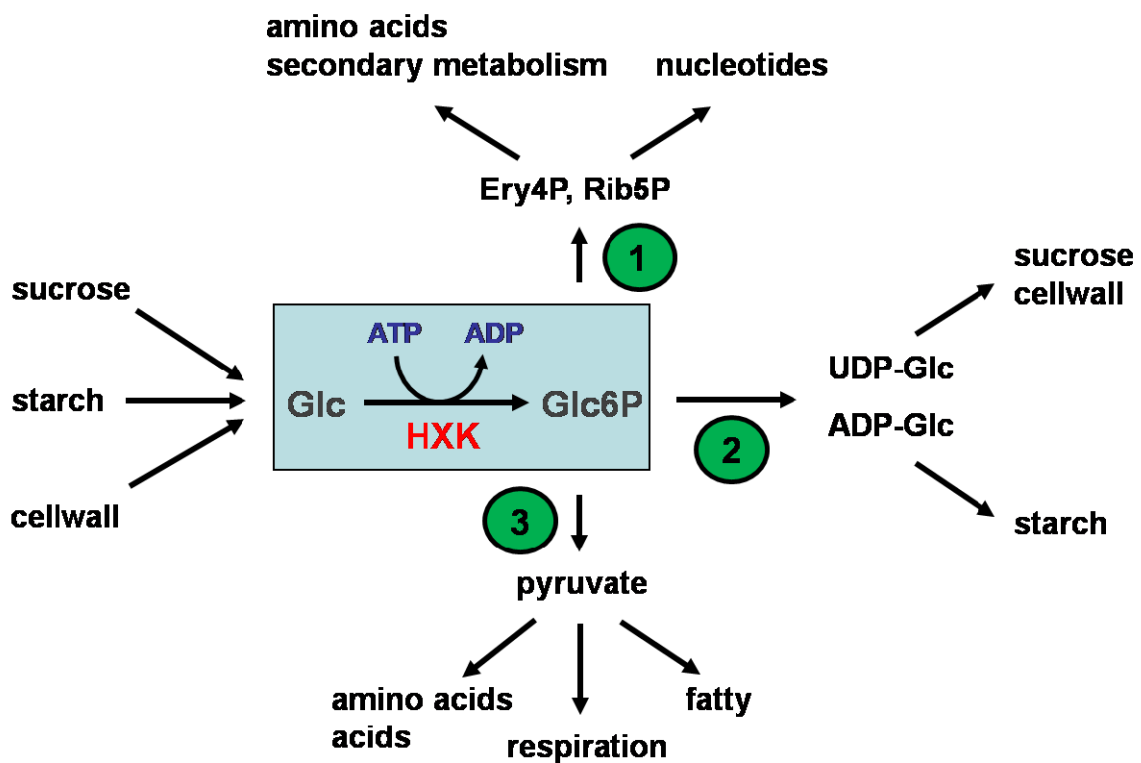


**Figure 2:** Central role of HXK in the Glc metabolism of plants.

Framed is the HXK reaction. **1:** Glc6P dehydrogenase (Glc6P-DH) supplies the OPPP, **2:** phosphoglucomutase (PGM) supplies the synthesis of UDP-Glc and ADP-Glc, **3:** phosphoglucoisomerase (PGI) supplies the glycolysis. Taken from Giese (*dissertation*, 2005).

## 1.4 Multiple HXK isoforms are common in Planta

In the last two decades HXK genes were isolated by PCR and other cloning techniques demonstrating that various plant species harbour and express up to ten HXK genes. In *Arabidopsis thaliana* (thale cress), six HXK genes have been identified, whereas three encode catalytically active and the other three encode noncatalytic proteins, which have been recently renamed as hexokinase-like (HKL) proteins (Karve *et al.*, 2008). Four HXK's isoforms have been identified in tomato (*Solanum lycopersicon*) (Kandel-Kfir *et al.*, 2006), ten isoforms in rice (*Oryza sativa*) (Cho *et al.*, 2006) and seven isoforms were found in tobacco (*Nicotiana tabacum*) during a previous study in our group (Giese, *dissertation*, 2005). Southern and gene sequence analysis in *Nicotiana sylvestris* revealed the existence of three more isoforms with homology to the isoforms 2, 3 and 6 leading to the assumption that in total at least 10 isoforms may exist in *N. tabacum* (Table 1 specifies nine identified *N. sylvestris* isoforms).

Name, Accession	cDNA	AA
HXK1, AF118133	1827	497
HXK1a, AY553214	1853	497
HXK2, AY553215	2300	499
HXK3, AY553216	1849	497
HXK4a, AY553217	1568	498
HXK4b, AY553218	1568	498
HXK5, AY553219	1966	499
HKL1, AY553220	1824	510
HXK7, AY664410	1916	497

**Table 1:** List of identified cDNA sequences with corresponding accession numbers, cDNA length in bp and corresponding protein sequence in amino acids (Giese, 2005).

The expression of multiple HXK isoforms with different kinetic attributes and subcellular localizations may indicate that each individual isoform has a well-defined physiological role within the plant (Claeyssen and Rivoal, 2007). Recently, the sequences of HXK genes from the lower plants *Physcomitrella patens* and *Sellaginella mollendorffii*, the eudicot species *Populus trichocarpa*, *Ricinus communis* and *Vitis vinifera* and the monocots *Sorghum bicolor* and *Zea mays* with the isoforms from *Arabidopsis*, tobacco and rice were compared and displayed in a phylogenetic tree (Karve *et al.*, 2010). The outcome of this phylogenetic

analysis, however, has been questioned and especially the phylogenetic position of tobacco HXK's has been corrected using sequence homology comparison based on the previously published data (Giese *et al.* 2005) (Fig.3).

**Figure 3:** Phylogenetic tree taken from Karve *et al.* (2010) with corrections (according to Giese *et al.*; 2005) indicated in red.

The specific function of individual HXK's is still poorly understood. To understand the individual roles of HXK isoforms it is essential to know where they occur within the plant. Tissue specificity and subcellular localization can provide valuable hints to specific functions performed by single HXK's. The function of only one isoform of HXK was elucidated recently in rice. Suppression of the *OsHXK10* gene whose gene product is located in the cytoplasm showed that the anthers of some flowers were unable to open (dehisce) and release their pollen. The pollen germination capacity was distinctly decreased and the proportion of empty seeds was significantly increased demonstrating that OsHXK10 plays an essential role in anther dehiscence, pollen germination and thereby grain filling (Xu *et al.*, 2008). Plant HXK's were found to be targeted to various subcellular compartments including the cytosol, chloroplasts, mitochondria and nucleus (Cho *et al.*, 2006; Claeysen and Rivoal, 2007). According to phylogenetic analyses, plant HXK's can be divided into two groups: chloroplast imported type A (Olsson *et al.*, 2003; Giese, *dissertation*, 2005) and mitochondria membrane

associated type B proteins (Cho *et al.*, 2009A; Cheng *et al.*, 2011). Up to now, the type-A HXK's NtHXK2, OsHXK4 and AtHXK3 were found to be localized in the chloroplast stroma (Giese *et al.*, 2005; Cho *et al.*, 2006; Karve *et al.*, 2008). In these studies only the physiological role of NtHXK2 has been further examined. It was demonstrated that NtHXK2 was primarily expressed in sink tissues and likely involved in starch degradation rather than starch synthesis (Giese *et al.*, 2005). The type B proteins are divided into two subclasses: B1 isoforms are catalytic inactive HKL proteins while B2 proteins are HXK's which exhibit Glc phosphorylation activity (Karve *et al.*, 2010; Fig.3). Type B HXK's occur predominantly, but not exclusively, associated with mitochondria (Karve *et al.*, 2008). AtHXK1 is primarily associated with mitochondria, but can additionally be found in the nucleus (Cho *et al.*, 2006), whereas AtHXK1 in both locations is able to modulate gene expression. In rice and maize one or more cytosolic HXK's have been described (da Silve *et al.*, 2001; Cheng *et al.*, 2011), though cytosolic isoforms might only occur in monocots (Damari-Weissler *et al.*, 2006).

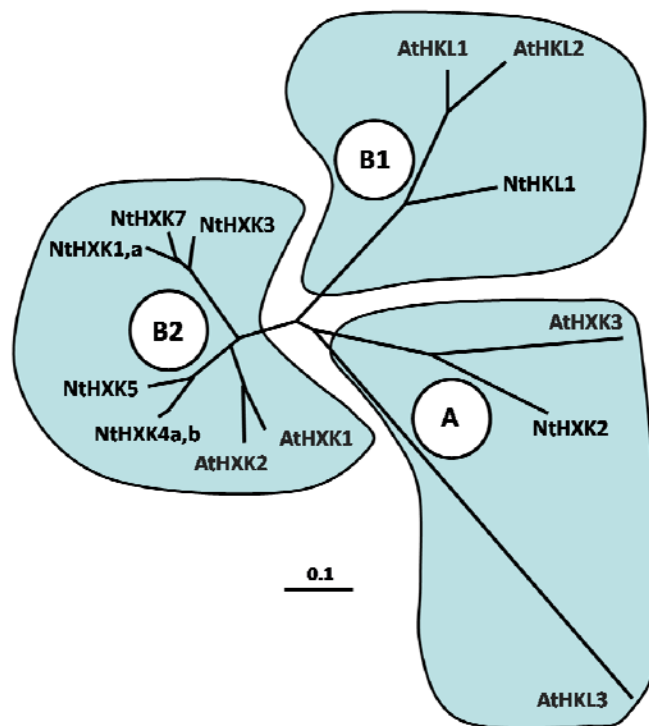


**Figure 4:** Radial phylogenetic tree with the HXK isoforms from Arabidopsis and tobacco.

Sequence comparison with ClustalX. Displayed with NJPlot (unrooted). **A:** proteins with plastid signal peptides and **B:** with N-terminal membrane anchor. The protein in subgroup B1 lacking the Glc phosphorylation activity. Taken from Giese (*dissertation*, 2005).

## 1.6 Hexokinase as glucose sensor

Sugars are energy-rich compounds with fundamental roles in energy metabolism, carbon storage, biosynthesis of carbonic acids or cell wall formation, but they also act as signaling molecules regulating physiological processes during the entire plant life cycle (Rolland *et al.*, 2006). To maintain normal growth and development, highly sophisticated sugar sensing and signaling systems have been evolved by plants that coordinate and modulate many essential metabolic pathways (Cho *et al.*, 2009A). These systems also involve an extensive coordination with plant hormone interactions (Rolland *et al.*, 2006). Glc is the most widely recognized sugar molecule that controls signaling pathways in plants (Cho *et al.*, 2009A). It has been described as a key regulator of many essential processes, including germination, seedling development, root, stem and shoot growth, photosynthesis, carbon and nitrogen metabolism, flowering, defense responses to biotic and abiotic stresses and senescence (Moore *et al.*, 2003). The role of a plant HXK as an evolutionary conserved Glc sensor was first recognized by the characterization of Arabidopsis plants with altered HXK levels, demonstrating that plants overexpressing AtHXK1 or AtHXK2 exhibited Glc hypersensitivity whereas antisense plants were hyposensitive (Jang *et al.*, 1997). A cast iron proof that HXK fulfills a sensing function turned up with the identification and characterization of the AtHXK1 null mutant *gin2* (*Glc insensitive 2*) for which multiple alleles do exist. This mutant displayed broad growth defects which became more severe with increasing light intensity. On the other hand, after germination on high Glc-containing (6%) Murashige and Skoog (MS) medium *gin2-1* showed normal growth after 6 days, while the wild type (*Landsberg erecta*) was inhibited in growth. *gin2-1* was not affected by the addition of Glc, explaining why it was referred to as *Glc insensitive* (*gin*). EMS mutagenesis of transgenic lines expressing the catalytic disabled AtHXK1 in the *gin2-1* background recovered the Glc sensitivity of the WT when grown on high Glc. Additionally, these lines exhibited normal growth under increasing light intensity. These experiments proved that the sensing function is uncoupled from the catalytic function. It was further shown, that AtHXK1-dependent Glc signaling interacts with plant hormone (auxin and cytokinin) signaling pathways (Moore *et al.*, 2003). Until now, a Glc sensing function has been described only for the Arabidopsis HXK's, AtHXK1 and AtHXK2 and recently for the rice HXK's, OsHXK5 and OsHXK6 which were able to restore the wild-type properties in the *gin2-1* background (Cho *et al.*, 2009A). Furthermore, Cho *et al.* (2009B) suggested that the nuclear localization of AtHXK1, OsHXK5 and OsHXK6 might be critical for Glc sensing and signaling. Up to now detailed characterizations of single HXK isoforms especially with focus on their physiological roles are still missing.



## 1.7 Using RNA interference pathways for the elucidation of gene functions

Forward genetics refers to an approach where the scientific approach attempts to identify a gene or a set of genes responsible for a specific phenotypic variation within genotypes of a species. On the contrary, in reverse genetics approaches the gene sequence is already known, but its exact *in vivo* function is uncertain and intended to be elucidated. Profiting from the rapid progress in whole-genome sequencing projects, reverse genetics have proven successful and to represent an efficient approach to discover the role of genes in the phenotypic variability of a trait and to determine gene functions (Tierney and Lamour, 2005; Gilchrist and Haughn, 2010). In reverse genetics, many techniques and strategies have been developed and applied to alter or disrupt DNA sequences, like non-targeted disruptions (e.g. transposon-mediated mutagenesis, chemical mutagenesis) and targeted alterations (e.g. site-directed mutagenesis, gene silencing). Gene silencing in particular exploits the RNA interference (RNAi) pathway and has evolved as a powerful tool in molecular biology in the last decade. This method is also referred to as *gene knockdown* or *posttranscriptional gene silencing* (PTGS) and aims at modulating the expression of target genes to investigate the resulting loss-of-function phenotypes. For the RNAi pathway the generation of small interfering RNAs (siRNAs; 20-25 nucleotide long RNAs) by processing of longer double stranded RNA (dsRNA) or stem loop precursors (so called hairpin RNAs) is essential. These two effectors of RNAi are formed in transgenics which produce hairpin RNAs with sequences homologous to sequences of the target gene, or via the infection with recombinant RNA viruses (viral-induced gene silencing, VIGS). Antisense and co-suppression are additional modes of gene silencing that require the RNAi machinery. SiRNAs are produced by ATP-dependent cleavage of dsRNA or hairpin RNA by the RNase III endonuclease ‘Dicer’. Single siRNAs are subsequently unwound into two single-stranded RNAs (ssRNAs), referred to as passenger strand and guided strand. The guided strand is incorporated into the RNA-induced silencing complex (RISC) while the passenger strand is degraded. Pairing of the guided strand with a complementary sequence of a mRNA initiates the active component of RISC, the so-called argonaute, which cleaves the target mRNA and prevents its functional translation (Small, 2006; Angaji *et al.*, 2010). SiRNAs are also able to mediate transcriptional gene silencing (TGS) by shifting chromatin configuration or methylation status at the siRNA-binding sites on the chromosomes. In plants, RNA interference has been evolved as an effective cellular defense system against viruses and transposons and as mediator in the regulation of gene expression.

## 1.8 Characterization of HXK's in tobacco

*Nicotiana sylvestris* has turned out suitable to investigate HXK isoforms due to fact that tobacco is one of the most widely used and best studied model plants in the field of biochemistry, molecular biology and genetic engineering. Previous work on the identification and functional characterization of tobacco HXK's was essentially based on two different approaches (Giese, *dissertation*, 2005). First, by screening of a tobacco leaf cDNA library under low stringency conditions with the cDNA sequence of the *Arabidopsis AtHXK1* the tobacco hexokinase homologues *NtHXK1*, *NtHXK1a*, *NtHXK2* and *NtHXK3* were identified. Another isoform, *NtHXK6*, was found in the same way using the *AtHXK2* cDNA sequence as a probe. Second, further isoforms *NtHXK4a*, *NtHXK4b*, *NtHXK5* and *NtHXK7* were isolated by PCR-based sequence amplification using degenerated primers derived from highly homologous sequences.

The paired protein sequence analysis revealed that the isoforms *NtHXK1*, *NtHXK1a*, *NtHXK3* and *NtHXK7* as well as *NtHXK4a*, *NtHXK4b* and *NtHXK5* compose groups of close relationship (Fig. 5; Giese, *dissertation*, 2005). *NtHXK1* and *NtHXK1a* as well as *NtHXK4a* and *NtHXK4b* appear to represent two alleles of the same gene.

<b>HXK1</b>								
<b>HXK1a</b>	<b>97</b>							
<b>HXK3</b>	<b>88.3</b>	<b>88.7</b>						
<b>HXK7</b>	<b>91.8</b>	<b>92</b>	<b>86.1</b>					
<b>HXK4a</b>	71.2	72.3	71.1	72.5				
<b>HXK4b</b>	70.6	71.1	70.2	71.9	<b>97.2</b>			
<b>HXK5</b>	69.9	69.6	69.4	69.8	<b>87.2</b>	<b>86</b>		
<b>HXK2</b>	57.5	57.8	57.1	57.1	56.2	55.6	58.1	
<b>HKL1</b>	53.6	53.9	52.7	53.3	53.8	53.6	56.3	52.6
	<b>HXK1</b>	<b>HXK1a</b>	<b>HXK3</b>	<b>HXK7</b>	<b>HXK4a</b>	<b>HXK4b</b>	<b>HXK5</b>	<b>HXK2</b>

**Figure 5:** Comparison of sequence homology of tobacco hexokinases. The percentage homology is calculated from the amino acid sequence. Groups of closely related isoforms (over 85% identity) are highlighted in bold letter. Taken from Giese (*dissertation*, 2005).

In order to investigate the intracellular distribution of the NtHXX isoforms GFP-fusion constructs and immunogold localization studies were conducted showing that the type A protein NtHXX2 is located in the stroma of chloroplasts and the type B proteins are associated with mitochondria (Fig. 6). Furthermore, the 5'UTRs of NtHXX1 (1.4kb) and NtHXX2 (0.9 kb) were isolated and used to create stable transgenic lines expressing promoter-GUS constructs that allowed monitoring the tissue-specific expression of these genes in the plant. Transgenic plants harbouring the *NtHXX1-Prom::GUS* constructs showed no GUS activity in any of the investigated lines, most likely due to a flaw in the construct design: The promoter part still contained the translation start sequence (TSS) of the *NtHXX1* gene sequence which possibly led to a frame shift in the transcripts of the GUS sequence. The plants with the *NtHXX2-Prom::GUS* construct showed specific GUS activity in the starch sheath (cylinder of starch storing cells in the vascular tissue of stems), xylem parenchyma, guard cells and root tips. Transgenic lines with tobacco *HXX* genes under the control of constitutive 35S-promoters were generated and subjected to activity measurements. In a simple feeding experiment, leaf samples were collected and placed for 24 h in 300 mM Glc solution. A determination of starch contents revealed increased starch concentrations in leaves of NtHXX4-, NtHXX5- and NtHXX6-overexpressing plants, no significant difference in leaves of NtHXX2- and NtHXX3-overexpressing plants and a clear decrease in leaves of NtHXX1-overexpressing plants compared to the WT. However, a confirmation of these findings by the analysis of knockout or knockdown plants is still lacking but could allow elucidating specific roles of individual HXX isoforms.

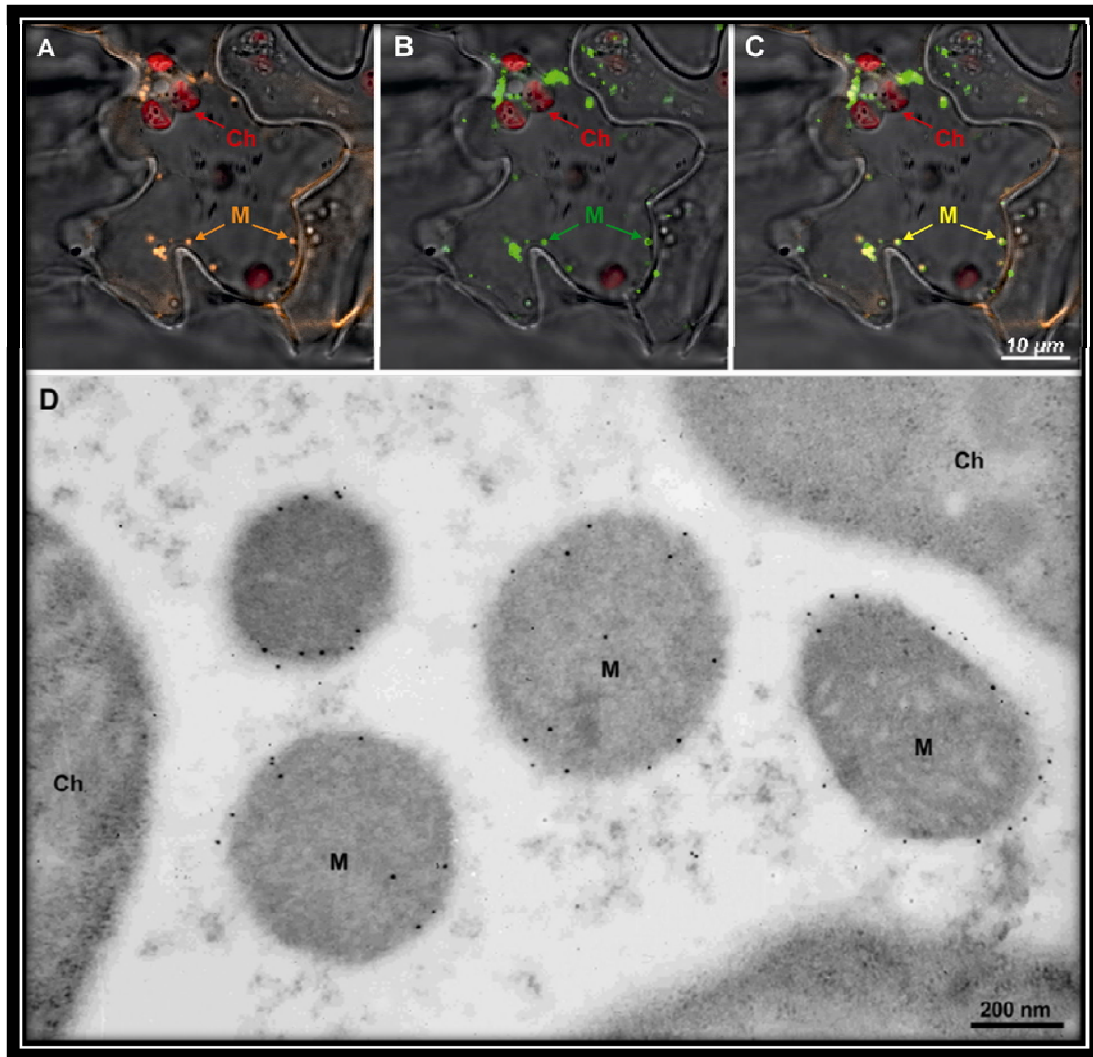


**Figure 6:** Intracellular localization of NtHXX1.

Distribution of NtHXX1:GFP in a leaf epidermis-cell: (A) detection of mitochondria by staining with “Mito Tracker CMTMRos” (orange staining) (B), detection of GFP (510-525nm) and (C) both signals merged. (D) Immunolocalization with NtHXX1 antibody via transmission electron microscopy (TEM). Immunogold labeling (dots) concentrated on mitochondria membrane surface. Taken from Giese (*dissertation*, 2005)

## 1.9 Aim of this study

The original aim of the project was the functional characterization of the entire HXK gene family in tobacco, which was soon recognized not to be feasible in the frame of one PhD dissertation. RNA interference (RNAi)-constructs from the NtHXK isoforms 1, 2, 4 and 6 were generated and used for transformation of tobacco plants. The isoforms 3, 5 and 7 were excluded due to their close relation to the selected isoforms. While generating homozygous T<sub>2</sub>-lines, we discovered that the plants with silenced *NtHXX1* gene expression displayed strong growth defects and distinct phenotypical aberrations. In addition, further experimental

evidence led to the presumption that NtHXK1 performs a crucial role in tobacco plants. In particular, the following aims have been addressed in the present work:

1. Determination of tissue- and organ-specific localization of *NtHXK1* expression to better understand the function of NtHXK1.
2. Physiological analysis of RNAi lines with repressed expression of HXK1.
3. Complementation of the *gin2-1* mutant to verify if NtHXK1 can take over sensing functions and plays a role in sugar sensing.

The outcome of these approaches should allow creating a detailed functional model of NtHXK1, demonstrating its individual role in the primary metabolism of tobacco plants.

## 2 Material & Methods

### 2.1 Plant material and growth conditions

#### 2.1.1 Tobacco

Virginian tobacco (*Nicotiana tabacum* L.) is one of the best studied model plant systems since it can be easily transformed and has a relative short generation time. *N. tabacum* is a member of the agriculturally important *Solanaceae* family, which also includes petunia, tomato, potato, eggplant and pepper crop plants. It is an amphiploid species ( $2n=48$ ) from an interspecific cross between *N. sylvestris* ( $2n=24$ ) and *N. tomentosiformis* ( $2n=24$ ) and has a relatively large genome size. With approximately 4.5 billion base pairs, its genome is 1.5 times the size of the human and 40 times the size of the *Arabidopsis thaliana* genome. The wild type variety Samsun NN (SNN; provided by Vereinigte Saatzuchten EG, Ebstorf, Germany) and transgenic plants were cultivated on Murashige and Skoog media (MS, 2% Suc) at 24°C in a light/dark cycle of 16h/8h and, if not stated otherwise, transferred to soil at 25°C/18°C under a 16 h light/8 h dark photoperiod in the greenhouse.

#### 2.1.2 *Arabidopsis*

Thale cress (*Arabidopsis thaliana* L.) is the most suitable model plant for genetic studies. Its small genome (157Mbp;  $2n=10$ ), small size, rapid life cycle, selfing nature and high seed productivity made *Arabidopsis* to a powerful genetic model organism for over 50 years. It was the first plant to have its genome sequenced in 2000 and reams of phenotypic and physiologic mutants have been studied and described. The routine transformation by floral dip avoids the necessity of either tissue culture or plant regeneration.

The wild type (Landsberg erecta ecotype, Ler-0; from the IPK Genebank, Gatersleben, Germany), *gin2-1* mutant (supplied by *Arabidopsis* Biological Resource Center, Columbus, USA) and transgenic plants were cultivated after stratification (2 days in dark at 4°C) on half strength MS (2% Suc, 1x Gamborg Vitamin Solution) at 21°C in a light/dark cycle of 16h/8h.

### 2.2 Bacteria strains

*E.coli* **TOP10F'** (Invitrogen, Karlsruhe): *mcrA*,  $\Delta(mcrBC-hsdRMS-mrr)$ , *endA1*, *recA1*, *relA1*, *gyrA96*,  $\Phi80lacZ\Delta M15$ , *deoR*, *nupG*, *araD139*,  $F\{lacI^q, Tn10(Tet^r)\}$ , *galU*,  $\Delta lacX74$ , *galK*,  $\Delta(ara-leu)7697$ .

*E.coli* **XL1-Blue MRF'** (Stratagene, California):  $\Delta$  (mcrA )183,  $\Delta$ (mcrCB-hsdSMR-mrr )173, endA1, supE44, thi-1, recA1, gyrA96, relA1, lac [F 'proAB lacI<sup>q</sup> Z  $\Delta$ M15 Tn 10 (Tet<sup>r</sup> )].

*Agrobacterium tumefaciens* (Deblaere *et al.*, 1985): pGV2260 in C58Cl

## 2.3 Yeast strain

*Saccharomyces cerevisiae* **YSH7.4-3C** (de Winde *et al.*,1996): W303-1A with hxx1 $\Delta$ ::HIS3 hxx2 $\Delta$ ::LEU2 glk $\Delta$ ::LEU2

## 2.4 Vector construction

### 2.4.1 Tissue-specific localization

To examine the tissue-specific localization of NtHXX1, the genomic region (Accession No. AY664411) -1384 to -21 bp upstream of *HXX1* transcription start sequence (TSS) was amplified to also add the *HindIII* and *AatI* (for GUS) as well as *EcoRI* and *XhoI* (GFP) restriction sites. The fragments were ligated into binary vectors pGUSI (Hood *et al.*, 1993) and pGFP\_amp and further transferred by *SfiI* digestion into the vector pNOS9. The primers were:

HXX1\_Prom\_FP 5'-CTCTAATTTGGTGTATCCCACTCAT-3' and

HXX1\_Prom\_RP 5'-AGGAATTGGAGGTTGGCTAAAAGTT-3'

For the colorimetric detection of GUS activity tissue samples were stained at 37°C in a buffer containing 100 mM sodium phosphate, pH 7.2, 0.1% Triton X-100, 15 mM  $\beta$ -mercaptoethanol and 1mM X-Glc.

### 2.4.2 Yeast complementation

In the past, plant HXX genes were identified by complementation approaches with yeast mutants (Cho *et al.*, 2006). The first isolated plant HXX (AtHXX1) was characterized by complementation of a yeast triple mutant (hxx1, hxx2 and glk1) (Dai *et al.*, 1995). Likewise, the two isoforms AtHXX1 and AtHXX2 were identified from an expression library in the yeast double mutant DBY 2219 (hxx1 and hxx2) (Jang *et al.*, 1997). To complement the Glc phosphorylation inactive yeast triple mutant YSH7.4-3C (ScHXX1, ScHXX2, ScGK1) full-length *NtHXX* open reading frames (ORFs) were isolated from cDNA libraries with additional restriction sites and placed under the control of the constitutive PMA1 promoter in the yeast high copy vector pDR196 (kindly provided by Doris Rentsch, University of Bern, Switzerland; Rentsch *et al.*, 1995). The primers were:

NtH XK1\_Primer\_FP\_SpeI 5'-ACTAGTATGAAGAAAGCGACGG-3' and  
 NtH XK1\_Primer\_RP\_SmaI 5'-CCCGGGGGACTTATCTTC-3',  
 NtH XK3\_Primer\_FP\_SpeI 5'-ACTAGTTGAGCGGATAACAATTTTCACACAG-3' and  
 NtH XK3\_Primer\_RP\_XhoI 5'-CTCGAGGAGGTCATTACTGGATCTATCAA-3',  
 NtH XK4\_Primer\_FP\_SpeI 5'-ACTAGTATGGGAAAAGTGGTGGTGGG-3' and  
 NtH XK4\_Primer\_RP\_XhoI 5'-CTCGAGTCAAGATTCCTCCAGTCCGA-3',  
 NtH XK5\_Primer\_FP\_SpeI 5'-GGACTAGTATGGGAAAATTGGTTGTAGGTG-3' and  
 NtH XK5\_Primer\_RP\_Sall 5'-ACGCGTCGACTCATGATTCCTCGAGATCTGTGTAT-  
 TGGGAA-3',  
 NtH XK7\_Primer\_FP\_SpeI 5'-ACTAGTATGAAGAAAGTGACGGTGG-3' and  
 NtH XK7\_Primer\_RP\_SmaI 5'-CCCGGGCTAAGCTTGATC-3'.

### 2.4.3 Overexpression of tobacco hexokinase 1

Stable transgenic tobacco lines with *NtH XK1* under the control of the 35S-promoter were generated in a preliminary work (Giese, *dissertation*, 2005). To constitutively express *NtH XK1* in *Arabidopsis*, the full-length ORF was amplified from cDNA with additional *BamHI* and *Sall* restriction sites and ligated into the pCR blunt vector (Invitrogen, Carlsbad, CA, USA) and subsequently placed under the control of the cauliflower mosaic virus (CaMV) 35S promoter using the pBinAR (Höfgen and Willmitzer, 1990) vector (Fig. 7). The primers were:

H XK1\_FP 5'-GGATCCCCGTAT-GCGCAAAGT-3' and  
 H XK1\_RP 5'-GTCGACACCAATGCCAGA-ACCATC-3'.

### 2.4.4 Silencing of tobacco hexokinase 1

To suppress *NtH XK1* in tobacco, a 728 nucleotide long fragment (+90 to +818 downstream of TSS) was amplified from cDNA, cloned into the gateway entry vector pENTR (Invitrogen) and further transferred to the RNA interference destination vector Pk7GWIWG2(II) (Karimi *et al.*, 2002; Fig. 7). The primers were:

H XK1\_RNAi\_FP 5'-GTCGCTGATGCTATGACCGTCGAG-3' and  
 H XK1\_RNAi\_RP 5'-GTGGCGTGATCA-TACTGTGTCAAG-3'



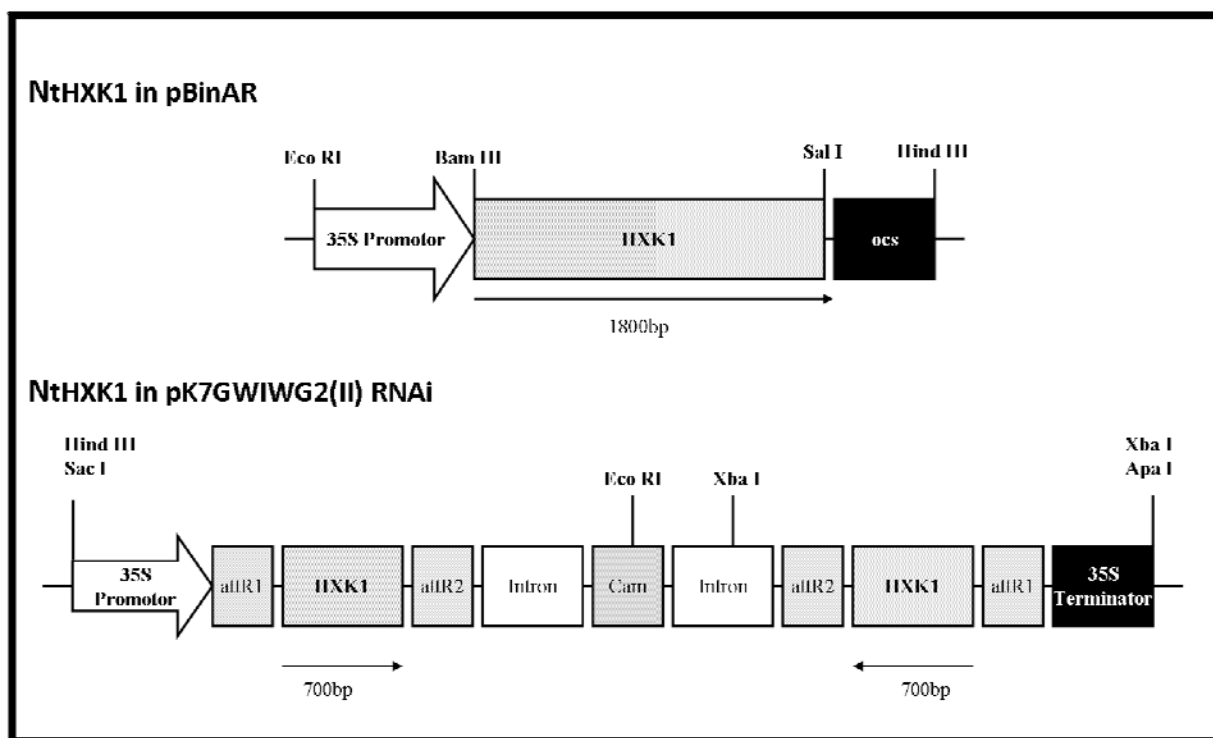


**Figure 7:** Schematic representation of the overexpression (upper) and the silencing construct (lower) of NtHXK1 isoform in tobacco

## 2.5 Plant transformation

### 2.5.1 Tobacco

Stable plant transformation by *Agrobacterium tumefaciens* mediated DNA transfer was performed using the strain C58C1 with the helper plasmid pGV2260 (Deblaere *et al.*, 1985). The cultivation of *Agrobacterium* was carried out in YEB media (Vervliet *et al.*, 1975) while their transformation with binary vectors was accomplished following the method of Höfgen and Willmitzer (1990). The stable transformation of tobacco was performed according to Rosahl *et al.* (1987). Transgenic individuals were selected by antibiotic resistance and further propagated. Homozygous T2 lines were used for further investigation. One sample consisted of at least 3 samples from individual plants of each line. Samples were at identical time points and pooled for different analyses or assays.

### 2.5.2 *Arabidopsis*

Prior to transformation, *Arabidopsis thaliana* plants were cultivated for 4 weeks under short day conditions and further transferred to long day, to trigger flower induction. 8 week old plants were transformed by the floral dip method as previously described (Clough and

Bent, 1998). To obtain homozygous plants, positive plants were selected by antibiotic resistance and propagated for at least two further generations.

## **2.6 Yeast transformation**

Yeast cells were transformed using the lithium acetate/single stranded carrier DNA/PEG method according to the protocol from Gietz and Schiestl (2007). The yeast strain to be transformed was streaked from a frozen glycerol stock on an YPD-Gal (1% (w/v) Bacto yeast extract, 2% (w/v) Bacto peptone, 2% (w/v) galactose, 2% Difco Agar for solid medium plate and incubated at 30°C for 3 days, until single colonies were visible. A single colony was picked, inoculated into a test tube containing 5 ml liquid YPAD-Gal (1% (w/v) Bacto yeast extract, 2% (w/v) Bacto peptone, 2% (w/v) galactose, 80 mg l<sup>-1</sup> adenine hemisulfate medium and incubated overnight at 200 rpm and 30°C. A bottle of 2x YPAD-Gal medium and a 250 ml culture flask were placed in a 30°C incubator overnight. After 16 h of growth, the optical density at 600 nm (OD<sub>600</sub>) was determined in a 100-fold dilution in disposable cuvettes. The volume of the overnight culture was added to 50 ml pre-warmed 2x YPAD-Gal in order to achieve a final OD<sub>600</sub> of 0.17. The culture was then incubated at 30°C and 200 rpm for 4h. The cell titer was supposed to achieve after this period an OD<sub>600</sub> of 0.6-0.7. Microcentrifuge tubes containing carrier DNA (salmon sperm DNA dissolved in sterile 10 mM Tris-HCl, 1 mM Na<sub>2</sub>-EDTA, pH 8.0) were denatured for 5 min at 99°C and immediately chilled on ice (single stranded carrier DNA). The yeast cells were harvested by pouring the 50 ml yeast suspension in a 50 ml centrifuge tube, centrifuged at 3000 g and 20°C for 5 min and the supernatant was discarded. For washing, the yeast pellet was resuspended in 25 ml water by vortexing and centrifugation at 3000 g and 20°C for 5 min. This washing step was repeated twice. The cells were resuspended in 1 ml water. The yeast suspension was transferred to a 1.5 ml tube, centrifuged for 30 s at 13.000 g and the supernatant was discarded. Cells were resuspended in 1 ml water and 100 µl samples were transferred into 1.5 ml tubes, one for each transformation. Tubes were centrifuged at 13.000 g for 30s and the supernatant was removed. Sufficient transformation mix was prepared and thoroughly vortexed. The components of the mix were cooled to 4°C before mixing and kept on ice after mixing to maintain the salmon sperm DNA denatured.

## Yeast transformation mix components

• PEG 4000 [50% (w/v)]	Volume	240 $\mu$ l
• water	Volume	32 $\mu$ l
• LiAc (1.0 M)	Volume	36 $\mu$ l
• Single-stranded carrier DNA (2.0 mg ml <sup>-1</sup> )	Volume	50 $\mu$ l
	Total volume	358 $\mu$ l

358  $\mu$ l of transformation mix were added to each transformation tube containing the cell pellet. 2  $\mu$ l plasmid DNA was added to each of the tubes. A negative control tube containing cell pellet and transformation mix without plasmid DNA was included. The cell pellet was resuspended by vortexing vigorously. The tubes were then incubated at 42°C for 40 min in a thermomixer. After the heat shock, the tubes were centrifuged at 13.000 g for 30 s and the supernatant was removed with a pipette. The pellet was resuspended in 1.0 ml water.

1%, 10% and 100% (diluted with water) of the cell suspension were plated onto solid YNB-Gal medium. The plates were incubated at 30°C for at least 5 days until single colonies were visible.

## 2.7 RNA isolation and quantitative real-time PCR

Total RNA was extracted from different tissues according to the Single-Step Method (Chomczynski and Sacchi, 1987). After DNase treatment the RNA samples were quantified and used for the synthesis of single-stranded complementary DNA (cDNA) with an oligo-dT-primer and the RevertAid<sup>TM</sup> First Strand cDNA Synthesis Kit (Fermentas, St. Leon-Rot, Germany). The resulting cDNA was used for the quantitative real-time PCR (qPCR) with HXK specific primers and control primers for the housekeeping/reference gene EF-1 $\alpha$  (Elongation factor 1 $\alpha$ ; Schmidt and Delaney, 2010). The primers were:

<b>NtHXK1</b>	5'-GAGATGAATTGGCGACAAGC-3' and 5'-GCTTGATGGTATAATCCGGAGA-3',
<b>NtHXK2</b>	5'-TGGATCTGGAATTGGAGCTG-3' and 5'-TCGTACCAAACGAGCCCTTA-3',
<b>NtHXK3</b>	5'-AGCCGCAAATGATGGTTCT-3' and 5'-CAAGCACAAGTGCTGCAAAA-3',
<b>NtHXK4</b>	5'-TGGTGGTGGGTGCAGCAGTAGTA-3' and 5'-CCACCTTCAGAAGCAAGACCAGC-3',

**NtHXK5** 5'-GCATGCTGGACTTGCTTCTGA-3' and  
5'-GCACACGCATCACACGAAAGT-3',  
**NtHXK6** 5'-TTAGCAGCTGCTGGTATCGTGGG-3' and  
5'-CCCTGATCCATCTTCCATGACCC-3',  
**NtHXK7** 5'-GAAGGACTTGCTCGGAGAGG-3' and  
5'-CCGAAAATGCTTGAGAGCAAA-3' and  
**EF-1 $\alpha$**  5'-CTCTCAGGCTCCCACTTCAG-3' and  
5'-AAGAGCTTCGTGGTGCATCT-3'.

The qPCR was performed with the Mastercycler® ep *realplex* (Eppendorf, Hamburg, Germany) and the iQ™ SYBR® Green Supermix (Bio-Rad Laboratories, Hercules, CA, USA). Relative quantification was calculated by comparative C<sub>t</sub> Method ( $2^{-[\Delta][\Delta]C_t}$ ) with EF-1 $\alpha$  as reference. The experiments were conducted with two biological and two technical replicates (n=4) for each primer pair and cDNA variant.

## 2.8 Northern Blot analysis

Between 10 to 50  $\mu$ g of total RNA were separated after denaturation on a 1.5% (w/v) formaldehyde-agarose gel and blotted via capillary transfer onto GeneScreen membranes (NEN, Boston, USA). By UV-light the RNA samples were then covalently linked on the blotting membrane. After the probes (cDNA fragments that are complement to the RNAs of interest) have been labeled with the usage of the “High Prime” kit (Boehringer, Mannheim) and the radioactive labeled [ $\alpha$ -<sup>32</sup>P]-dCTP (Amersham, Freiburg), they were hybridized to the RNA on the membranes in church buffer (Church and Gilbert, 1984) according to the description in Herbers *et al.* (1995). The membranes were thoroughly washed and rinsed to avoid background signals and the hybrid signals were detected by X-ray film (Kodak, Stuttgart) or by phosphor imaging (Fuji FLA-3000; Fuji, Tokio, Japan).

## 2.9 Western Blot analysis

Plant tissue samples were homogenized in 2x SDS buffer [50 mM tris-HCl pH 6.8, 5% (v/v)  $\beta$ -mercaptoethanol, 10% (v/v) glycerin, 2% (w/v) SDS]. After a heat denaturing step for 10 min the cell-debris were pelletized and similar volumes of supernatants were separated on 10 –15% (v/v) SDS-polyarylamide gels (Lämmli, 1970). The proteins were transferred by electroblotting onto nitrocellulose membranes (Porablot, Macherey-Nagel, Düren). After blocking with bovine serum albumin (BSA) the hybridization with two antibodies according

the two-step method was performed. The unbound antibodies were washed away and the membranes were developed in TBS/T buffer [20 mM tris, 500 mM NaCl, 0.1 % (w/v) Tween 20] with NtHXX1 specific primary antibodies as well as fluorescence-tagged secondary antibodies (Alexa Fluor® 790; infrared). Images were taken with a Li-Cor Odyssey® Imaging System (Li-Cor Inc., Lincoln, NE, USA).

## 2.10 Protoplast isolation

Tobacco mesophyll protoplasts were isolated based on the method of Yoo *et al.* (2007). Leaves of 6 weeks old plants were cut into 1-2 mm strips with a razor blade (around 1-1.5 g) and incubated for 1 h in 0.5 M mannitol (Man) in a Petri dish. After removal of Man, 10 ml digestion buffer [1% (w/v) cellulase R10, 0.25% (w/v) macerozyme R10, 0.4 M Man, 20 mM MES (pH 5.7), 20 mM KCl, 10 mM CaCl<sub>2</sub>] was added and the dish was then put under vacuum for 30 min at room temperature. The dish was then placed in the dark for 12-20 h at room temperature. After filtering the crude solution into a 50 ml tube with MiraCloth (pore size 22-25 µm; CalBiochem®, San Diego, CA, USA) the protoplast were collected by centrifugation (100 x g, 4°C and 10 min). The pellet was washed twice with 10 ml W5 buffer (154 mM NaCl, 125 µM CaCl<sub>2</sub>, 5 mM KCl and 2 mM MES pH 5.7), resuspended in 10 ml W5 buffer and kept at 4°C for 30 min. The protoplasts were collected again by centrifugation (100 x g, 4°C and 10 min), washed with 10 ml Mg solution (0.4 M Man, 15 mM MgCl<sub>2</sub>, 4 mM MES pH 5.7) and resuspended in 5 ml Mg solution.

## 2.11 Glucose phosphorylation activity

Plant material from source leaf lamina was homogenized in 50 mM Tris-HCl, pH 6.8, 5 mM MgCl<sub>2</sub>, 5 mM β-mercaptoethanol, 15% glycerol, 1 mM EDTA, 1 mM EGTA, 0.1 mM pefabloc and 1% Triton X-100. Crude extracts were centrifuged at 4°C and 14000 rcf for 10 minutes and clear supernatants were used for activity assays. HXK activity was determined by monitoring the formation of NADH (Wiese *et al.*, 1999). The formation of NADH was determined by measuring the absorbance change at 340 nm using a 96-well microtiterplate reader (EL 808, BioTek, Winooski, VT, USA).

The reaction mixture contained 100 mM Tris/HCL, pH 8.0, 5.5 mM MgSO<sub>4</sub>, 4 mM ATP, 0.8 mM NAD and 0.5 U glucose-6-phosphate-dehydrogenase from *Leuconostoc mesenteroides*. Reaction was initiated by the addition of 2 mM Glc.

## 2.12 Photosynthetic activity

Photosynthesis respectively net CO<sub>2</sub> uptake rates as well as dark respiration rates were measured by gas exchange with an Infra-Red Gas Analyzer (IRGA) LI-6400 Portable Photosynthesis System (Li-Cor Inc., Lincoln, NE, USA) essentially as described by Hajirezaei *et al.* (2002). Photosynthetic Photon Flux Density (PPFD) values varied between 0 and 2000  $\mu\text{mol photons m}^{-2} \text{ s}^{-1}$ , CO<sub>2</sub> concentration of the air entering the chamber was adjusted to 400  $\mu\text{mol mol}^{-1}$  and leaf temperature was maintained at 20°C. Dark respiration rates represent CO<sub>2</sub> exchange rates at the PPFD of 0  $\mu\text{mol photons m}^{-2} \text{ s}^{-1}$ .

## 2.13 Chlorophyll determination

Chlorophyll extraction and measurement were performed essentially according to Lichtenthaler (1987). Leaf discs of known diameter (to calculate the exact area) were homogenized thoroughly in 80% acetone solution, centrifuged (3000 rpm for 15 min at 4°C) and the supernatant was immediately used to measure chlorophyll contents by spectrophotometry. The absorbance of chlorophyll a and b were recorded at 645 nm and 663, respectively. Chlorophyll concentrations were determined according to following calculations:

$$\text{chlorophyll a (mg l}^{-1}\text{)} = [12.7 \times A_{663} - 2.69 \times A_{645}] \times V$$

$$\text{chlorophyll b (mg l}^{-1}\text{)} = [22.9 \times A_{645} - 4.86 \times A_{663}] \times V$$

$$\text{total chlorophyll (mg l}^{-1}\text{)} = [8.02 \times A_{663} + 20.20 \times A_{645}] \times V$$

where V = volume of the extract (l), A<sub>645</sub> = absorption at 645 nm, A<sub>663</sub> = absorption at 663 nm.

## 2.14 Nitrogen and carbon determination

Nitrogen and carbon content were measured from dry leaf material by an elemental analyzer (Euro EA CHNSO-Analyzer, EuroVector SpA, Milan, Italy). 10 mg of dry leaf material was used for each measurement and the average of 20 biological replicates was calculated. The elemental analyzer employs dynamic combustion with subsequent chromatographic separation for the exact determination of C and N.

## 2.15 Soluble sugar and starch determination

Soluble sugars were extracted and analyzed essentially as described by Ahkami *et al.* (2009) by incubating leaf material in 80 % (v/v) ethanol for 1h at 80°C followed by an

enzymatic assay. Homogenized samples were centrifuged for 5 min at 4°C and at 14,000 rpm. Supernatant was completely dried under vacuum at 50°C and re-suspended in 0.25 ml *aqua dest.*. Determination of glucose, fructose and sucrose contents was performed in a measuring buffer containing 100 mM imidazol-HCl (pH 6.9), 5 mM MgCl<sub>2</sub>, 2.25 mM NAD, 1 mM ATP and 20 µl of the sugar extract in a final volume of 300 µl using corresponding auxiliary enzymes according to Hajirezaei *et al.* (2000). Starch was subsequently decomposed from the remaining insoluble material with 0.2 N KOH for 1 h at 95°C and homogenized. After neutralization of pH with 1 N acetic acid, starch samples were hydrolyzed with amyloglucosidase (2 U / ml, Boehringer, Mannheim, Germany) overnight at 37°C. The quantification of produced Glc was carried out as described above.

In addition, Glc, Fru and Mal were measured using a HPLC system from the Dionex company consisting of a pump GP50, an autosampler AS50, an eluent generator EG50 producing a gradient with KOH and an amperometric detector ED50. For separation of the sugars a CarboPac PA200 column with 4 µm diameter and 250 mm length was used (Dionex, Sunnyvale, CA, USA). The concentration of different sugars was calculated based on external standards and generation of a calibration curve with more than five different standard concentrations. The Software Chromeleon release 6.8 was used for the calculation of the results.

For visualization of starch, whole leaves were kept in darkness for 24 h and then destained overnight with 80 % ethanol. Starch staining was performed with Lugol's solution (5 % iodine, 10 % potassium iodide). The stained leaves were photographed on light background (paper).

## 2.16 Glucose repression assay

For Glc-repression assays in *Arabidopsis*, seedlings were grown on half strength MS medium containing no Glc, 6 % Glc, or 6 % Man, respectively, for 6 days at a light intensity of 100 µmol m<sup>-2</sup> s<sup>-1</sup>. To examine the growth phenotype, WT, *gin2-1* and transgenic plants expressing NtHKK1 were grown on soil for 18 d under low (100 µmol m<sup>-2</sup> s<sup>-1</sup>) and high (240 µmol m<sup>-2</sup> s<sup>-1</sup>) light conditions in a light/dark cycle of 16 h/8 h. To examine the growth phenotype in tobacco, WT and silenced *NtHKK1* and *NtHKK1* over-expressing plants were grown for 18 days on soil under ambient greenhouse with an average light intensity of 250 µmol m<sup>-2</sup> s<sup>-1</sup> and a light/dark cycle of 16 h/8 h as well as at high light conditions with a constant light intensity of 500 µmol m<sup>-2</sup> s<sup>-1</sup>.

## 2.17 Metabolite profiling

Metabolite profiling was performed using the ICS3000 system (Dionex) coupled to an API 4000 triple quadrupole mass spectrometer (AB SCIEX, Foster City, CA, USA) providing a simple, rapid, specific and sensitive method for the simultaneous detection and quantification of several primary metabolites involved in the TCA cycle and glycolysis pathway (Rolletschek *et al.*, 2011). Samples from homogenized leaf material were extracted with chloroform/methanol/water [1:1:3] according to Heinzl and Rolletschek (2011). Separation was performed over an IonSwift™ MAX-100 column (1x250 mm, Dionex). The column temperature was constant at 40°C and the total flow was 150 µl/min. Sodium hydroxide was used as eluent with the following gradient: t = 0 min (5 mM); t = 10 min (5 mM); t = 16 min (12 mM); t = 28 min (25mM); t = 32 min (100 mM); t = 38 min (100 mM); t = 42 min (5mM) and t = 56 min (5mM). The samples were measured on MS in negative mode. Nitrogen was used as a curtain gas, nebulizer gas, heater gas, and collision gas. The identification of the detected metabolites was executed by specific MS/MS transitions. The ion spray voltage was set to -4000V and the capillary temperature at 450°C. A table with detailed detection parameters can be found elsewhere (Heinzl and Rolletschek, 2011).



### 3. Results

#### 3.1 Phylogenetic analysis

The generation of a phylogenetic tree by alignment of the predicted protein sequences of the HXK gene families from *Nicotiana tabacum*, *Arabidopsis thaliana* and *Oryza sativa* (Fig. 8) was executed in order to look into evolutionary relationships and common features of related isoforms. Furthermore, the identities in percentage of the amino acid sequences of the tobacco isoforms in comparison to sequences of the *Arabidopsis* and rice isoforms were integrated in a table (Table 2). The catalytic active and mitochondria associated Type B2 proteins (Fig.3; *Introduction*) NtHXK1, NtHXK3, NtHXK4, NtHXK5 and NtHXK7 are clustered together with AtHXK1 and AtHXK2, which are described to be additionally involved in sugar sensing and signaling (Jang *et al.*, 1997). The plastidic isoform NtHXK2 is found in the same cluster as the isoforms OsHXK4 (69.5 % identity with NtHXK2) and AtHXK3 (63.1 %), which were also found to be localized in plastids. Finally NtHKL1 forms a cluster together with the catalytic inactive B1-proteins AtHKL1 (70.1 % identity with NtHKL1) and AtHKL2 (66.3 %) which comprise N-terminal membrane anchors. AtHKL1 was recently found to be a negative regulator of plant growth (Karve and Moore, 2009) and mediates certain aspects of crosstalk between Glc and ethylene response pathways (Karve *et al.*, 2012).

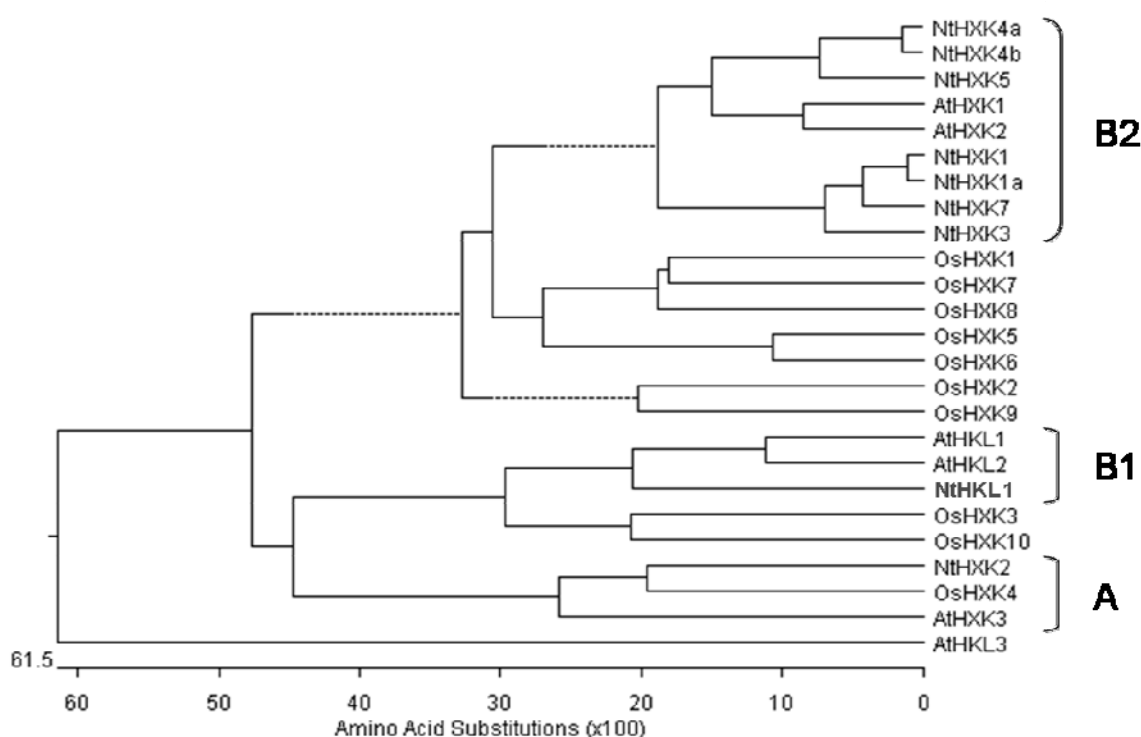


**Figure 8:** Phylogenetic tree of the HXK isoforms from tobacco (Nt), rice (Os) and *Arabidopsis* (At) ClustalW sequence comparison of the corresponding protein sequences (found via NCBI)

	NtHXK1	NtHXK1a	NtHXK2	NtHXK3	NtHXK4a	NtHXK4b	NtHXK5	NtHXK7	NtHKL1
<i>Arabidopsis thaliana</i>									
<b>AtHXK1</b>	<b>69.8</b>	<b>70.2</b>	55.0	<b>70.6</b>	<b>76.2</b>	<b>75.6</b>	<b>74.5</b>	<b>71.8</b>	54.6
<b>AtHXK2</b>	<b>69.8</b>	<b>69.6</b>	53.4	<b>70.2</b>	<b>76.9</b>	<b>76.3</b>	<b>74.4</b>	<b>70.8</b>	53.1
<b>AtHXK3</b>	49.7	50.7	<b>63.1</b>	49.9	49.8	49.6	51.5	48.7	46.4
<b>AtHKL1</b>	51.7	52.5	47.3	51.7	51.1	51.1	50.8	51.9	<b>70.1</b>
<b>AtHKL2</b>	49.1	49.1	45.3	48.9	50.1	50.3	50.6	48.9	<b>66.3</b>
<b>AtHKL3</b>	42.0	42.6	39.8	41.4	42.7	41.9	42.8	41.6	37.7
<i>Oryza sativa</i>									
<b>OsHXK1</b>	55.3	55.9	51.0	56.6	56.1	56.5	55.1	55.7	50.8
<b>OsHXK2</b>	<b>66.5</b>	<b>66.7</b>	56.9	<b>68.3</b>	<b>69.7</b>	<b>69.7</b>	<b>68.2</b>	<b>67.7</b>	55.4
<b>OsHXK3</b>	53.1	53.7	47.6	52.9	53.1	52.5	54.6	53.5	<b>65.2</b>
<b>OsHXK4</b>	52.1	52.3	<b>69.5</b>	53.3	52.9	52.1	53.6	51.9	48.3
<b>OsHXK5</b>	59.7	59.9	53.9	59.7	<b>63.2</b>	<b>62.8</b>	<b>63.3</b>	<b>60.1</b>	49.3
<b>OsHXK6</b>	<b>61.4</b>	<b>62.0</b>	53.5	<b>62.4</b>	<b>65.8</b>	<b>65.0</b>	<b>65.1</b>	<b>62.6</b>	49.6
<b>OsHXK7</b>	<b>62.2</b>	<b>62.6</b>	55.6	<b>63.5</b>	<b>63.9</b>	<b>63.9</b>	<b>63.2</b>	<b>62.9</b>	54.9
<b>OsHXK8</b>	<b>60.9</b>	<b>61.4</b>	54.4	<b>62.4</b>	<b>62.4</b>	<b>62.4</b>	<b>61.7</b>	<b>62.9</b>	54.8
<b>OsHXK9</b>	57.5	57.5	52.4	58.1	59.1	58.9	<b>60.4</b>	57.7	51.1
<b>OsHXK10</b>	48.3	48.1	46.7	46.4	45.0	44.8	47.3	47.2	59.0

**Table 2:** Percent identity of hexokinase amino acid sequences from tobacco compared to rice and *Arabidopsis*. Sequence alignment was performed by Clustal W method (Thompson *et al.*, 1994). Identities over 60% are highlighted in bold letters.

### 3.2 Expression analysis of HXK's in tobacco plants

In order to quantify mRNA, quantitative real-time PCR (qPCR) or more precisely reverse-transcription qPCR (qRT-PCR), real-time PCR combined with reverse transcription has become the method of choice in the past years for the validation of microarray results and the quantification of gene expression. Quantitative RT-PCR with primers for EF-1 was employed as reference for normalization and non-specific dsDNA-intercalating dye (SYBR Green) for detection of PCR products (see Material and Methods 2.7).

#### 3.2.1 Expression of the tobacco *HXK* isoforms in different plant organs

The quantitative RT-PCR analysis of the tobacco HXK isoforms 1 to 7 in different plant organs (flower, bud, sink leaf, source leaf, stem and root) revealed strongest expression of *NtHXK1* in flower samples (Figure 9A). Furthermore, the comparison of the different isoforms revealed a predominant expression of *NtHXK1* in all aerial organs (Fig. 9A-9E). Interestingly, *NtHXK4* was expressed in a predominant manner in roots (Fig. 9F) while only marginally detectable in the remaining organs. The expression level of *NtHXK3* (11-fold less in flower compared to *NtHXK1*) and particularly *NtHXK7* (almost not detectable in all investigated organs), which share very close sequence homology to *NtHXK1*, were considerably lower and therefore these isoforms were supposed to be rather redundant and not further considered in the following experiments.

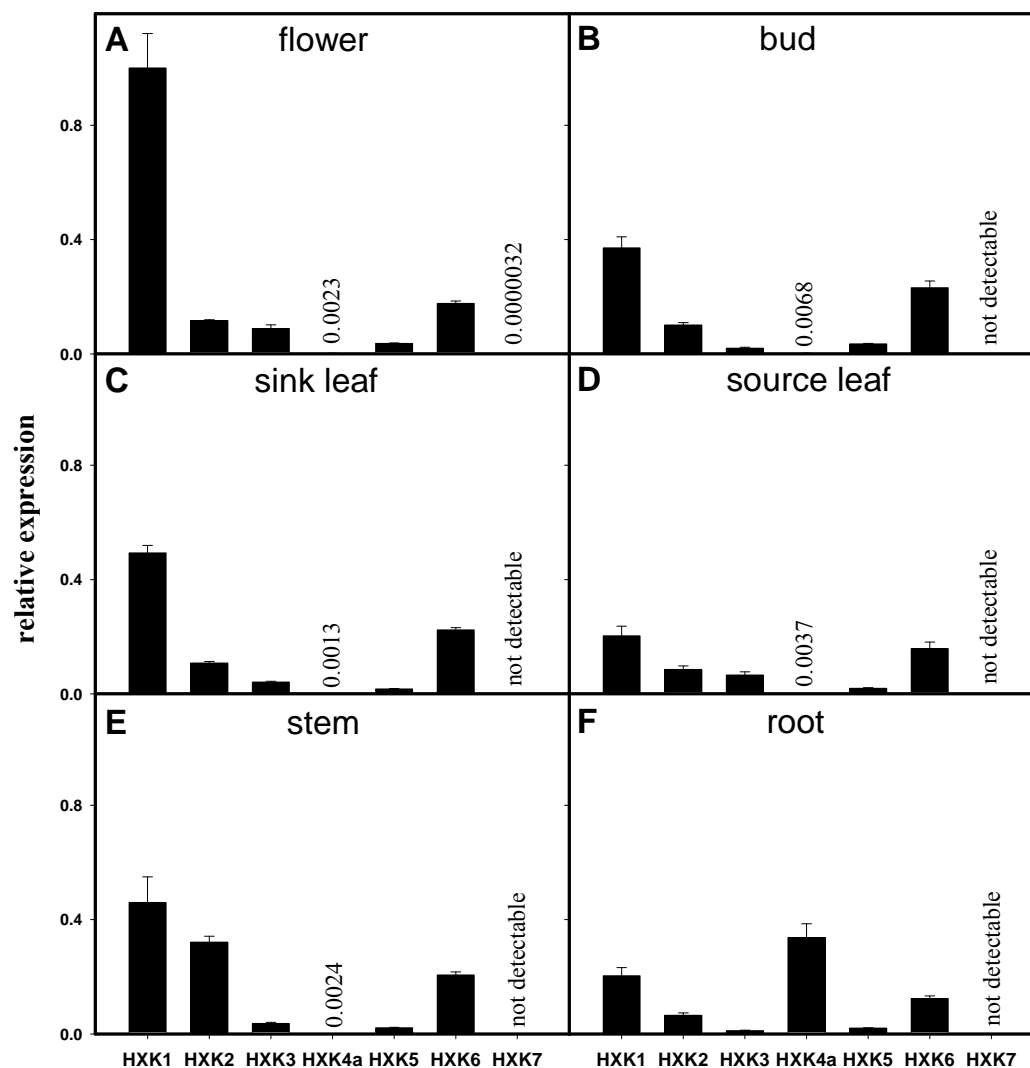


**Figure 9:** Expression analysis of hexokinases in different plant organs.

(A-F) Relative mRNA levels of seven HXK isoforms in different tobacco organs. Wild type plants were grown for 5 weeks in the greenhouse. Quantitative PCR was performed with gene-specific primers on wild type cDNA and expression levels were normalized to EF-1 $\alpha$  expression. Bars indicate means  $\pm$  SD, n = 4. HXK6 = HKL1.

### 3.2.2 Diurnal rhythm of *NtHXK1* expression

In order to investigate the *NtHXK1* expression during the course of the day and night samples were collected from tobacco wild type plants (sink and source leaves) every 2 hours over a period of 24 h and determined relative *NtHXK1* mRNA levels by qRT-PCR. In sink and source leaves, the highest amounts of *NtHXK1* transcripts were found at 4 am in the night. With the beginning of the light period (6 am), mRNA levels of HXK1 in sink leaves decreased, then an increase peaking at daytime around 6 pm (Fig.10A), followed by another

decrease till dusk and an increase to the highest level at 4 am (Fig.10A). In principle, the same diurnal variation in expression levels was observed for HXK1 in source leaves, except that the peak at daytime was at 2-4 pm. The difference between the bars in the light phase and in the dark phase in mature source leaves displays a significant increase of *NtHXK1* expression in the dark phase compared to the light phase.

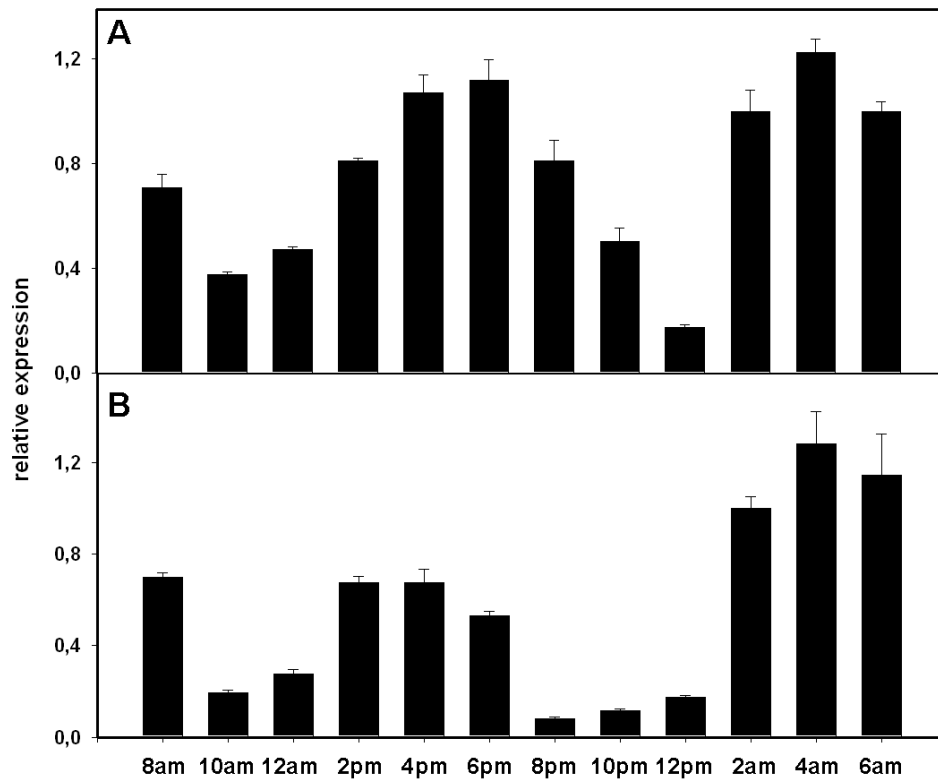


**Figure 10:** Time course of *NtHXK1* mRNA content in sink (A) and source (B) leaves determined by qRT-PCR (n=4). Light phase started at 6 am and ended at 10 pm.

### 3.3 Tissue-specific localization

Since the subcellular localization of NtHXK1 was successfully accomplished and delivered evidence for its association with the outer membrane of mitochondria, only the question of the tissue- or organ-specific localization remained to be resolved. Therefore, the 5'UTR of *NtHXK1* (-1384 to -21 upstream of the TSS) containing the putative promoter was inserted in front of the TSS of GFP and GUS, respectively, and introduced into tobacco plants to localize the promoter activity of *NtHXK1* (see Material and Methods 2.4.1). This time, both reporter signals were detectable indicating the correct function of the promoter sequence (compared to Giese *dissertation*, 2005).

### 3.3.1 Localization of *NtHXX1* promoter:GFP activity

Selected plants expressing the GFP reporter construct only showed green fluorescence under the fluorescence microscope in developing pollen but not in mature pollen or pollen of earlier developmental stages (Fig. 11A-11F). The microscopic analysis did not reveal any detectable fluorescence elsewhere in the remaining plant tissues of the three investigated independent lines cultivated in the greenhouse.

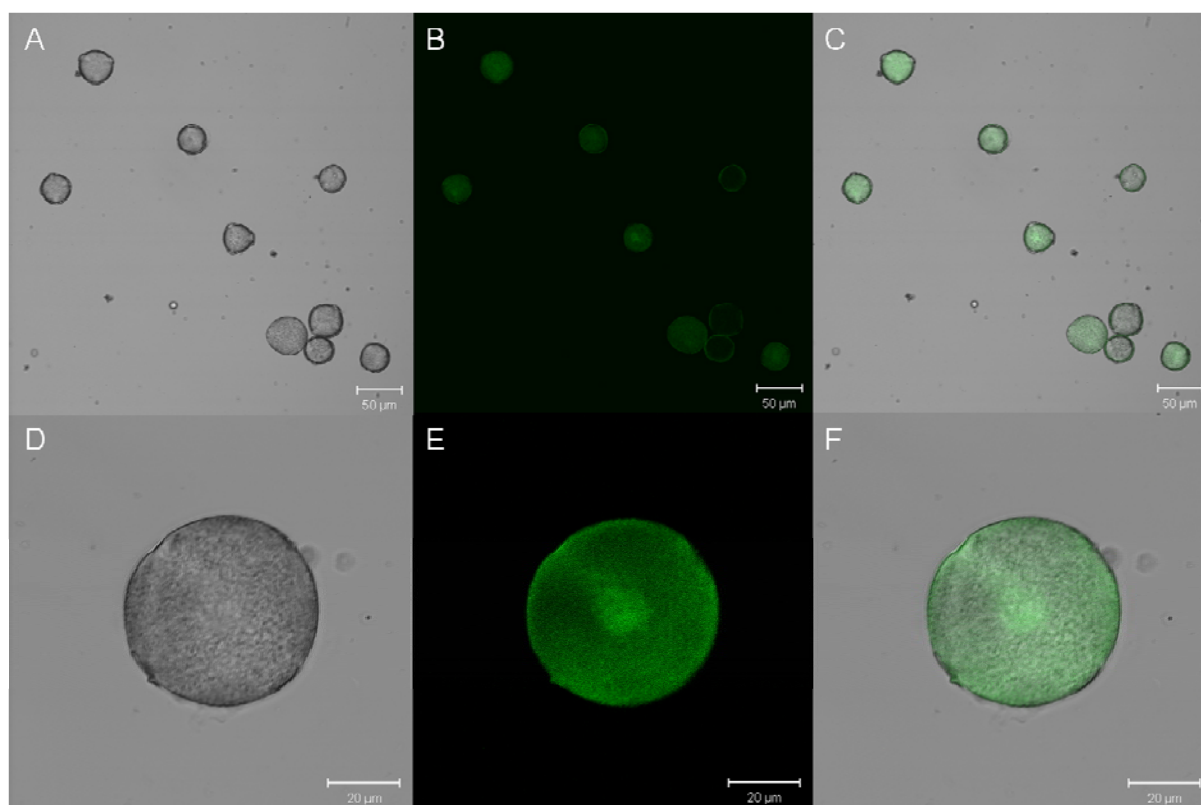


**Figure 11:** Pollen of plants expressing *NtHXX1* promoter::GFP construct.

Microscope images of pollen in two magnifications [lower A-C) and higher [D-F)]. (A) and (D) show bright field, (B) and (E) GFP fluorescence, (C) and (F) show light field and GFP fluorescence images merged.

### 3.3.2 Localization of *NtHXX1* promoter:GUS activity

Transgenic plants expressing a *NtHXX1* promoter:GUS reporter construct displayed GUS activity only in anthers/pollen (Fig. 12A and 12B) and ovaries/egg cells (Fig. 12C). No activity was detectable in early or mature stages of pollen respectively egg development. The *NtHXX1* promoter appeared to be very active in the developing reproductive system but less active in other flower parts. Since it was found by qRT-PCR that *NtHXX1* mRNA levels are comparatively high in other organs too, these results appeared contradictory but might be

explained by posttranscriptional regulation of *NtH XK1* expression independent from the promoter activity.

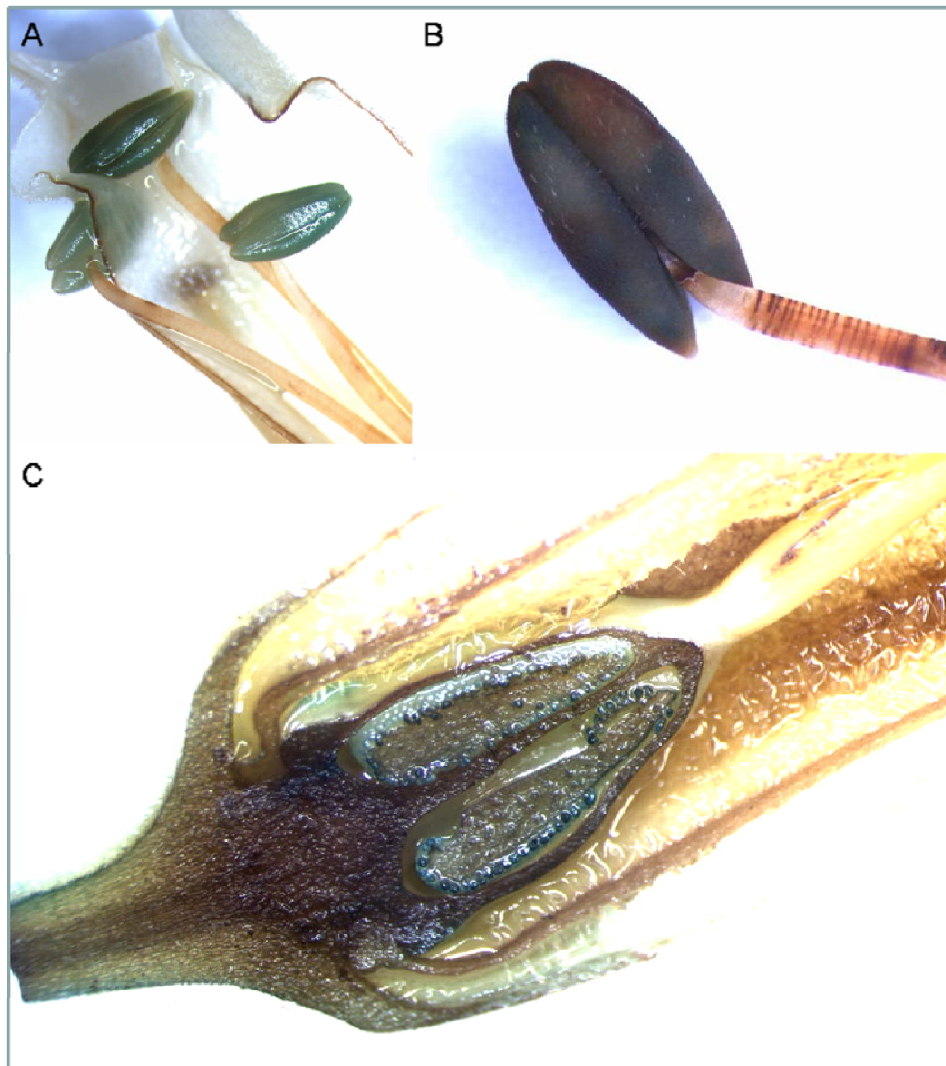


**Figure 12:** GUS activity in flower tissues of plants expressing a *NtH XK1* promoter::GUS construct. Anthers with lower (A) and 3 times higher (B) magnification. (C) Ovary with GUS activity in egg cells.

### 3.4 Functional expression of NtH XK1 in yeast

In order to confirm the hexose phosphorylation activity, the cDNA clones of all group B2 HXK's from tobacco (*NtH XK1*, *NtH XK3*, *NtH XK4*, *NtH XK5*, *NtH XK7*) were used to complement growth of the yeast triple mutant YSH7.4-3C (knockouts of *h xk1*, *h xk2*, *g l k1*) (De Winde et al. 1996; see Material and Methods 2.4.2)), which is lacking endogenous hexokinase activity. Yeast cells transformed with the empty vector pDR196 showed delayed growth on these selection media. All of the yeast cells transformed with full-length *NtH XK* cDNAs grew better on selection medium containing glucose or fructose as the sole carbon source (Fig.13A and 13B), showing that all examined *NtH XK*s complement glucose

phosphorylation activity in the yeast mutant and fructose phosphorylation activity as well. Yeast cells expressing NtHXX5 showed the strongest growth with supplemented glucose or fructose.

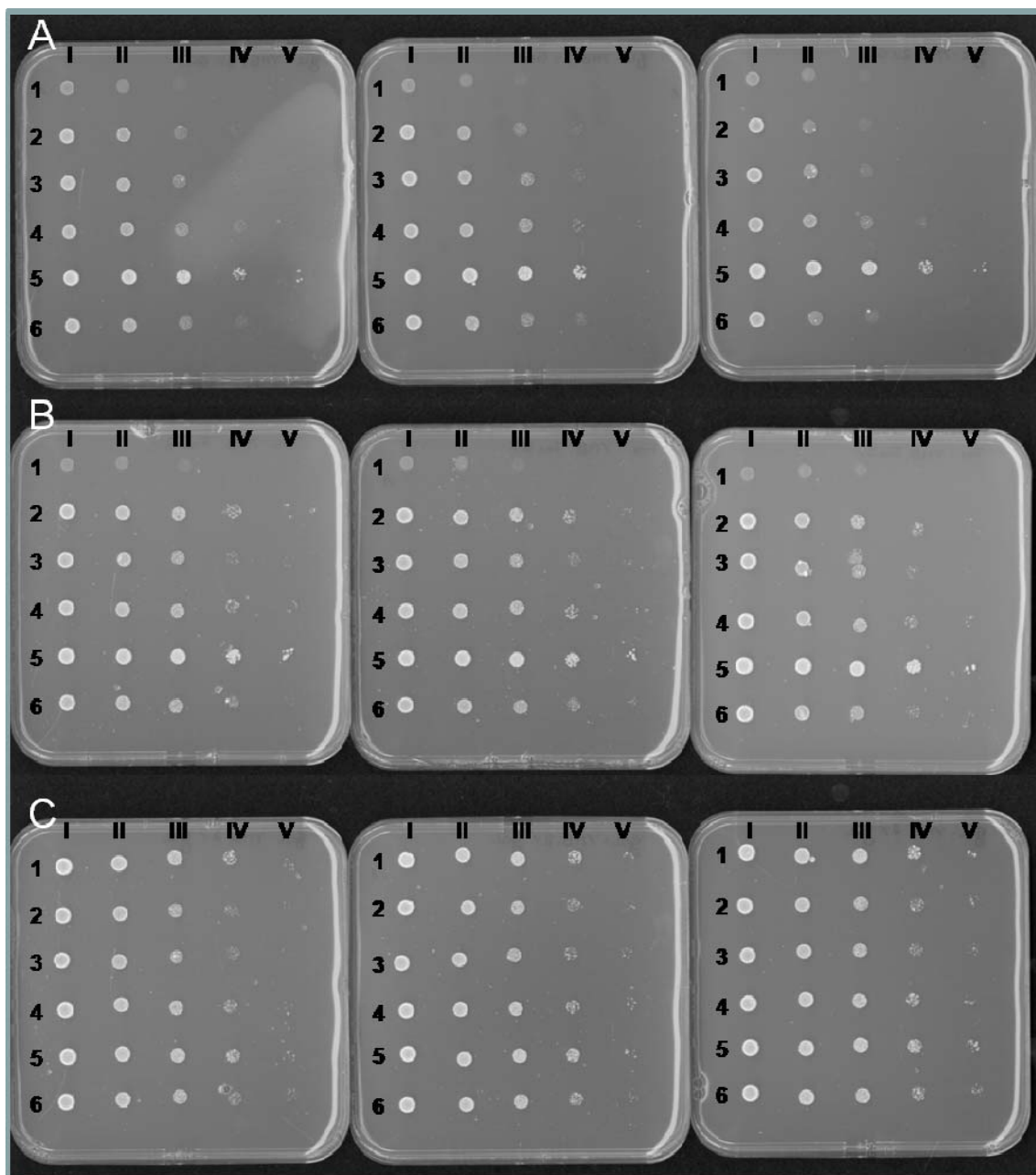


**Figure 13:** Growth complementation of the hexokinase-deficient yeast triple mutant YSH7.4-3C with the empty vector pDR196 (first row), or pDR196 harbouring *NtHXX1* (second row), *NtHXX3* (third row), *NtHXX4* (fourth row), *NtHXX5* (fifth row), *NtHXX7* (sixth row). The transformed colonies were spotted and grown on a medium containing 2% D-glucose (A), D-fructose (B) or galactose (C) as the sole carbon source and grown for 4 days at 30°C. 10 µl of a dilution series from OD<sub>600</sub> of 1 (I), 10<sup>-1</sup> (II), 10<sup>-2</sup> (III), 10<sup>-3</sup> (IV) and 10<sup>-4</sup> (V) of the cell suspension (left to right) was used. Three replicates are shown.

### **3.5 Generation of transgenic tobacco plants with constitutively decreased expression of *NtH XK1***

In order to study the functional role of NtH XK1 *in vivo* a reverse genetics approach was conducted. Transgenic tobacco plants with suppressed *NtH XK1* expression were generated using an RNAi strategy. To this end, a 728 bp fragment of the NtH XK1 ORF (-90 to -819 downstream of TSS) was amplified by PCR with the primers NtH XK1\_RNAi\_FP and NtH XK1\_RNAi\_RP, cloned into the gateway entry vector pENTR and further transferred to the RNAi destination vector Pk7GWIWG2(II) (Fig. 7; Material & Methods 2.4.4). The RNAi-cassette containing the gene-specific fragments in sense and antisense orientation and interspersed by a short sequence [chloramphenicol resistance gene (*cam*) flanked by two introns] included a 35S *CaMV* promoter. The resulting RNAi construct was subsequently introduced into tobacco plants via *Agrobacterium*-mediated gene transfer (see Material & Methods 2.5.1).

### **3.6 Analysis of transgenic lines with elevated or reduced *NtH XK1* expression**

Selection of transgenic lines showing *NtH XK1* overexpression (HXK1-10, HXK1-11 and HXK1-15; see Material and Methods 2.4.3) or *NtH XK1* suppression (HXK1-19, HXK1-24 and HXK1-64; see Material and Methods 2.4.4) was performed by protein gel blot analysis (see Material and Methods 2.9), qRT-PCR and Glc phosphorylation activity assays (see Material and Methods 2.11) on samples of fully expanded leaves, in order to confirm that these lines exhibit the desired alteration in the expression of *NtH XK1*.

#### **3.6.1 Protein detection using protein gel blot analysis**

The level of NtH XK1 protein in *NtH XK1*-silenced lines, *NtH XK1*-overexpression lines and WT were estimated by a protein gel blot and hybridization with an antibody raised against NtH XK1 (Fig. 14). Samples derived from the overexpression lines HXK1-10 and HXK1-15 showed elevated protein levels at approximately 50 kDA, whereas the samples of the silenced lines displayed either undetectable protein levels (HXK1-19), intermediate (HXK1-24) or slightly reduced (HXK1-64) protein levels relative to wild-type samples.



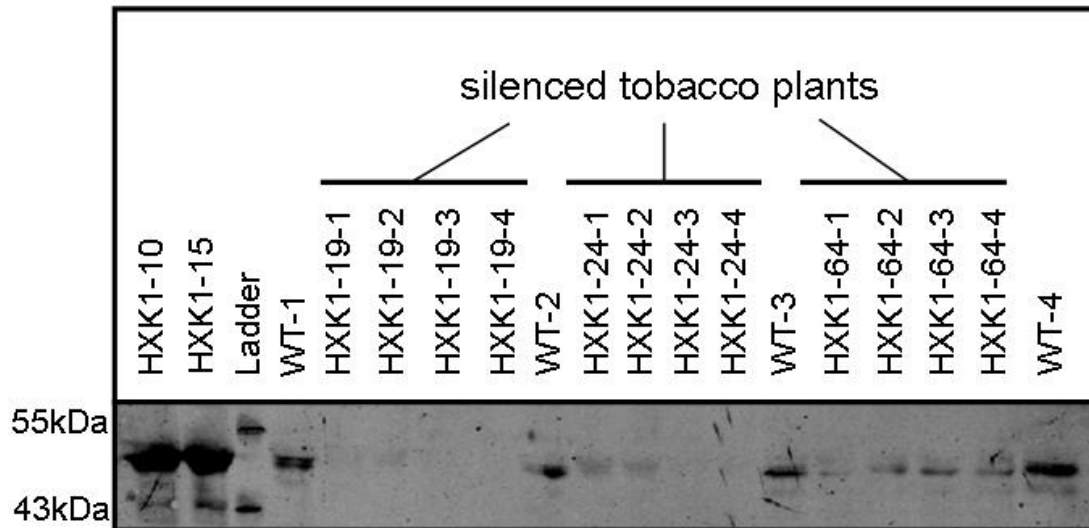


**Figure 14:** Detection of NtHKK1 protein by protein gel blot analysis. Total protein was isolated from mature leaves of the indicated transgenic lines as well as the respective wild type controls. Identical amounts of protein were separated by SDS-PAGE, transferred to a nitrocellulose membrane, and probed with a polyclonal antibody raised against NtHKK1. 55 and 43 kDa indicate the respective molecular weight according to band positions of the molecular marker.

### 3.6.2 Gene expression analysis

The determination of relative *NtHKK1* expression levels by quantitative RT-PCR was performed using either expanded leaf material (black bars; Fig. 15) or isolated mesophyll protoplasts (white bars; see Material and Methods 2.10). *NtHKK1* expression levels in protoplasts were always higher than in total leaves indicating that *NtHKK1* templates were enriched and that *NtHKK1* is preferentially expressed in mesophyll cells of tobacco leaves. The overexpression lines NtHKK1-10, NtHKK1-11 and NtHKK1-15 exhibited a strong increase in the expression of *NtHKK1* compared to the wild type (Fig.15A). *NtHKK1* expression levels in all three transgenic RNAi lines were strongly suppressed (Fig.15B), whereas HXK1-19 displayed strongest suppression, less in HXK1-24 and weakest in HXK1-64. In summary, leaf expression of *NtHKK1* was increased to 370 % in HXK1-10, 320 % in HXK1-11, 259 % in HXK1-15, but decreased to 12 % in HXK1-19, 22.5 % in HXK1-24 and 30 % in HXK1-64 relative to the wild type control.

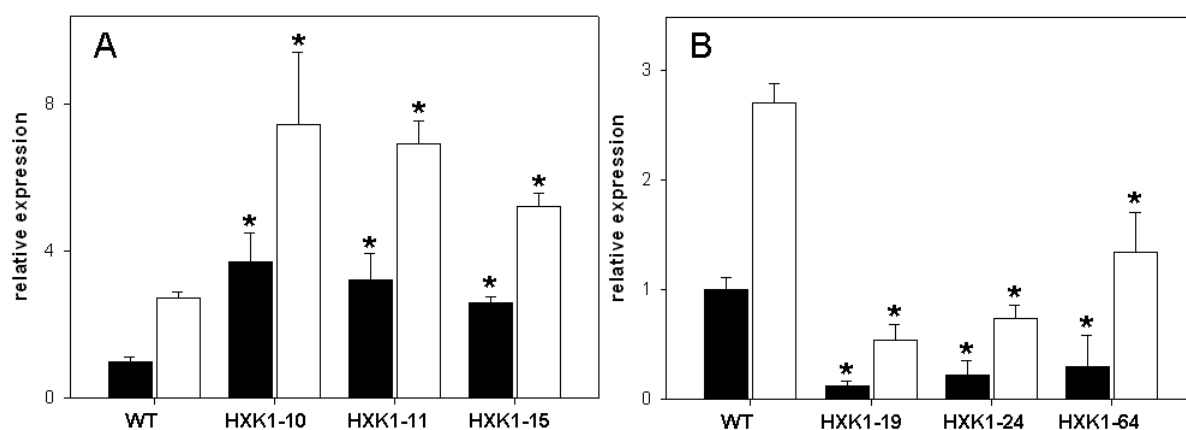


**Figure 15:** Expression analysis of A) the *NtHKK1* overexpression lines HKK1-10, HKK1-11 and HKK1-15 and B) the *NtHKK1* RNAi lines HKK1-19, HKK1-24 and HKK1-64 relative to the wild type control in total leaf (black bars) and isolated mesophyll protoplasts (white bars) by qRT-PCR (n = 4; \*: P < 0.001).

### 3.6.3 Hexokinase activity assay

The analysis of hexokinase activity, respectively Glc phosphorylation activity increased by up to 13.2-fold in the investigated overexpression lines relative to the wild type control (Fig.16A). Furthermore, the relative activity was decreased by 2.1-fold in HKK1-19, 1.8-fold in HKK1-24 and 1.1-fold in HKK1-64 (Fig. 16B). The results particularly of the RNAi lines fit suitably to the data from the qRT-PCR analysis (Fig. 15B). It is crucial to bear in mind that the HXK activity is formed by the sum of the combined activities of all expressed HXK isoforms and is not only dependent on *NtHKK1* expression exclusively.

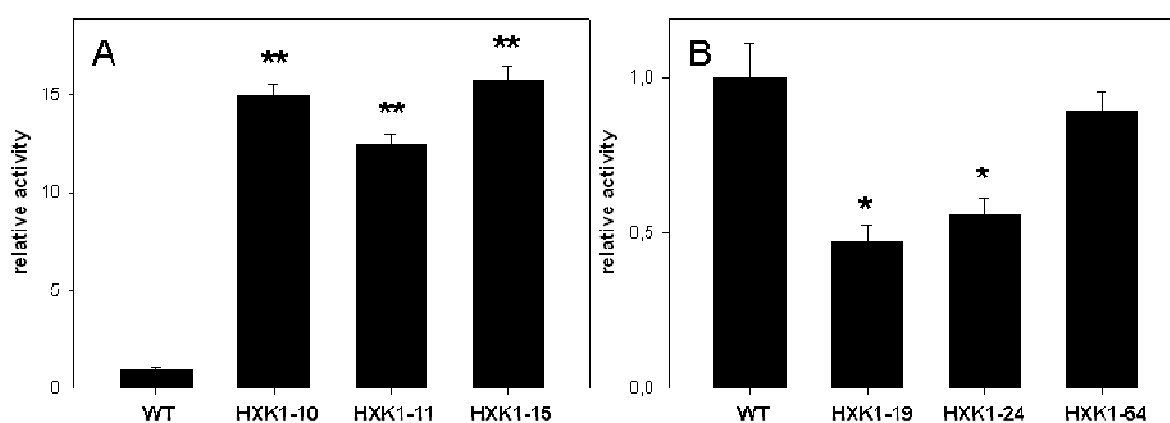


**Figure 16:** Relative glucose phosphorylation activity in (A) *NtHKK1* overexpressing and (B) *NtHKK1* RNAi lines in comparison to the wild type. Values are means of 5 individual replicates (source leaf samples)  $\pm$  SD. \*: P < 0.05 and \*\*: P < 0.0001.

### 3.7 Expression of active NtH XK isoforms in a selected *NtH XK1* RNAi line

In order to investigate the effect of *NtH XK1* silencing on the expression of the remaining catalytic active NtH XK isoforms a qRT-PCR was performed with specific primers for the genes of the catalytic active isoforms NtH XK1, NtH XK2, NtH XK3, NtH XK4, NtH XK5 as well as NtH XK7 using RNA extracts from mature leaves of the *NtH XK1* suppressed line HXK1-19 and the wild type control (Fig. 17). Simultaneous with the suppression of *NtH XK1* (13% of wild type expression) the expression of *NtH XK3* was found to be decreased (13%), most likely due to the high sequence homology (88.3 %, Fig.5). As suspected, both transcripts are targeted by RNAi in the transgenic lines. A slight increase of *NtH XK2* transcripts (135%) and a small decrease in *NtH XK5* expression (61%) were observed which might be due to physiological changes within the silenced plants rather than by a direct influence of the RNAi transcripts. The expression levels of *NtH XK4* and *NtH XK7*, which are only found in traces in leaves, were reduced down to 64% and 48% of the wild type control, respectively.

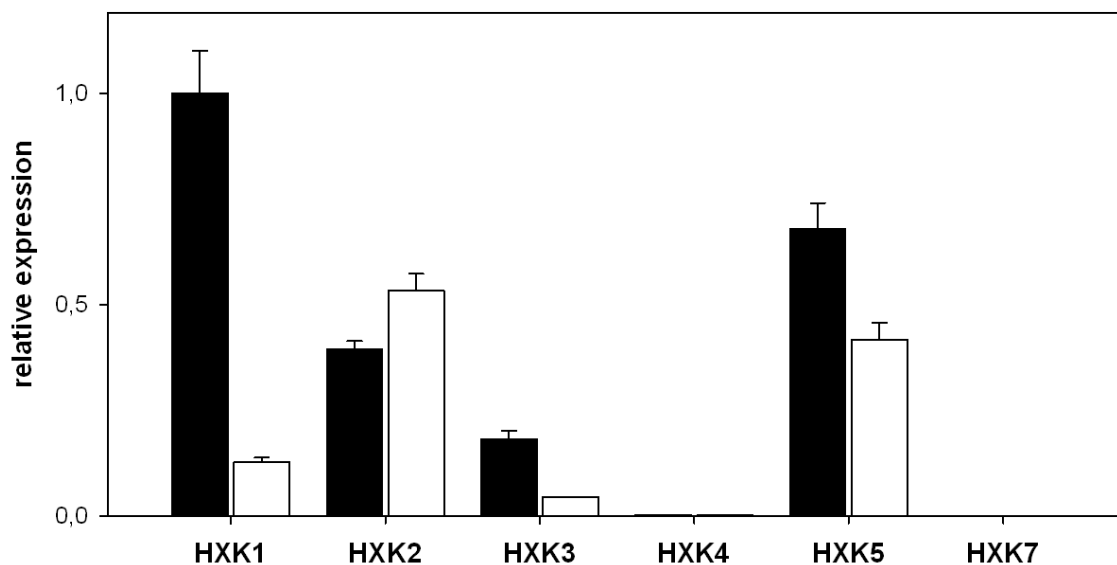


**Figure 17;** Quantitative RT-PCR for gene expression analyses of the catalytic active NtH XK isoforms. Plants were grown for 8 weeks in the greenhouse for subsequent RNA extraction from mature leaves from wild type (black bars) and HXK1-19 (white bars) plants. Bars indicate means  $\pm$  SD; n = 4).

### 3.8 Physiological characterization of *NtH XK1* RNAi lines

#### 3.8.1 Phenotypic analysis

Silencing of *NtH XK1* affected plant growth and development massively (Figure 18). Plants from the selected RNAi lines HXK1-19, HXK1-24 and HXK1-64 as well as the wild

type were grown in the greenhouse (see Material and Methods 2.1.1). Images were taken 2-3 weeks (Fig. 18A), 5-6 weeks (Fig. 18B) and 9-10 weeks (Fig. 18C) after germination. According to the level of *HXK* gene suppression plants, the silenced line HXK1-19 showed severe growth retardation, while plants of line HXK1-24 exhibited milder inhibition in growth as well as development and plants of line HXK1-64 displayed no difference in comparison to the wild type control. Furthermore, the growth defects were accompanied by extensive leaf bleaching in plants of the line HXK1-19, diffusely bleached leaves on plants of line HXK1-24, stunted leaf shapes (Fig. 19) as well as a delay in fluorescence, reduction/arrest in leaf size, in flower development, capsule size and seed number (observations not documented).

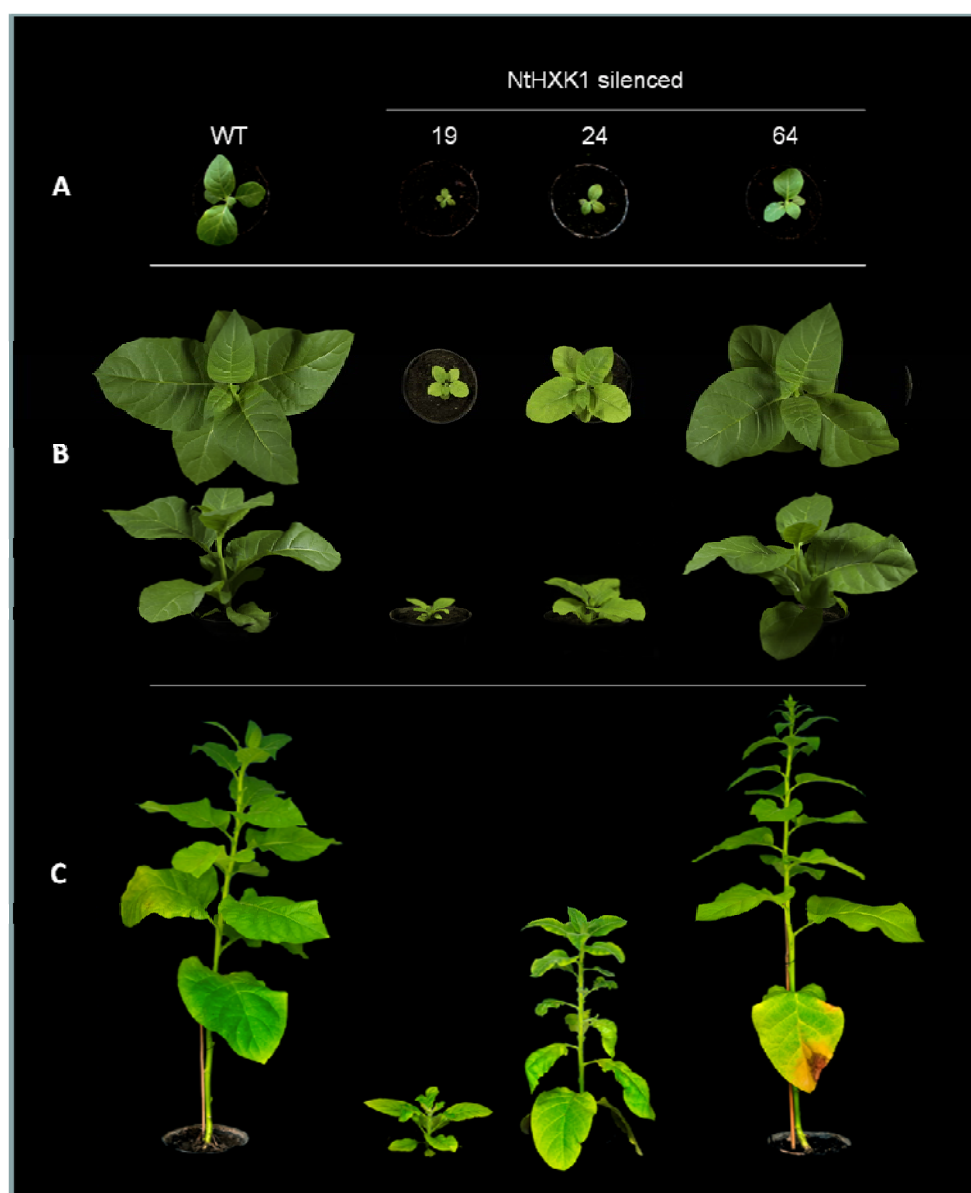


**Figure 18:** Growth of untransformed wild type plants and three transgenic lines (T2 generation) of HXK1-19, HXK1-24 and HXK1-64 for 16-19 days (A), 38-42 days (B) or 64-68 days (C) old plants, from left to right: WT, HXK1-19, HXK1-24 and HXK1-64. Plants were grown at  $250 \mu\text{mol m}^{-2} \text{s}^{-1}$  and a 16/8 h light/dark-cycle in a greenhouse.



**Figure 19:** Close up of plants from A) wild type (7 weeks), B) line HXK1-19 (9-10 weeks) and C) line HXK1-24 (9-10 weeks). Transgenic plants exhibit chlorosis of mature source leaves and deformation of developing sink leaves.

### 3.8.2 Ultrastructural analysis of HXK1-deficient tobacco plants

Electron microscopy was used to analyze changes in leaf tissue structure of transgenic plants with impaired NtHKK activity. To avoid starch accumulation in leaves, plants were kept for 24 hours in the dark prior to sample preparation for microscopy. Leaves of *NtHKK1*-silenced plants showed different defects in chloroplast structure. In sink leaves of both wild type and NtHKK1-19 plants, the overall organization of the cell structure was retained (Fig. 20A, B, E and F) with intact grana stacks (Fig. 20I, J, M and N). The only visible difference was the number of starch bodies that was enhanced in the sink leaves of silenced *NtHKK1* plants (Fig. 20J) compared to those of wild type leaves (Fig. 20I). However, in source leaves of the transgenic line NtHKK1-19 the organization of mesophyll cells was altered, as palisade parenchyma cells were more stretched and chloroplasts were disorganized and largely degraded (Fig. 20C, D and 20G, H). Magnification of cell structures showed that chloroplasts of wild type plants were characterized by intact grana stacks (Fig. 20-O), while chloroplasts in source leaves of silenced *NtHKK1* plants displayed features of partial degradation such as an

increase in the number of plastoglobuli and loosening of the thylakoid and grana stack organisation (Fig. 20P, 20L).

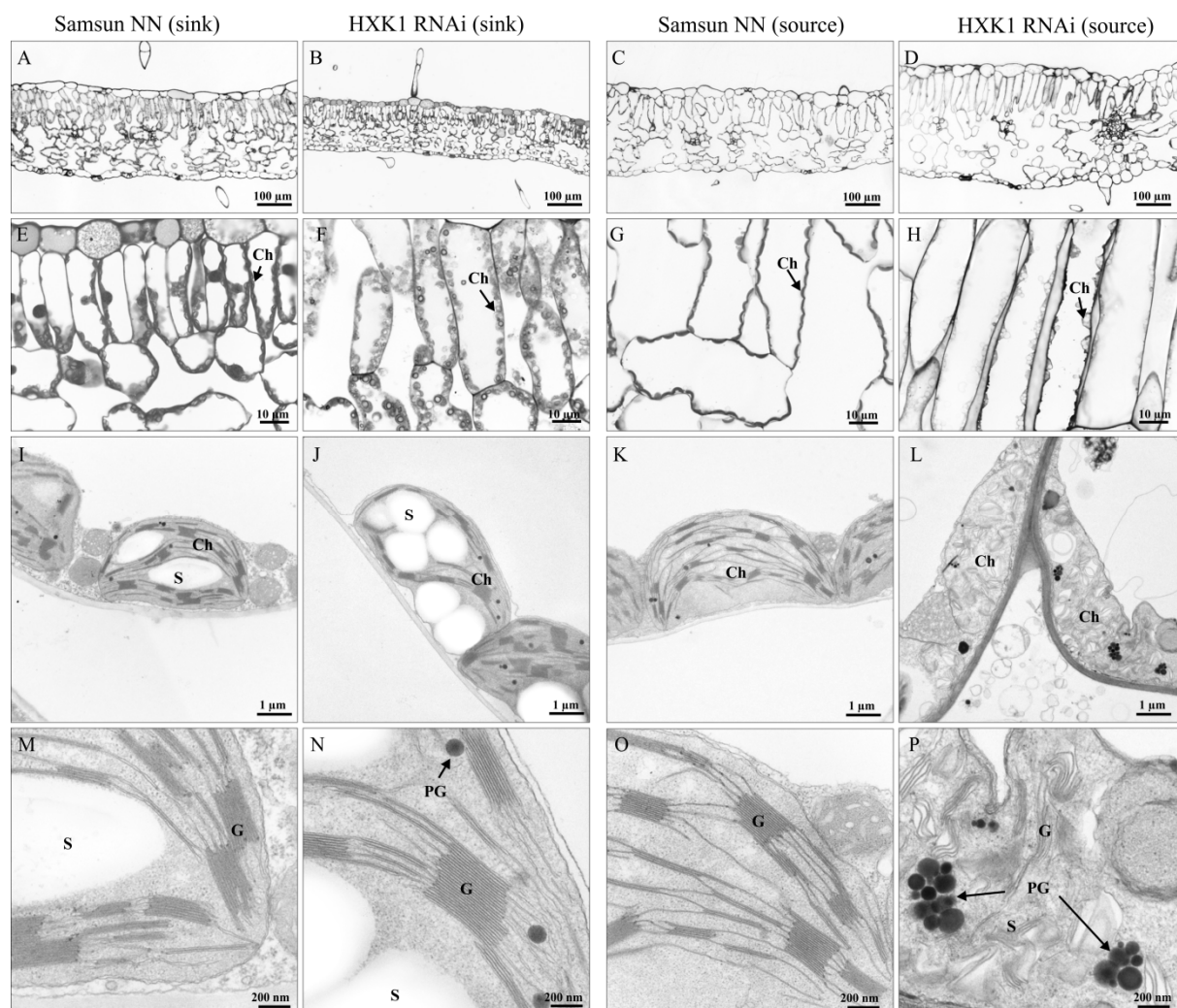


**Figure 20:** Light and transmission electron microscopy of leaf cross sections.

Histological (A-H) and ultrastructural analysis (I-P). Wild-type sink (A, E, I and M) and source leaf (C, G, K and O). *NtHXK1* sink (B, F, J and N) and source leaf (D, H, L and P). Leaf samples were prepared for microscopy analysis from plants grown in a greenhouse at ambient conditions with an average light intensity of  $250 \mu\text{mol m}^{-2} \text{s}^{-1}$  and exposed to an extended dark period of 24 hours. Ch, chloroplast; G, grana; PG, plastoglobuli; S, starch.

### 3.8.3 Photosynthesis, chlorophyll content and respiration

Tobacco plants with different levels of *NtHXK1* expression were grown for 8-10 weeks after germination on soil under ambient conditions in a greenhouse. Measurement of the net  $\text{CO}_2$  fixation rate per photosynthetic active photon flux density (PPFD, light response curve; see Material and Methods 2.12) was executed on the youngest fully expanded leaves, corresponding to the 6<sup>th</sup> leaf from the bottom of the plants (Fig. 21A). As illustrated in the

Figure 21, the net CO<sub>2</sub> uptake was inhibited in *NtHXX1*-silenced plants. While wild type plants exhibited maximal photosynthetic rates of 15  $\mu\text{mol CO}_2 \text{ m}^{-2} \text{ s}^{-1}$  in average, plants with an excessive reduction in NtHXX1 activity (HXX1-19) showed only a maximal photosynthetic rate of about 3.7  $\mu\text{mol CO}_2 \text{ m}^{-2} \text{ s}^{-1}$ . A strong decrease in photosynthetic activity was also observed in transgenic plants with a moderate reduction in NtHXX1 activity (HXX1-24). On the contrary, transgenic plants with a small reduction in NtHXX1 activity (HXX1-64) had a maximal photosynthetic rate of 12  $\mu\text{mol CO}_2 \text{ m}^{-2} \text{ s}^{-1}$  at high light intensities, and thus only slightly but significantly lower than that of the wild type (Fig. 21A). Low CO<sub>2</sub> assimilation was accompanied with decreased chlorophyll concentrations (Fig. 21B). Plants of lines HXX1-19 and HXX1-24 displayed a decrease in total chlorophyll concentration by 79% and 66%, respectively (Fig. 21B). The dark respiration rate as calculated from a non-linear curve-fitting was reduced in HXX1-19, HXX1-24 and HXX1-64 plants to 0.39; 0.45; 0.50  $\mu\text{mol m}^{-2} \text{ s}^{-1}$  respectively in comparison to the dark respiration rate of  $0.66 \pm 0.14$  in leaves of the wild type control (Fig. 21C).

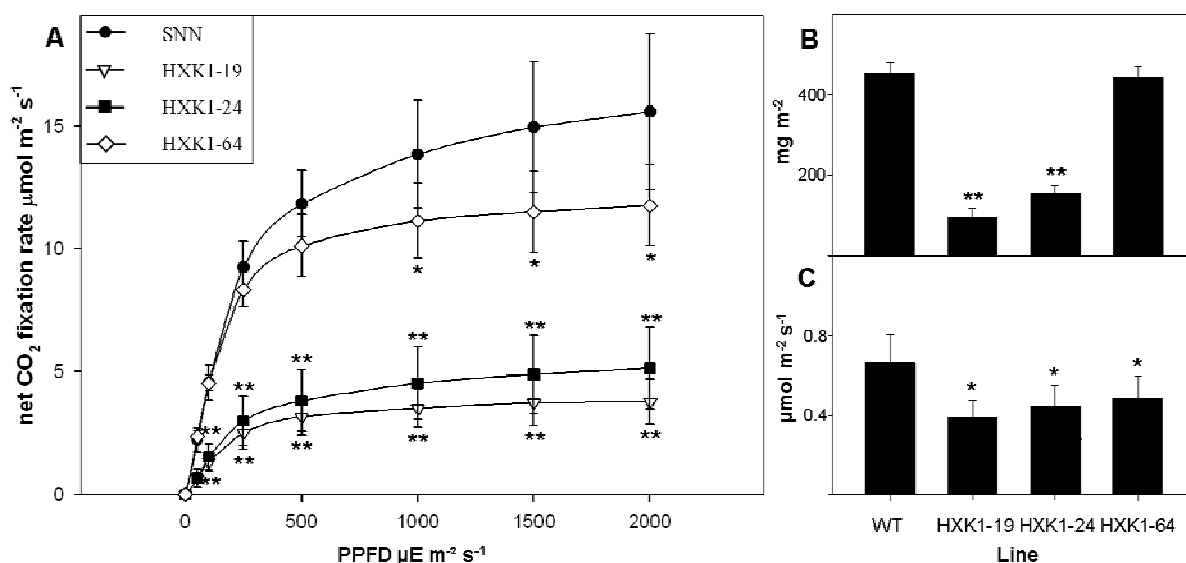


**Figure 21:** Photosynthetic activity, chlorophyll content and respiration rates in WT and the *NtHXX1* RNAi lines (A) Net CO<sub>2</sub> uptake rates measured in the youngest fully expanded leaves at Photosynthetic Photon Flux Density (PPFD) values between 20 and 2000  $\mu\text{mol m}^{-2} \text{ s}^{-1}$  and 400 ppm CO<sub>2</sub>. Values are means of 16-20 biological replicates  $\pm$  SD. (B) Concentration of total chlorophyll and (C) the rate of respiration in the dark in leaves of wild type and transgenic plants with various degrees of *NtHXX1* inhibition. Values are means of 12 (chlorophyll) and 16 (respiration) biological replicates  $\pm$  SD\*:  $P < 0.05$  and \*\*:  $P < 0.0001$ .



### 3.8.4 Carbon-to-nitrogen ratio

Organic matter is composed of considerable amounts of the element carbon together with smaller amounts of nitrogen. The ratio of the mass of carbon to the mass of nitrogen in a plant organ or the whole plant is generally referred to as the C:N ratio and used as an indicator of the C or N nutritional status. C compounds include carbohydrates and structural building blocks for example in the cell wall. N compounds are either inorganic like ammonium and nitrate or organic like amino acids. The C/N balance needs to be tightly coordinated within plants and other cellular organisms to ensure optimal growth and development (Zheng, 2009). The determination of carbon and nitrogen by elemental analysis (see Material and Methods 2.14) was applied to dry leaf material from the lines HXK1-19, HXK1-24, HXK1-64 as well as from the wild type (Fig. 22). The C:N ratio altered from 6.8:1 in the wild type control to 21.9:1 and 19.3:1 in the transgenic lines HXK1-19 and HXK1-24, respectively. The ratio in the line HXK1-64 was with 6.9:1 comparable to the wild type.

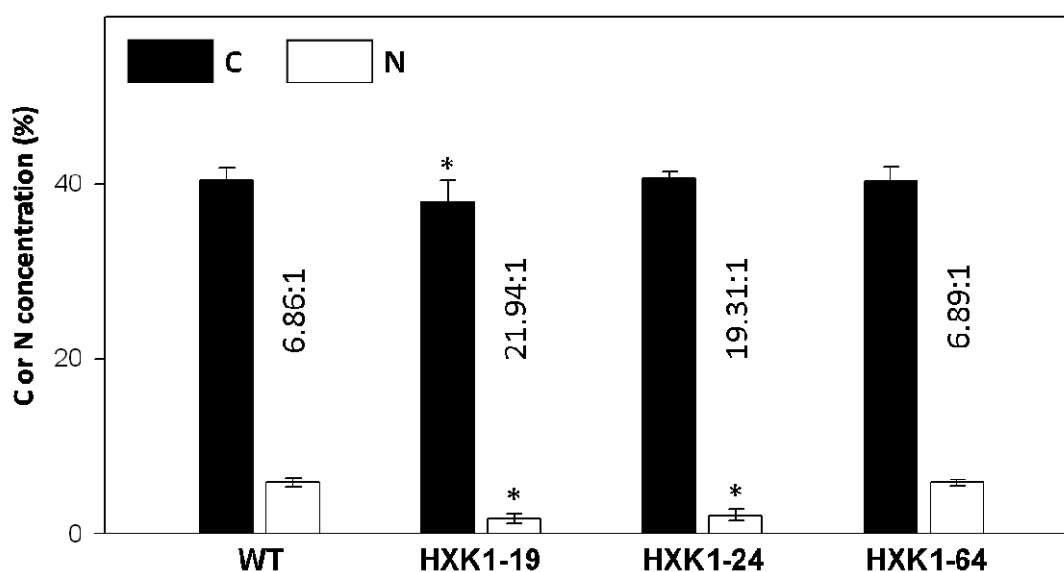


**Figure 22:** Carbon and nitrogen concentrations in leaves of WT, HXK1-19, HXK1-24 or HXK1-64 as determined by an elemental analyzer. The corresponding ratios are included into the graph. Values are means of 20 biological replicates  $\pm$  SD. \*:  $P < 0.05$

### 3.8.5 Qualitative determination of starch in leaves

In order to validate the measured accumulation of starch in the leaves of *NtHXK1* RNAi plants, leaves were stained by iodine after a prolonged dark period (24 h) subsequent to 12 h of illumination (Fig. 23). In leaves of control plants starch was almost completely depleted after 24 h of dark treatment, whereas in leaves of transgenic plants with strong and



moderate inhibition of NtH XK1 activity, starch accumulated in source and sink leaves of line H XK1-19 and in source and intermediate leaves of line H XK1-24 (Fig. 23). In leaves of plants with minor *NtH XK1* suppression (H XK1-64) weak staining was only visible in tips of fully expanded leaves. In addition, transgenic plants with strong or moderate inhibition of NtH XK1 activity were characterized by an increased number of leaves (40 leaves) which were considerably smaller in size compared to the leaves of wild type or transgenic plants with the weakest reduction in NtH XK1 activity (H XK1-64 with 26 leaves).

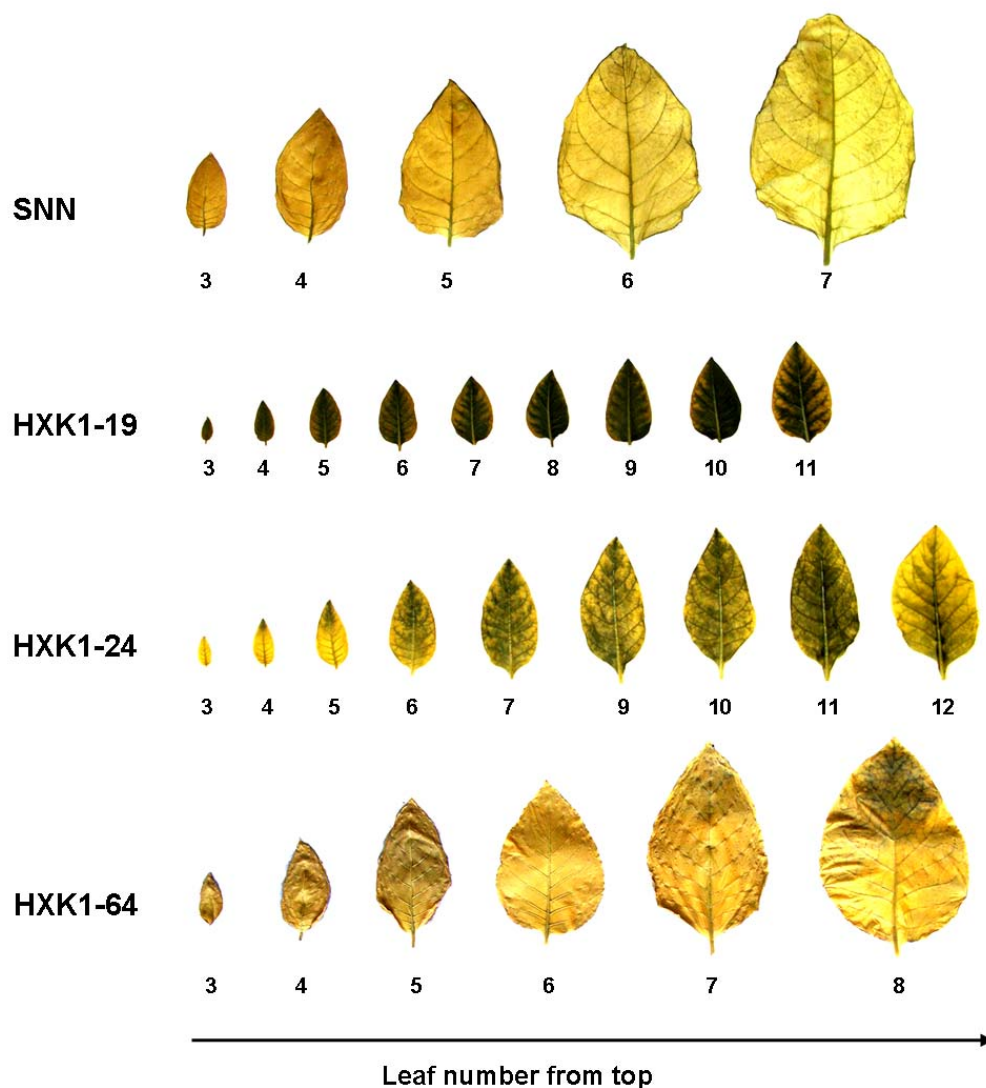


**Figure 23:** Visualization of starch in leaves of *NtH XK1* RNAi and wild type plants. After a 12 h light period plants were kept for 24 h in darkness. Leaves were bleached with ethanol and then stained with Lugol's solution (Material and Methods 2.15).

### 3.8.6 Determination of insoluble sugars during a day cycle

In order to investigate the impact of *NtHKK1* suppression on starch levels in leaves during the course of day, samples from fully expanded leaves of 8-10 week old plants were collected every two hours from the beginning of the light period (6 am) to its end (10 pm) and starch concentrations were measured (see Material and Methods 2.15). In the wild type, starch was only marginally detectable at the end of the dark period/the beginning of the light period and was then continuously increasing till midday, holding a similar level till the end of the day (Fig. 24). The starch concentration in leaves of plants with weak *NtHKK1* suppression (HKK1-64) was already starting off at a higher level than in the wild type and was increasing steadily during the whole light period. The starch level after midday was similar in wild type and HKK1-64. In leaves of plants with intermediate suppression of *NtHKK1* (HKK1-24) starch was found to be higher at the beginning of the light period than in the wild type at the end of the day. The starch level was decreasing slightly during the course of the day in HKK1-24 but was always above the levels of the wild type control. In sharp contrast to the wild type, plants with strong suppression of *NtHKK1* transcripts (HKK1-19) displayed an extreme accumulation of starch in the leaves at the end of the night that slightly decreased during the light period. In summary, starch accumulation particularly at the end of the dark period respectively at the beginning of the light period was increased according to the level of *NtHKK1* transcript suppression and the reduction NtHKK activity.

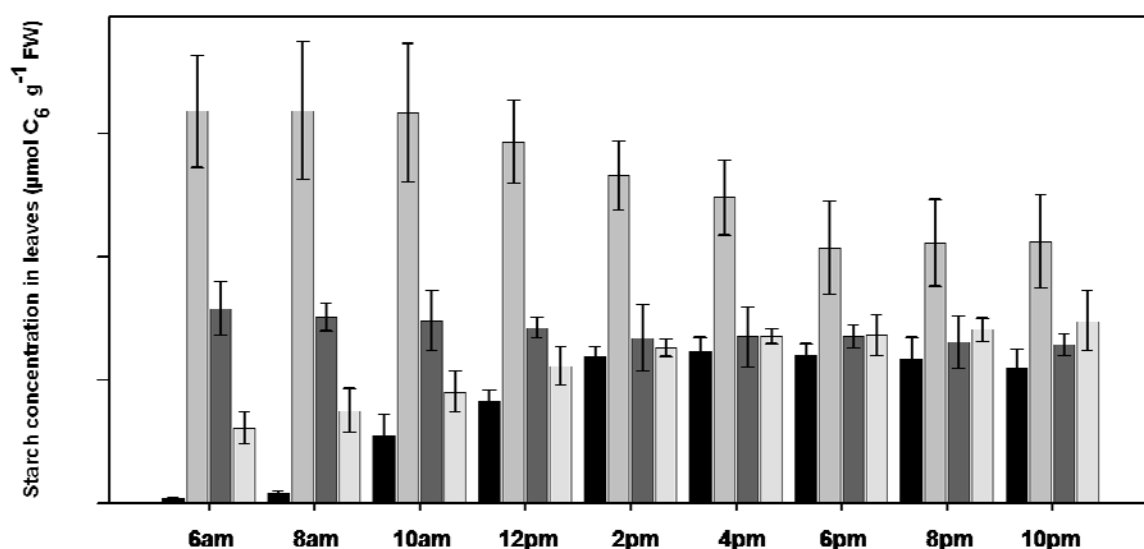


**Figure 24:** Changes in starch concentrations during the course of the day. Samples from wildtype (black), HKK1-64 (grey), HKK1-24 (dark grey) and HKK1-19 (light grey) were analysed. Values are means of 5 individual biological replicates  $\pm$  SD. \*:  $P < 0.05$ , \*\*:  $P < 0.005$  and \*\*\*:  $P < 0.0001$ .

### 3.8.7 Determination of sugar concentrations in leaves

The concentrations of the soluble sugars including Glc, Fru, Suc and Mal were determined (see Material and Methods 2.15) from comparable leaf material (source leaves from 8 week old plants) used for starch measurements and harvested at midday (see 3.8.6, Fig. 25). A significant increase in glucose and fructose concentrations was observed in all transgenic lines, which coincided with *NtH XK1* transcript levels. Compared to the concentrations in wild type leaves, Glc concentrations increased by 43-fold, 22-fold and 7-fold (Fig. 25A) and Fru concentrations by 28-fold, 11-fold and 7-fold (Fig. 25B) in the transgenic lines NtH XK1-19, NtH XK1-24 and NtH XK1-64, respectively.

Furthermore, an accumulation of sucrose (Suc) and maltose (Mal) was detected in plants with strong and intermediate reduction of *NtH XK1* transcript levels. Suc was found to be 9 times and 4 times (Fig. 25C) higher while Mal was 2830 times and 1074 times higher (Fig. 25D) in source leaves of H XK1-19 and H XK1-24 plants, respectively, than in wild type plants.

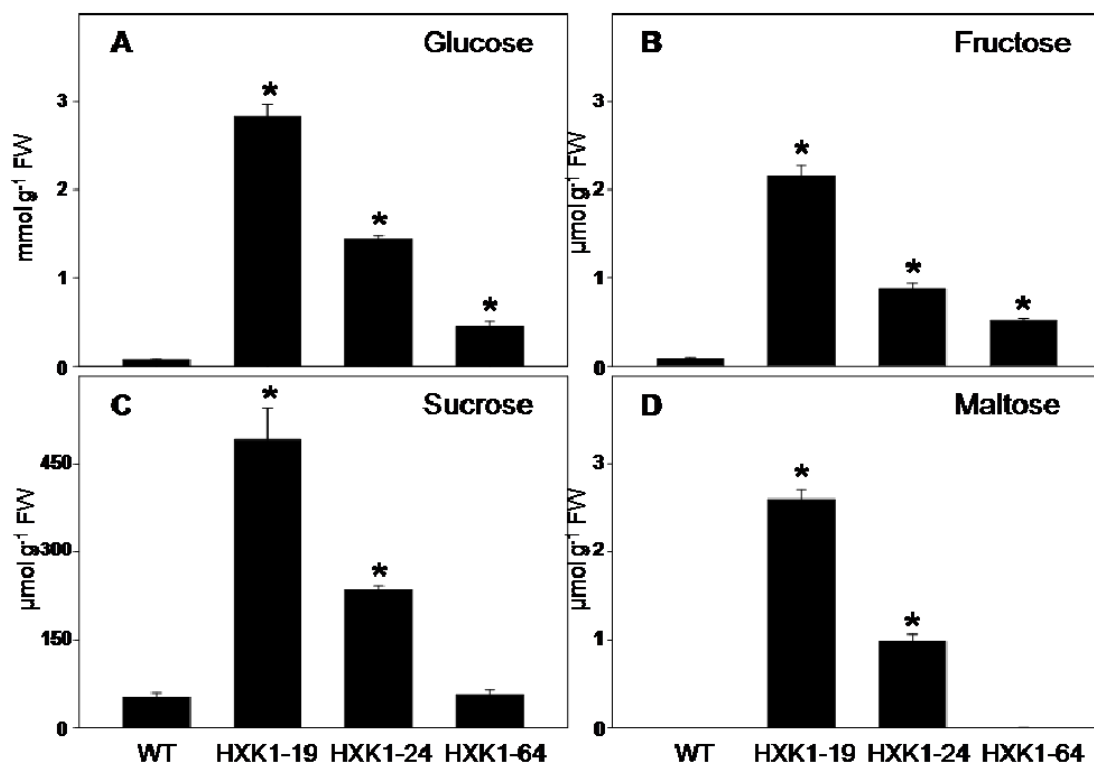


**Figure 25:** Soluble sugars, glucose, fructose and maltose concentrations in fully expanded leaf samples of wild type and *NtH XK1*-silenced plants grown in a greenhouse at ambient light conditions with an average irradiance of  $250 \mu\text{mol m}^{-2} \text{s}^{-1}$  (A: glucose; B: fructose; C: sucrose and D: maltose). Values are means of 5 individual biological replicates  $\pm$  SD. \*:  $P < 0.05$

### 3.8.8 Metabolite profiling

The results of the above experiments pointed towards severe alterations in the carbon metabolism of the *NtHXK1*-suppressed RNAi lines. In order to investigate these changes in detail a targeted LC-MS based metabolite profiling (see Material and Methods 2.17) was performed with mature leaves of *NtHXK1* RNAi (HXK1-19, HXK1-24 and HXK1-64), three independent *NtHXK1* overexpression lines (HXK1-10, HXK1-11 and HXK1-15) as well as the wild type control (Tab. 2). Samples were harvested from plants of similar developmental stage (before formation of inflorescence, from approximately 8-9 week old plants in WT, HXK1-64 and the overexpression lines) at midday (about 6 h into the photoperiod). We could not harvest leaf material from strongly inhibited *NtHXK1* plants (HXK1-19 and HXK1-24) at the same developmental age due to the slowdown in growth. This might be the cause of few discrepancies in the results of these lines. Nevertheless, the metabolite profiling revealed an increase of Suc6P in the RNAi lines HXK1-19 (2.8-fold) and HXK1-24 (2.3-fold) in contrast to a decrease of Suc6P in the overexpression lines (up to 2.6-fold) compared to the wild type. An increase of Suc6P was accompanied by an overall Suc accumulation in leaves of *NtHXK1* silenced plants (Fig. 25C). The results also showed increased levels of Tre6P especially in HXK1-19 (5.5-fold) compared to the control (Table 3). Additionally, an increased concentration of ADP-Glc was found in leaves of the *NtHXK1* suppressed lines HXK1-19 (3.6-fold) and HXK1-24 (1.3-fold) compared to the wild type. Furthermore, decreased levels were detected for the nucleotides ADP, ATP, UDP and UTP, the nucleotide sugar UDP-Glc as well as of the glycolytic intermediates 3PGA (to 43-fold in HXK1-19) and PEP (to 15-fold in HXK1-19) in all RNAi lines, which again coincided with the level of *NtHXK1* suppression.

nmol / g FW	Wildtype	HXK19	HXK24	HXK64	HXK10	HXK11	HXK15
<i>Nucleotides</i>							
ADP	3.72 ± 0.3	0.70 ± 0.01	0.92 ± 0.05	3.11 ± 0.7	2.73 ± 0.3	2.83 ± 0.5	2.82 ± 0.6
ATP	11.1 ± 1.9	n.d.	3.46 ± 0.5	5.56 ± 1.5	4.11 ± 1.0	4.76 ± 1.2	4.28 ± 1.2
UDP	2.02 ± 0.4	0.35 ± 0.08	1.68 ± 0.3	0.78 ± 0.1	1.38 ± 0.2	1.87 ± 0.2	1.25 ± 0.1
UTP	3.24 ± 0.2	0.03 ± 0.01	2.42 ± 0.5	0.88 ± 0.1	1.39 ± 0.3	2.02 ± 0.2	1.38 ± 0.2
<i>Nucleotide sugars</i>							
ADP-Glc	3.43 ± 0.5	12.4 ± 1.1	4.32 ± 0.2	2.10 ± 0.3	0.25 ± 0.2	3.43 ± 0.3	1.42 ± 0.7
UDP-Glc	86.3 ± 12	38.4 ± 4.4	94.2 ± 4.0	29.4 ± 4.0	61.8 ± 12	77.6 ± 8.6	77.7 ± 3.8
<i>Sugar phosphates</i>							
Glc-6-P	57.8 ± 3.8	28.4 ± 5.8	79.3 ± 16	46.5 ± 7.2	62.0 ± 13	85.2 ± 7.0	75.2 ± 6.5
Fru1,6bisP	7.2 ± 1.2	3.66 ± 0.7	4.53 ± 0.8	3.03 ± 0.6	3.61 ± 0.4	4.59 ± 0.6	3.33 ± 0.3
Sucrose-6-P	4.4 ± 0.9	12.3 ± 2.7	10.1 ± 2.2	2.98 ± 0.5	1.67 ± 0.4	2.42 ± 0.2	2.14 ± 0.4
Trehalose-6-P	0.33 ± 0.09	1.80 ± 0.3	0.17 ± 0.01	0.48 ± 0.06	0.08 ± 0.02	0.16 ± 0.06	0.10 ± 0.02
<i>Glycolysis</i>							
3PGA	1529 ± 309	35.9 ± 3.8	350 ± 46	760 ± 149	973 ± 133	1159 ± 129	830 ± 129
PEP	206 ± 23	13.3 ± 1.3	97.9 ± 10	126 ± 8.5	159 ± 20	185 ± 5.3	153 ± 11
<i>Citric acid cycle</i>							
Citrate	243 ± 91	273 ± 98	354 ± 32	298 ± 4.6	751 ± 80	849 ± 96	800 ± 61
Isocitrate	89.6 ± 11	109 ± 16	75.3 ± 8.4	42.0 ± 7.9	79.8 ± 10	110 ± 11	114 ± 16
Fumarate	379 ± 39	216 ± 20	211 ± 24	411 ± 62	220 ± 78	261 ± 65	241 ± 70
Malate	2543 ± 513	320 ± 105	1150 ± 96	5034 ± 419	2901 ± 788	4625 ± 118	3591 ± 246

**Table 3:** Metabolite levels in mature leaves of *NtHXK1* silenced and over-expressing tobacco plants. LC-MS based profiling of wild type; *NtHXK1* silenced lines (HXK19=HXK1-19, HXK24=HXK1-24 and HXK64=HXK1-64) and *NtHXK1* over-expressing lines (HXK10=HXK1-10, HXK11=HXK1-11 and HXK15=HXK1-15). Values are given as the mean of 4-5 individual biological replicates ± SD.

### 3.9 Complementation of the mutant *gin2-1* by *NtHXK1*

The *Arabidopsis* HXK1 (AtHXK1) null mutant *glucose insensitive 2-1* (*gin2-1*) became a useful tool to investigate glucose sensing functions of plant hexokinases. It displays broad growth defects, which become more intense with increased light intensity indicating a role of AtHXK1 in growth processes. On the contrary, supplementation with elevated glucose contents allows *gin2-1* to exhibit normal growth, while wild type plants are strongly impaired

in development (Moore *et al.*, 2003). In order to investigate a possible role of NtHXX1 in glucose sensing and signaling, a full-length *NtHXX1* cDNA sequence was placed under the control of the CaMV 35S promoter (see Material and Methods 2.4.3) and the resulting over-expression construct was used for transformation of the *gin2-1* mutant by floral-dip (Clough and Bent, 1998; see Material and Methods 2.5.2). Three independent homozygous lines were selected and propagated for subsequent experiments. On half-strength MS media with 6 % Glc the growth of the transgenic plants was considerably suppressed along with small cotyledon sizes and anthocyanin accumulation (Fig. 26A). Transgenic lines did not show any differences when growing on MS with 6% Man suggesting that there was no influence by osmotic pressures on the development of the mutant and transgenic lines. Furthermore, in order to investigate whether the expression of *NtHXX1* was able to compensate for the growth defect phenotype of *gin2-1*, plants of the wild type, the *gin2-1* mutant and the transgenic lines were grown under low ( $100 \mu\text{mol m}^{-2} \text{s}^{-1}$ ) and high ( $240 \mu\text{mol m}^{-2} \text{s}^{-1}$ ) light conditions (Fig. 26B). Under low light conditions these plants did not show significant differences after 18 days. On the contrary, under high light conditions only *gin2-1* plants exhibited impaired development mainly at the basal leaf rosette, whereas the transgenic *gin2-1* plants expressing *NtHXX1* were able to restore plant growth and leaf expansion comparable to the wild type control.

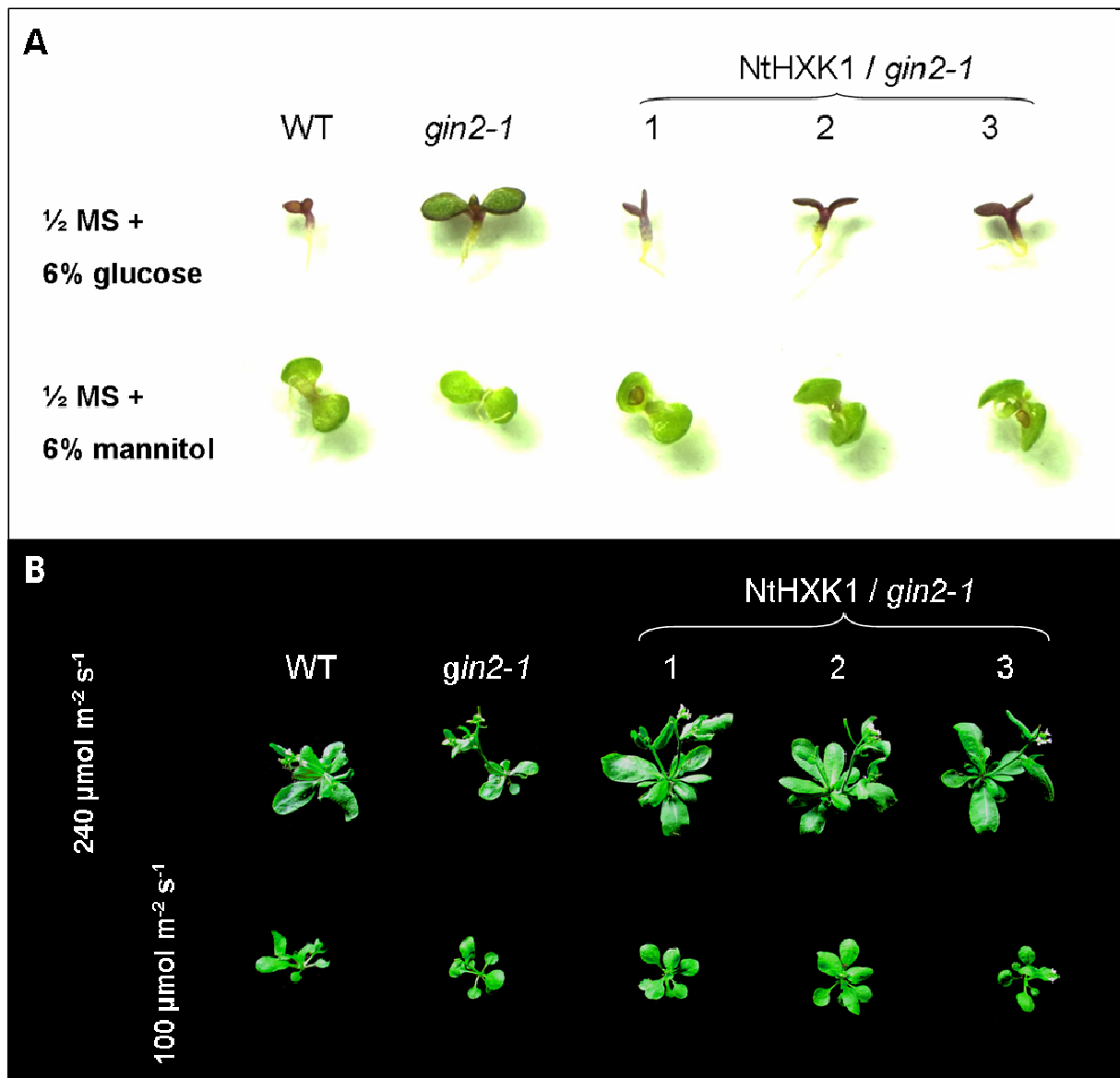


**Figure 26:** Complementation of the *Arabidopsis* glucose insensitive mutant *gin2-1* by tobacco HXK1. (A) Plants were grown on MS medium containing 6% glucose or 6% mannitol under 100  $\mu\text{mol m}^{-2} \text{s}^{-1}$  constant light for 6 days. (B) Plants were grown on soil under high light (240  $\mu\text{mol m}^{-2} \text{s}^{-1}$ ) and low light (100  $\mu\text{mol m}^{-2} \text{s}^{-1}$ ) in an 18 h/6h light/dark-cycle for 18 days.

### 3.10 Plant growth under different light conditions

Since tobacco HXK1 was able to restore AtHXK1 functions in glucose sensing and signaling in *Arabidopsis thaliana* the question whether NtHXK1 may act as a Glc sensor in tobacco as well emerged. Growth experiments on Glc supplemented media did not confirm glucose insensitivity in the *NtHXK1* suppressed lines or enhanced glucose sensitivity in *NtHXK1* overexpression lines compared to the wild type control (data not shown). In order to examine if NtHXK1 plays a similar role in growth promotion in tobacco as AtHXK1 does in *Arabidopsis*, transgenic plants with reduced *NtHXK1* expression were grown under constant

high light ( $500 \mu\text{mol m}^{-2} \text{s}^{-1}$ ) or under ambient light conditions in the greenhouse in a 16h/8h light/dark-cycle for 28 days (Fig. 27). Under constant high light the wild type plants displayed enhanced growth compared to their siblings in the greenhouse. Also plants with intermediate (HXK1-24) or weak suppression of *NtHXK1* expression (HXK1-64) showed enhanced development compared to the greenhouse equivalents (Fig. 27, upper part). In contrast, plants with strong suppression of *NtHXK1* expression revealed reduced growth in comparison to the plants grown in the greenhouse, which suggested a similar role of NtHXK1 in growth promotion as reported for AtHXK1 (Fig. 27, upper part).

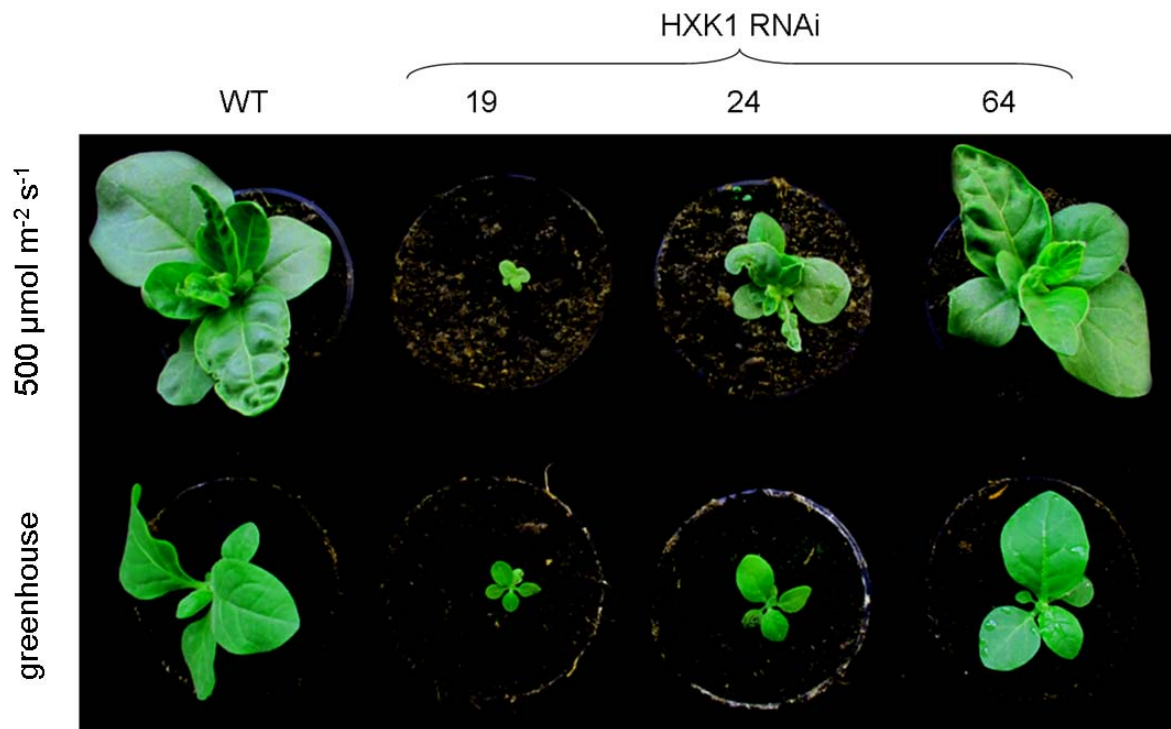


**Figure 27:** Effect of silenced *NtHXK1* expression on plant growth at different light conditions. Tobacco plants were cultivated after germination at constant high light of  $500 \mu\text{mol m}^{-2} \text{s}^{-1}$  or in ambient conditions in a greenhouse with an average irradiance of  $250 \mu\text{mol m}^{-2} \text{s}^{-1}$ .



## 4. Discussion

In the past decade the interest on hexokinase research rose with the discovery that plant hexokinases are involved in sugar perception and signalling. Nevertheless, a detailed study of the physiological role or function of individual hexokinase isoforms remained open. In the previous work of Jens-Otto Giese (*dissertation*, 2005), 9 different cDNA sequences encoding HXK proteins were identified (Tab. 1; Introduction). The subcellular localization accomplished by protein-GFP fusion constructs and immunolocalization confirmed that NtHXK1 proteins are strongly associated with mitochondria (Fig. 6). Feeding experiments, in which leaf discs were placed for 24 h on a concentrated Glc solution under the exclusion of light, resulted in decreased amounts of starch in leaves of plants overexpressing *NtHXK1* compared to the wild type control (Giese, 2005). In contrast, starch levels did not significantly change in plants overexpressing *NtHXK2* and *NtHXK3* but increased in plants overexpressing *NtHXK4*, *NtHXK5* and *NtHKL1*. These results indicated individual roles of single HXK isoforms in tobacco carbohydrate metabolism. In the present work, the expression of all tobacco HXK isoforms in different plant organs was investigated by qRT-PCR. A predominant expression of *NtHXK1* in all examined aerial parts could be observed. Furthermore, while screening and propagating tobacco RNAi plants with transcripts targeting the tobacco HXK's 1, 2, 4 and HKL1, it was observed that only plants with targeted silencing of *NtHXK1* exhibited obvious phenotypical changes (Fig. 18). Both findings led to the presumption that NtHXK1 holds a crucial physiological role in the development of tobacco plant and encouraged the investigation of its role in more detail (Kim *et al.*, 2013).

### 4.1 *NtHXK1* is expressed in all aerial organs especially during the night

The expression analysis of HXK genes in wild type tobacco via qRT-PCR revealed a predominant expression of *NtHXK1* in all examined tissues (flower, bud, source leaf, sink leaf and stem) except for roots, where *NtHXK4* turned out to be the predominant HXK isoform (Fig. 9). Interestingly, *NtHXK4* expression was only detectable in small traces in the remaining tissues suggesting a physiological function of this isoform in roots. Nevertheless, compared to other tissues *NtHXK1* was highly expressed in flowers, i.e. at 2-fold higher levels than in sink leaves and 4-fold higher levels than in source leaves. Using GFP- and GUS-constructs under control of the *NtHXK1* promoter sequence (-1384 to -21 bps upstream TSS) introduced in tobacco plants, GFP signals were detectable only in developing pollen and GUS activity in anthers and ovaries (Fig. 12). The physiological function of NtHXK1 in developing pollen and egg cells will be discussed in an upcoming paragraph. GFP emission or GUS

activity could not be detected in other organs or tissues which was quite contradictory to the results of the qRT-PCR. This might be due to the low sensitivity of these methods or due to posttranscriptional regulation of *NtH XK1* transcripts. A similar phenomenon was observed during the analysis of overexpression lines where *NtH XK1* transcript levels in leaves increased up to 3.7-fold compared to the control (HXK1-10; Fig. 15a) while the overall HXK activity increased by 12.1-fold (HXK1-10; Fig. 16a) indicating that NtH XK1 protein levels are not exclusively dependent on mRNA expression levels. Furthermore, the time-course qRT-PCR experiment with *NtH XK1* sequence-specific primers (Fig. 10) showed that *NtH XK1* is expressed higher in the dark period, peaking around 4 am (2h before the end of dark period/onset of light period) than during the light period, which was found to hold true particularly in mature source leaves (Fig. 10b). Major expression of *NtH XK1* during the dark period implies a definite function of NtH XK1 mainly during the night.

## **4.2 Transgenic plants display elevated and suppressed *NtH XK1* expression**

To further characterize the function of NtH XK1 in tobacco, transgenic plants were generated successfully by an RNAi strategy (Fig. 7; Material and Methods). Three independent lines HXK1-19, HXK1-24 and HXK1-64 with various degrees of *NtH XK1* suppression were selected for further investigation. The Western Blot analysis with NtH XK1 specific antibodies revealed a reduction of NtH XK1 protein in these RNAi lines as well as an increase in the over-expression lines HXK1-10, HXK1-11 and HXK1-15 (generated by Jens-Otto Giese, 2005) compared to the wild type control (Fig. 14). In addition, these results were confirmed by quantitative PCR with NtH XK1-specific primers on leaf material and isolated mesophyll protoplasts of the same lines (Fig. 15). In leaves, HXK1-19 displayed 12%, HXK1-24 22.5% and HXK1-64 30% of the wild type expression. Furthermore, *NtH XK1* expression levels were found to be on average 2-3 times greater in protoplast (Fig. 15) than in total leaf material suggesting its major occurrence in the mesophyll, the primary location for photosynthesis in the plant. The RNAi plants further displayed reduced Glc phosphorylation activity according to the level of *NtH XK1* suppression whereas the over-expression plants exhibited exceptionally enhanced enzyme activity (12.1-fold in HXK1-10 compared to wild type), which cannot be simply explained by the increase of *NtH XK1* expression only (3.7-fold) (Fig. 16). Further posttranscriptional modifications on transcript or protein levels are most likely required to boost up the HXK activity as observed in this case. As an example, exogenous sugars have been found to act selectively on RNA and protein stability, on translation and on post-translational modification on enzymes (Smith and Stitt, 2007).

Additionally, a qRT-PCR on leaves of line HXK1-19 with primers each active HXK isoform showed that the RNAi transcripts also target and suppress *NtHXK3* as well as *NtHXK7* expression (Fig. 17). The observed changes in the expression of the remaining isoforms are most likely the result of physiological changes within the plant rather than caused directly by the RNAi transgene.

### **4.3 Starch-excess phenotype is triggered by silencing *NtHXK1***

As described in the introduction, gene silencing became a useful tool in reverse genetics to elucidate the influence of genes on phenotype and furthermore to determine their biological functions (Gilchrist and Haughn, 2010). In the present study three individual RNAi lines with altered levels of *NtHXK1* suppression as well as distinct morphological changes could be selected for a detailed phenotypical and biochemical analysis. This enabled us to follow the effect of *NtHXK1* silencing in a more structured and comprehensive manner.

Plants with strong reduction of *NtHXK1* expression (HXK1-19) exhibited severe growth retardation after transfer to a greenhouse accompanied by leaf chlorosis and lesions (Fig. 18 and 19). Interestingly, plants with suppressed expression of *NtHXK1* down to 30% of the wild type expression level (HXK1-64) showed no obvious phenotypical changes while plants with a reduction to 22.5% of the wild type (HXK1-24) already displayed broad growth and developmental defects indicating a mandatory threshold between 22.5 and 30% *NtHXK1* expression to sustain normal plant growth and development in tobacco. Furthermore, the cutback to 12% of the wild type *NtHXK1* expression level as found in plants of HXK1-19 caused such significant consequences that a complete loss of *NtHXK1* expression (e.g. by knockout) is in all probability lethal for the tobacco plant. The TEM analysis revealed huge starch bodies incorporated in chloroplasts of sink leaves and degraded chloroplasts as well as disordered mesophyll architecture in source leaves of *NtHXK1*-silenced plants (HXK1-19) (Fig. 20). In addition, gas exchange experiments and chlorophyll measurements showed that photosynthetic activities, respiration rates and chlorophyll concentrations were reduced consistent with the degree of *NtHXK1* suppression (Fig. 21). These results are clearly due to the massive impact on chlorophyll architecture observed under the TEM.

The excessive imbalance within the C:N-ratios observed in the RNAi lines HXK1-19 and HXK1-24 in comparison to HXK1-64 and the wild type control (Fig. 22) already pointed to vast physiological changes triggered by silencing *NtHXK1*. The vast accumulation of starch leads to a severe shift towards carbon. By iodine staining of leaves after an extended dark period (Fig. 23) and measurement of starch levels during the course of a day (Fig. 24)

transgenic plants with decreased *NtHXX1* expression less than or equal to 22.5% of the level of control plants were exposed to display clear *starch-excess* (sex) phenotypes. *Starch-excess* is defined by retaining high levels of starch in photosynthetic cells at the end of the night phase, in general along with plant growth defects. Moreover, extremely elevated levels of the soluble sugars Glc, Fru, Suc and in particular Mal were found especially in the lines HXX1-19 and HXX1-24 (Fig. 25) as well as a reduction of glycolytic intermediates and nucleotides (Fig. 26). Mutants with defective genes of starch breakdown frequently exhibit sex phenotypes, due to a discrepancy between the starch synthesis rate during the day and the starch degradation rate during the night. The isolation and investigation of *starch-excess* mutants strongly contributed to identify enzymes involved in the starch degradation pathway and uncovered this pathway (Stitt *et al.*, 2010). The most pronounced sex phenotype was observed in mutants with impaired GWD (glucan water dikinase) (Yu *et al.*, 2001), explained by its key position at the beginning of the pathway. Mutations concerning steps downstream of GWD were found to produce milder sex phenotypes. In addition, some sex mutants were described to accumulate intermediates of the starch breakdown pathway. In 2009, Stettler *et al.* demonstrated that the starch-excess mutant *mex1* (*Arabidopsis* mutant of MEX1, *maltose-excess* 1, a chloroplast envelope maltose transporter; Niitylä *et al.*, 2004) displayed a chlorotic phenotype with autophagy-like chloroplast degeneration unlike other sex mutants, probably due to massive accumulation of maltose and malto-oligosaccharides. These findings are to some extent in agreement with our results. The hypothesis that NtHXX1 is the pivotal HXX isoform involved in transitory starch degradation catalyzing primarily Glc deriving from starch breakdown in the night evolved. The predominant expression of *NtHXX1* during the dark period in wild type leaves supports this hypothesis. Inhibition of *NtHXX1* leads to a holdup in starch breakdown causing a high accumulation of products respectively intermediates from it, which in turn results in a feedback inhibition of starch breakdown and the observed *starch-excess* phenotype. In contrast to the described sex mutants *NtHXX1* transcripts were only knocked down and not completely lost. Furthermore, the growth defects observed in sex mutants appear to be considerably minor compared to the present study.

#### 4.4 NtHXX1 performs as glucose sensor

The phylogenetic analysis (Figure 8) revealed that NtHXX4 (over 75 % identity with AtHXX1) and NtHXX5 (74.5 %) exhibit a closer relation to the known Glc sensors from *Arabidopsis* and rice than NtHXX1 (about 70%), NtHXX3 (70.6 %) or NtHXX7 (71.8 %) suggesting a high probability that these isoforms cover a Glc sensing function as well. Among

the tobacco HXK cDNAs, NtHXK1 is able to recover hexokinase activity in the triple knockout mutant YSH7.4-3C (*hxx1*, *hxx2* and *glk1*) (De Winde et al. 1996) and to restore functional Glc and Fru utilization (Fig. 13). However, the complementation of the AtHXK1 null mutant *gin2-1* with NtHXK1 showed that NtHXK1 is able to restore the wild type phenotype under defined conditions and replace AtHXK1 as a Glc sensor in *Arabidopsis thaliana* (Fig. 26). It was previously demonstrated that the sensing function is uncoupled from the catalytic function (Moore *et al.*, 2003; Cho *et al.*, 2009). Furthermore, the plant Glc-sensors NtHXK1 and probably OsHXK5 as well as OsHXK6 are present in nuclei, albeit in hardly detectable amounts, enabling them to interact with other nuclear proteins in order to mediate sugar sensing and signaling (Cho et al., 2006b; Cho et al., 2009a). The nuclear interaction partners of AtHXK1 *vha-B1* and *rpt5b* have been identified by yeast two-hybrid (Y2H) assays and mutants of *vha-B1* and *rpt5b* were shown to share similar phenotypes like *gin2-1*. A nuclear localization of NtHXK1 couldn't be confirmed but the major association with mitochondria does not exclude the possibility that NtHXK1 is also present within nuclei *in vivo*, too. The probability rises in the light of the fact that they all perform similarly under the same conditions. The rice Glc-sensors OsHXK5 and OsHXK6 are expressed in all examined tissues like leaf, root, flower and immature seed, which suggests that they function as Glc sensors in sink and source organs of rice plants additionally to their function in sugar metabolism as glycolytic enzymes. Interestingly, expression of AtHXK1 in tomato (*Lycopersicon esculentum*) produced plants with inhibited growth, decreased chlorophyll content and reduced photosynthetic rates, probably due to different sugar levels in tomato compared to *Arabidopsis* (Dai *et al.*, 1999). Growth experiments with *NtHXK1* RNAi plants under high and ambient light conditions revealed that NtHXK1 exerts a comparable function in growth promotion in tobacco plants as AtHXK1 realizes in *Arabidopsis* (Fig. 27). However, the existence of other Glc and sugar signaling pathways independent from the sensing function of HXKs has been revealed in the last decade, like the regulator of G-protein signalling1 (RGS1), whereas mutants of AtRGS1 exhibit Glc insensitive phenotypes (Rolland *et al.*, 2006; Chen *et al.*, 2006).

#### 4.5 Pivotal role of NtHXK1 in the transition of starch to energy

Our results lead to the conclusion that tobacco hexokinase 1 is the primary HXK isoform that phosphorylates Glc deriving from transitory starch breakdown. This allows sustaining leaf respiration and continuous sucrose synthesis. Thus, NtHXK1 takes in the role of a key link between the starch breakdown pathway and glycolysis, which cannot be

compensated by other HXK isoforms. In accordance to the upper findings and recent literature, NtHXK1 was integrated into a model (Fig. 28), which emphasizes its relevance for tobacco plants. Most discoveries and insights on transitory starch breakdown were achieved in *Arabidopsis thaliana* which is why most denotations from our model are originating from *Arabidopsis* research even though modified. Recent findings showed that the text book knowledge of starch breakdown is essentially correct but needs in-depth revision (Stitt *et al.*, 2010). Key steps in the starch breakdown pathway in leaves are most likely highly conserved within higher plants and the achieved data should be employed to elucidate recent findings from other plant species as well. As mentioned before, in leaves starch and sucrose are synthesized together as the products of photosynthetic carbon assimilation during the day. While sucrose is primarily exported to sink organs, starch is accumulated in chloroplasts. In *Arabidopsis*, approximately half of the assimilated carbon is employed in starch synthesis (Zeeman *et al.* 2005). The initial step of transitory starch degradation is executed by glucan, water dikinase (GWD) which catalyzes the transfer of  $\beta$ -phosphate from ATP to the C6 position of glucosyl residues of amylopectin (Zeeman *et al.*, 2007, Stitt *et al.*, 2010). This step is a requisite for the action of a second enzyme, phosphoglucan, water dikinase (PWD), to phosphorylate amylopectin on the C3 position of the glucosyl residues. Phosphate groups first need to be added and subsequently removed for functional starch breakdown, which is catalysed by SEX4, a phosphoglucan phosphatase, in *Arabidopsis*. The reason why this procedure is necessary still needs clarification (Zeeman *et al.*, 2007). The interaction of different amylases ( $\alpha$ - and  $\beta$ - amylases as well as isoamylase) and debranching enzymes leads to the products Mal and Glc. Mal export from chloroplasts into the cytosol is the predominant route of carbon deriving from starch breakdown as indicated by experiments with isolated chloroplasts from bean (*Phaseolus vulgaris*), spinach (*Spinacia oleraceae*) or thale cress (*Arabidopsis thaliana*) (Weise *et al.*, 2004). The export of Glc and Mal from chloroplasts to the cytosol is carried out by distinct transporters (GLT respectively MEX) (Nittylä *et al.*, 2004, Stettler *et al.*, 2009). In the cytosol, Mal is metabolized by DPE2 in *Arabidopsis*, a glucosyltransferase, which transfers one glucosyl residue to an acceptor molecule, like glycogen, amylopectin and oligosaccharides, and releases Glc (Zeeman *et al.*, 2007). The liberated Glc as well as the Glc exported from chloroplasts are phosphorylated by NtHXK1 to supply sucrose synthesis and glycolysis. Interestingly, the enzymes involved in glycolysis were found to be associated with the surface of mitochondria like NtHXK1, suggesting that the whole glycolytic pathway is associated with plant mitochondria and this micro-compartmentation allows pyruvate to be directly used as substrate for respiration (Giese *et al.*,

2003). Furthermore, the organization of a multi-protein complex might be imaginable to realize channeling of substrates directly along the pathway.

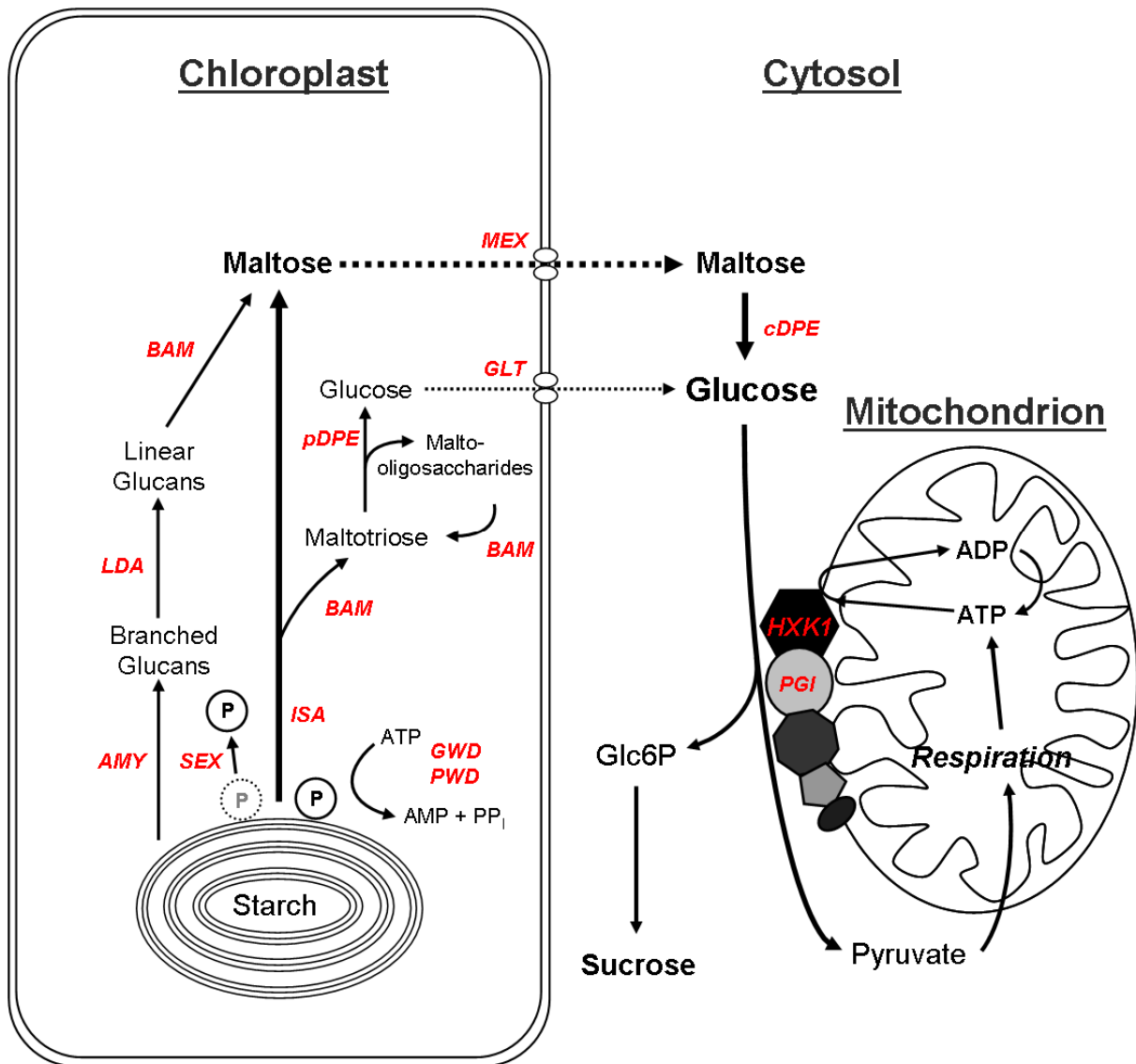


**Figure 28:** Pathway of starch breakdown in photosynthetic cells at night. Starch is primarily degraded over a hydrolytic pathway to produce Mal and lesser amounts of Glc, which are exported from the chloroplast to the cytosol, where they are further processed to supply cellular respiration and uninterrupted sucrose synthesis for sink export. The major enzyme activities and transporters are indicated in red. GWD is glucan, water dikinase, PWD is phosphoglucan, water dikinases, SEX is a phosphoglucan phosphatase, ISA is isoamylase (debranching enzyme), BAM is β—amylase, pDPE is plastidic deproportionating enzyme, AMY is α-amylase, LDA is limit dextrinase, MEX is a Mal transporter, GLT is Glc transporter, cDPE is cytosolic deproportionating enzyme and a glucosyltransferase, HXK1 is tobacco hexokinase 1 and PGI is phosphoglucoisomerase.

#### **4.6 The role of NtH XK1 in non-autotrophic cells**

Tobacco hexokinase 1 was found to be expressed predominantly in all aerial organs of the tobacco plant. The major expression of NtH XK1 particularly in flowers confirmed by qRT-PCR and promoter-reporter constructs suggests a crucial role of NtH XK1 in pollen and egg maturation. Additionally the reductions of flower development, number of capsules and seed quantity per capsule in NtH XK1 silenced plants were observed, which was unfortunately not documented. Starch synthesis and storage was monitored during pollen development but starch was found totally or partially converted to pectins, Suc, Glc and Fru before or after anther dehiscence (Pacini *et al.*, 2005). Soluble sugars and carbohydrates are supplied by the tapetum, absorbed by pollen and in case of surplus temporarily stored as starch during growth (Pacini, 1996). Starch is converted when required to sustain pollen growth and to modify internal turgor pressure to hinder uncontrolled water loss or gain. Carbohydrates can also mediate signals to influence development *in vivo* and *in vitro* (Goetz *et al.*, 2001). Furthermore, sucrose seems to stabilize plasma membranes of pollen, assuring viability during water loss and transport (Pacini, 1996). A pivotal role of NtH XK1 in this context is possible. The requirement of NtH XK1 as a Glc sensor is very likely, with regard to sugar perception and modulation of the expression of specific target genes in reproductive organs. Likewise, the sensing and signaling function might be relevant in stems, too. Particularly the involvement of NtH XK1 in growth promotion and plant development might explain the high level of *NtH XK1* expression in stem tissues as well.

#### **4.7 Final conclusion**

In the present study evidence was obtained that tobacco hexokinase 1 is inevitable to sustain normal plant growth and development in tobacco (Kim *et al.*, 2013). A total loss of *NtH XK1* is most likely lethal. The observed phenotypes of NtH XK1-silenced plants are rather the result of the combined suppression of two confirmed functions, the signaling and the catalytic function since all described starch-excess mutants showed minor alterations than our NtH XK1 RNAi plants, line HXK1-19 in particular. Additionally, both HXK functions are interconnected within the same pathways of the carbohydrate metabolism. HXK-mediated Glc sensing has been proven essential for the perception of endogenous Glc levels and the modulation of gene expression in photosynthesis. It is further demonstrated that NtH XK1 is the key link between the glycolytic pathway and the catabolism of transitory starch, which in turn is a primary product of photosynthesis. Further experiments are necessary to verify this



conclusion, for instance the expression of catalytically inactive NtHXK1 protein in NtHXK1-silenced plants.

## 5. Summary

The allosteric enzyme hexokinase (HXK) is present in virtually all living organisms and catalyzes a key step in carbohydrate metabolism, which is the ATP-dependant phosphorylation of Glucose (Glc). Its main product, glucose-6-phosphate (G6P), is a substrate for the oxidative pentose phosphate pathway (OPPP), the NDP-glucose pathway and glycolysis. Furthermore, HXKs can mediate sugar sensing and signaling in plant cells thereby affecting growth promotion, plant development and probably senescence. The tobacco (*Nicotiana tabacum*) HXK gene family consists of at least 10 members. To dissect the individual roles of multiple HXKs in tobacco, nine HXK genes were isolated and subjected to RNAi-mediated suppression of their expression in transgenic plants. While the gene silencing of most NtHXK genes produced no or weak phenotypes, silencing of *NtHKK1* produced a distinct phenotype with strong growth defects, leaf chlorosis and stunted leaf development. By expression analysis in WT (SNN) NtHKK1 was found to be expressed predominantly in all aerial organs. The determination of soluble sugars and starch in mature leaves revealed that *NtHKK1* suppression generated a *starch-excess* phenotype, which is defined by retaining high levels of starch in photosynthetic cells after the night phase. High accumulation of maltose and Glc which are breakdown products of starch, were most likely responsible for the excess accumulation of starch. This was almost certainly due to a feedback inhibition of starch degradation. In addition, it was further shown that NtHKK1 is able to substitute for the sensing function of AtHKK1 in the Glc-hypersensitive Arabidopsis mutant *gin2-1* (glucose insensitive; AtHKK1 null mutant). Hereby, it was confirmed that NtHKK1 can function as a plant Glc sensor and may be involved in sugar sensing and signalling. Based on the obtained results, it can be concluded that in leaves NtHKK1 is the major isoform amongst another nine HXK isoforms. NtHKK1 primarily metabolizes Glc deriving from transitory starch breakdown in order to supply continuously sucrose for downstream metabolism during the dark, thus performing the pivotal role as a link between the breakdown of starch and glycolysis. It is proposed that the observed phenotypes produced by silencing of NtHKK1 are most likely the result of a loss of both functions, the catalytic and the sensing function of NtHKK1.

## 6. Zusammenfassung

Das allosterische Enzym Hexokinase (HXK) findet sich in nahezu allen lebenden Organismen und katalysiert die Schlüsselreaktion im Kohlenhydrat-Stoffwechsel, nämlich die ATP-abhängige Phosphorylierung von Glukose (Glc). Ihr Hauptprodukt, das Glukose-6-Phosphat (G6P), ist die Basis für den oxidativen Pentosephosphatweg (OPPP), den NDP-Glukoseweg und der Glykolyse. Zudem können Hexokinasen Anteil haben an der Perzeption von Zuckern als Signalstoffe und in der Vermittlung dieser Signale, womit sie Wachstum, Entwicklung und möglicherweise Seneszenz der Pflanzen mit beeinflussen können. Die Tabak (*Nicotiana tabacum*) - HXK - Genfamilie besteht aus mindestens 10 Mitgliedern. Um die individuellen Rollen der verschiedenen Hexokinasen in Tabak nachvollziehen zu können wurden neun HXK-Gensequenzen isoliert und für die RNAi-vermittelte Unterdrückung ihrer Expression in transgenen Pflanzen eingesetzt. Während die Stilllegung (*silencing*) der meisten NtHXK-Gene keine oder nur schwache Phänotypen schuf, erzeugt die Stilllegung von NtHXK1 einen ausgeprägten Phänotypen mit massiven Wachstumsdefiziten, Blattchlorose und verkümmerter Blattentwicklung. Über die Expressionsanalyse im Wildtyp (SNN) konnte gezeigt werden, dass NtHXK1 in allen oberirdischen Pflanzenteilen dominant exprimiert wird. Die Bestimmung von löslichen Zuckern und Stärke in ausgewachsenen Blättern offenbarte, dass die Stilllegung von NtHXK1 einen Stärke-Exzess (*starch-excess*) - Phänotyp erzeugte, welcher per Definition einen exzessiven Anstau an Stärke nach der Nachtphase aufweist. Hohe Anhäufung von Maltose (Mal) und Glukose, welches Abbauprodukte der Stärke sind, verursachen aller Wahrscheinlichkeit nach diesen exzessiven Anstau an Stärke. Dies wurde mit größter Sicherheit durch eine Art Rückkopplungshemmung im Stärkeabbau verursacht. Des Weiteren zeigte sich, dass NtHXK1 in der Lage ist die *sensing*-/Perzeptionsfunktion von AtHXK1 in der Glc-hypersensitiven Mutante *gin2-1* (glucose insensitive; AtHXK1 Nullmutante) wiederherzustellen. Hierdurch konnte bestätigt werden, dass NtHXK1 die Funktion eines Glukosesensors erfüllt und vermutlich eine Rolle in der Perzeption und Vermittlung von Zuckersignalen spielt. Aufgrund der gewonnen Ergebnisse konnte darauf geschlossen werden, dass NtHXK1 eine übergeordnete Funktion gegenüber den neun weiteren HXK-Isoformen spielt. NtHXK1 metabolisiert primär Glc welches aus dem Aufschluss transitorischer Stärke stammt. Dieser Aufschluss hat die Aufgabe während der Dunkelphase Downstream-Stoffwechselwege mit Saccharose zu versorgen. Somit erfüllt NtHXK1 die zentrale Rolle als Verbindungsstück zwischen Stärkeabbau und Glykolyse. Mit großer Wahrscheinlichkeit resultieren die durch die Stilllegung von NtHXK1

erzeugten Phänotypen aufgrund ihrer Ausprägung aus dem Verlust beider Funktionen, der katalytischen und der *sensing*-Funktion von NtHXX1.

## 7. References

- Ahkami AH, Lischewski S, Haensch KT, Porfirova S, Hofmann J, Rolletschek H, Melzer M, Franken P, Hause B, Druege U, Hajirezaei MR (2009) Molecular physiology of adventitious root formation in *Petunia hybrida* cuttings: involvement of wound response and primary metabolism. *New Phytologist* **181**: 613–625
- Angaji SA, Hedayati SS, Poor RH, Poor SS, Shiravi S, Madani S (2010) Application of RNA interference in plants. *Plant Omics Journal* **3**: 77-84
- Cardenas ML, Cornish-Bowden A, Ureta T (1998) Evolution and regulatory role of the hexokinases. *Biochim Biophys Acta* **1401**:242-264
- Chen Y, Ji F, Xie H, Liang J, Zhang J (2006) The regulator of G-protein signalling proteins involved in sugar and abscisic acid signalling in Arabidopsis seed germination. *Plant Physiology* **140**: 302–310
- Cheng W, Zhang H, Zhou X, Liu H, Li J, Han S, Wang Y (2011) Subcellular localization of rice hexokinase (OsHXK) family members in the mesophyll protoplasts of tobacco. *Biologia Plantarum* **55**: 173-177
- Cho JI, Ryoo N, Ko S, Lee SK, Lee J, Jung KH, Lee YH, Bhoo SH, Winderickx J, An G, Hahn TR, Jeon JS (2006) Structure, expression, and functional analysis of the hexokinase gene family in rice (*Oryza sativa* L.). *Planta* **224**: 598-611
- Cho YH, Yoo SD, Sheen J (2006b) Regulatory functions of nuclear hexokinase1 complex in glucose signaling. *Cell* **127**: 579–589
- Cho JI, Ryoo N, Eom JS, Lee DW, Kim HB, Jeong SW, Lee YH, Kwon YK, Cho MH, Bhoo SH, Hahn TR, Park YI, Hwang I, Sheen J, Jeon JS (2009A) Role of the rice hexokinases OsHXK5 and OsHXK6 as glucose sensors. *Plant Physiol* **149**: 745-759
- Cho JI, Ryoo N, Hahn TR, Jeon JS (2009B) Evidence for a role of hexokinases as conserved glucose sensors in both monocot and dicot plant species. *Plant Signaling & Behaviour* **4**: 908-910
- Chomczynski P and Sacchi N (1987) Single-step method of RNA isolation by acid guanidinium thiocyanate-phenol-chloroform extraction. *Anal Biochem* **162**: 156-159
- Church GM, Gilbert W (1984) Genomic Sequencing. *Proc Natl Acad Sci* **81**: 1991-1995
- Claeysen E, Rivoal J (2007) Isozymes of plant hexokinase: Occurrence, properties and functions. *Phytochem* **68**: 709-31

**Clough SJ, Bent AF** (1998) Floral dip: a simplified method for *Agrobacterium*-mediated transformation of *Arabidopsis thaliana*. *Plant Journal* **16**: 735–743

**da-Silva WS, Rezende GL, Galina A** (2001) Subcellular distribution and kinetic properties of cytosolic and non-cytosolic hexokinases in maize seedling roots: implications for hexose phosphorylation. *J Exp Bot* **52**: 1191–1201

**Dai N, Schaffer A, Petreikov M, Shahak Y, Giller Y, Ratner K, Levine A, Granot D** (1999) Overexpression of *Arabidopsis* hexokinase in tomato plants inhibits growth, reduces photosynthesis, and induces rapid senescence. *Plant Cell* **11**: 1253–1266.

**Dai N, Kandel M, Petreikov M, Hanael R, Levin I, Ricard B, Rothan C, Schaffer AA and Granot D** (2002). The tomato hexokinase *LeHXK1*: cloning, mapping, expression pattern and phylogenetic relationships. *Plant Science* **163**: 581-590

**Damari-Weissler H, Kandel-Kfir M, Gidoni D, Mett A, Belausov E, Granot D** (2006) Evidence for intracellular spatial separation of hexokinases and fructokinases in tomato plants. *Planta* **224**: 1495–1502

**de Winde JH, Crauwels M, Hohmann S, Thevelein JM, Winderickx J** (1996). Differential requirement of the yeast sugar kinases for sugar sensing in the establishing the cataboliterepressed state. *Eur J Biochem* **241**: 633-643

**Deblaere R, Bytebier B, De Greve H, Deboeck F, Schell J, Van Montagu M, Leemans J** (1985) Efficient octopine Ti plasmid-derived vectors for *Agrobacterium*-mediated gene transfer to plants. *Nucleic Acids Res* **13**: 4777-4788

**Gibon T, Bläsing OE, Palacios-Rojas N, Pankovic D, Hendriks JHM, Fisahn J, Höhne M, Günther, Stitt M** (2004) Adjustment of diurnal starch turnover to short days: depletion of sugar during the night leads to a temporary inhibition of carbohydrate utilization, accumulation of sugars and post-translational activation of ADP-glucose pyrophosphorylase in the following light period. *Plant J* **39**: 847-862

**Giese JO** (2005) Molekulare und biochemische Charakterisierung der Hexokinase-Genfamilie von *Nicotiana tabacum*. Dissertation vorgelegt der Mathematisch-Naturwissenschaftlich-Technischen Fakultät der Martin-Luther-Universität Halle-Wittenberg <http://sundoc.bibliothek.uni-halle.de/diss-online/05/05H322/prom.pdf>

**Giese JO, Herbers K, Hoffmann M, Klösgen RB, Sonnewald U** (2005) Isolation and functional characterization of a novel plastidic hexokinase from *Nicotiana tabacum*. *FEBS Lett* **579**: 827-831

**Gietz RD, Schiestl RH** (2007) Quick and easy yeast transformation using the LiAc/SS carrier DNA/PEG method. *Nat Protoc* **2**:35-7

**Gilchrist E, Haughn G** (2010) Reverse genetic techniques: engineering loss and gain of function in plants. *Briefings in Functional Genomics* **9**: 103-110

**Goetz M, Godt DE, Guivarc'h A, Kahmann U, Chriqui D, Roitsch T** (2001) Induction of male sterility in plants by metabolic engineering of the carbohydrate supply. *Proc Natl Acad Sci U S A*. **98**: 6522-6527

**Granot D** (2008) Putting plant hexokinases in their proper place. *Phytochem* **69**: 2649-2654

**Jang JC, León P, Zhou L, Sheen J** (1997) Hexokinase as a sugar sensor in higher plants. *Plant Cell* **9**: 5-19

**Hajirezaei M, Peisker, Tschiersch H, Palatnik F, Valle EM, Carrilo N, Sonnewald U** (2002) Small changes in the activity of chloroplastic NADP+-dependent ferredoxin oxidoreductase lead to impaired plant growth and restrict photosynthetic activity of transgenic tobacco plants. *Plant Journal* **29**: 281-294

**Heinzel N, Rolletschek H** (2011) Primary Metabolite Analysis of Plant Material Using a Triple Quadrupole MS Coupled to a Monolith Anion-Exchange Column. *Dionex, Customer application note CAN 109*

**Herbers K, Mönke G, Badur R, Sonnewald U** (1995) A simplified procedure for the subtractive cDNA cloning of photoassimilate-responding genes: isolation of cDNAs encoding a new class of pathogenesis-related proteins. *Plant Mol Biol* **29**: 1027-1038

**Höfgen R and Willmitzer L** (1990) Biochemical and genetic analysis of different patatin isoforms expressed in various organs of potato (*Solanum tuberosum*) *Plant Science* **66**: 221-230

**Hood EE, Gelvin SB, Melchers LS, and Hoekema A** (1993) New *Agrobacterium* helper plasmids for gene transfer to plants. *Transgenic Res* **2**: 208-218

**Karve A, Rauh BL, Xia X, Kandasamy M, Meagher RB, Sheen J, Moore BD** (2008) Expression and evolutionary features of the hexokinase gene family in *Arabidopsis*. *Planta* **228**: 411-25

**Karve A, Moore BD** (2009) Function of *Arabidopsis* hexokinase-like1 as a negative regulator of plant growth. *Journal of Experimental Botany* **60**: 4137–4149

**Karve A, Xia X, Moore BD** (2012) *Arabidopsis* Hexokinase-Like1 and Hexokinase1 Form a Critical Node in Mediating Plant Glucose and Ethylene Responses. *Plant Physiology* **158**: 1965-1975

**Karve R, Lauria M, Virnig A, Xia X, Rauh BL, Moore B** (2010) Evolutionary lineages and functional diversification of plant hexokinases. *Mol Plant* **3**: 334-46

**Kandel-Kfir M, Damari-Weissler H, German MA, Gidoni D, Mett A, Belausov E, Petreikov M, Adir N, Granot D** (2006) Two newly identified membrane-associated and plastidic tomato HXKs: characteristics, predicted structure and intracellular localization. *Planta* **224**: 1341-52

**Karimi M, Inzé D, Depicker A** (2002) GATEWAY™ vectors for *Agrobacterium*-mediated plant transformation *Trends in Plant Science* **7**: 193-195

**Kim YM, Heinzl N, Giese, JO, Koeber J, Melzer M, Rutten T, von Wirén N, Sonnewald U, Hajirezaei MR** (2013) A dual role of tobacco hexokinase I in primary metabolism and sugar sensing. *Plant, Cell and Environment* **36**: 1311-1327

**Lämmli UK** (1970) Cleavage of structural proteins during the assembly of the head of bacteriophage T4. *Nature* **227**: 680-685

**Lichtenthaler HK** (1987) Chlorophylls and carotenoids: Pigments of photosynthetic biomembranes. *Methods Enzymol* **148**: 350-382

**Lunn JE, Feil R, Hendriks JHM, Gibon Y, Morcuende R, Osuna D, Scheible W-R, Carillo P, Hajirezaei M-R, Stitt M** (2006) Sugar-induced increases in trehalose6-phosphate are correlated with redoxactivation of ADPglucose pyrophosphorylase and higher rates of starch synthesis in *Arabidopsis thaliana*. *Biochem.J.* **397**: 139-148

**Matic S, Akerlund HE, Everitt E, Widell S** (2004) Sucrose synthase isoforms in cultured tobacco cells *Plant Phys and Biochem* **42**: 299-306

**Moore B, Zhou L, Rolland F, Hall Q, Cheng WH, Liu YX, Hwang I, Jones T, Sheen J** (2003) Role of the *Arabidopsis* glucose sensor HXK1 in nutrient, light, and hormonal signaling. *Science* **300**: 332-336

**Niittylä T, Messerli G, Trevisan M, Chen J, Smith AM, Zeeman SC** (2004) A previously unknown maltose transporter essential for starch degradation in leaves. *Science* **303**: 87-89

**Olsson T, Thelander M, Ronne H** (2003) A novel type of chloroplast stromal hexokinase is the major glucose-phosphorylating enzyme in the moss *Physcomitrella patens*. *J. Biol. Chem.* **278**: 44439-44447

**Pacini E** (1996) Types and meaning of pollen carbohydrate reserves. *Sexual Plant Reproduction* **9**: 362-366

**Pacini E, Guarnieri M, Nepi M** (2006) Pollen carbohydrates and water content during development, presentation, and dispersal: a short review. *Protoplasma* **228**: 73-77



**Pellny TK, Ghannoum O, Conroy JP, Schluepmann H, Smeekens S, Andralojc J, Krause KP, Goddijn O, Paul MJ** (2004) Genetic modification of photosynthesis with *E. coli* genes for trehalose synthesis. *Plant Biotechnol. J.* **2**: 71–82

**Rentsch D, Laloi M, Rouhara I, Schmelzer E, Delrot S, Frommer WB** (1995) NTR1 encodes a high affinity oligopeptide transporter in *Arabidopsis*. *FEBS Lett* **370**: 264-268

**Rolland F, Baena-Gonzalez E, Sheen J** (2006) Sugar sensing and signaling in plants: conserved and novel mechanisms. *Annu. Rev. Plant. Biol.* **57**: 675-709

**Rolletschek H, Melkus G, Grafahrend-Belau E, Fuchs J, Heinzel N, Schreiber F, Jakob PM, Borisjuk L** (2011) Combined noninvasive imaging and modeling approaches reveal metabolic compartmentation in the barley endosperm. *Plant Cell* **23**: 3041 – 3054

**Schmidt GW, Delaney SK** (2010) Stable internal reference genes for normalization of real-time RT-PCR in tobacco (*Nicotiana tabacum*) during development and abiotic stress. *Molecular Genetics and Genomics* **3**: 233 – 241

**Schnarrenberger C** (1990) Characterization and compartmentation in green leaves of hexokinases with different specificities for glucose fructose and mannose and for nucleoside triphosphates. *Planta* **181**: 249 – 255

**Small I** (2007) RNAi for revealing and engineering plant gene functions. *Current Opinion in Biotechnology* **18**: 148-153

**Smith AM, Stitt M** (2007) Coordination of carbon supply and plant growth. *Plant, Cell and Environment* **30**: 1126–1149

**Stettler M, Eicke S, Mettler T, Messerli G, Hörtensteiner S, Zeeman SC** (2009) Blocking the metabolism of starch breakdown products in *Arabidopsis* leaves triggers chloroplast degradation. *Molecular Plant* **2**: 1233-1246

**Stitt M, Lunn J, Usadel B** (2010) Arabidopsis and primary photosynthetic metabolism – more than the icing on the cake *Plant J* **61**: 1067-1091

**Tierney MB, Lamour KH** (2005) An introduction to Reverse Genetic Tools for Investigating Gene Function. *The Plant Health Instructor* DOI: 10.1094/PHI-A-2005-1025-01

**VanGuilder HD, Vrana KE, Freeman WM** (2008) Twenty-five years of quantitative PCR for gene expression analysis. *BioTechniques* **44**: 619-626

**Vervliet G, Holsters M, Teuchy H, Van Montagu M, Schell J** (1975) Characterization of different plaque-forming and defective temperate phages in *Agrobacterium*. *J Gen Virol* **26**: 33-48

**Weise SE, Weber APM, Sharkey TD** (2004) Maltose is the major form of carbon exported from the chloroplast at night. *Planta* **218**: 474–482

**Wiese A, Gröner F, Sonnewald U, Deppner H, Lerchl J, Hebbeker U, Flügge U, Weber A** (1999) Spinach hexokinase I is located in the outer envelope membrane of plastids. *FEBS Lett* **461**: 13-18

**Wind J, Smeekens S, Hanson J** (2010) Sucrose: Metabolite and signaling molecule. *Phytochemistry* **71**: 1610-1614

**Xu, FQ, Li, XR, Ruan, YL** (2008) RNAi-mediated suppression of hexokinase gene OsHXK10 in rice leads to non-dehiscent anther and reduction of pollen germination. *Plant Sci* **175**: 674-684

**Yoo SD, Cho YH, Sheen J** (2007) *Arabidopsis* mesophyll protoplasts: a versatile cell system for transient gene expression analysis. *Nature Protocols* **2**: 1565-1572

**Yu TS, Kofler H, Häusler RE, Hille D, Flügge UI, Zeeman SC, Smith AM, Kossmann J, Lloyd J, Ritte G, Steup M, Lue WL, Chen Y, Weber A** (2001) The *Arabidopsis* *sex1* mutant is defective in the R1 protein, a general regulator of starch degradation in plants, and not in the chloroplast hexose transporter. *Plant Cell* **13**: 1907–1918

**Zeeman SC, Kossmann J, Smith AM** (2010) Starch: It's Metabolism, Evolution and Biotechnological Modification in Plants. *Annu Rev Plant Biol* **61**: 209-234

**Zeeman SC, Smith SM, Smith AM** (2007) The diurnal metabolism of leaf starch. *Biochem J* **401**: 13-28

**Zheng Z** (2009) Carbon and nitrogen nutrient balance signaling in plants. *Plant Signaling & Behavior* **4**: 584-561

## 8. Appendix

### 8.1 Data from Figure 9 – Expression analysis in different organs

<i>flower</i>	delta CT	delta delta CT	ratio	SD
HXK1	3,3200		1,0000	0,0120
HXK2	6,4200	-3,1000	0,1166	2,6517e <sup>-4</sup>
HXK3	6,8200	-3,5000	0,0884	1,3197e <sup>-3</sup>
HXK4	12,0700	-8,7500	2,3227e <sup>-3</sup>	1,7255e <sup>-5</sup>
HXK5	8,0800	-4,7600	0,0369	1,6421e <sup>-4</sup>
HXK6	5,8200	-2,5000	0,1768	8,5849e <sup>-4</sup>
HXK7	21,5800	-18,2600	3,1856e <sup>-6</sup>	9,4880e <sup>-9</sup>
<i>bud</i>	delta CT	delta delta CT	ratio	SD
HXK1	4,7500		1,0000	0,0103
HXK2	6,6300	-1,8800	0,2717	2,3775e <sup>-3</sup>
HXK3	8,9600	-4,2100	0,0540	7,6713e <sup>-4</sup>
HXK4	11,9400	-7,1900	6,8485e <sup>-3</sup>	4,8951e <sup>-5</sup>
HXK5	8,1600	-3,4100	0,0941	4,0424e <sup>-4</sup>
HXK6	5,4300	-0,6800	0,6242	6,2771e <sup>-3</sup>
HXK7			0,0000	
<i>sink leaf</i>	delta CT	delta delta CT	ratio	SD
HXK1	4,3400		1,0000	5,3235e <sup>-3</sup>
HXK2	6,5300	-2,1900	0,2192	1,1530e <sup>-3</sup>
HXK3	7,9100	-3,5700	0,0842	5,4149e <sup>-4</sup>
HXK4	13,9500	-9,6100	1,2797e <sup>-3</sup>	1,3404e <sup>-5</sup>
HXK5	9,1500	-4,8100	0,0356	2,7728e <sup>-4</sup>
HXK6	5,4800	-1,1400	0,4538	1,5768e <sup>-3</sup>
HXK7			0,0000	
<i>source leaf</i>	delta CT	delta delta CT	ratio	SD
HXK1	5,6200		1,0000	0,0167
HXK2	6,8700	-1,2500	0,4204	6,1167e <sup>-3</sup>
HXK3	7,2400	-1,6200	0,3253	5,3407e <sup>-3</sup>
HXK4	13,7100	-8,0900	3,6700e <sup>-3</sup>	1,3628e <sup>-5</sup>
HXK5	9,0000	-3,3800	0,0961	1,1729e <sup>-3</sup>
HXK6	5,9800	-0,3600	0,7792	0,0114
HXK7			0,0000	
<i>stem</i>	delta CT	delta delta CT	ratio	SD
HXK1	4,4400		1,0000	0,0194
HXK2	4,9600	-0,5200	0,6974	4,5192e <sup>-3</sup>
HXK3	8,0900	-3,6500	0,0797	8,8766e <sup>-4</sup>
HXK4	13,1300	-8,6900	2,4213e <sup>-3</sup>	1,7274e <sup>-5</sup>
HXK5	8,8500	-4,4100	0,0470	3,5330e <sup>-4</sup>
HXK6	5,6000	-1,1600	0,4475	2,3544e <sup>-3</sup>
HXK7			0,0000	
<i>root</i>	delta CT	delta delta CT	ratio	SD
HXK1	5,6200		1,0000	0,0143
HXK2	7,2600	-1,6400	0,3209	4,0407e <sup>-3</sup>
HXK3	9,8000	-4,1800	0,0552	7,8954e <sup>-4</sup>
HXK4	4,8900	0,7300	1,6586	0,0237
HXK5	8,9200	-3,3000	0,1015	5,1131e <sup>-4</sup>
HXK6	6,3300	-0,7100	0,6113	4,3648e <sup>-3</sup>
HXK7		0,0000		

## 8.2 Data from Figure 10 – Time course of NtHXK1 in sink and source

	<i>sink leaf</i>		<i>source leaf</i>	
	<b>ratio</b>	<b>SD</b>	<b>ratio</b>	<b>SD</b>
<b>8am</b>	0,7092	0,0500	0,6978	0,0200
<b>10am</b>	0,3767	0,0100	0,1946	0,0100
<b>12pm</b>	0,4730	0,0100	0,2774	0,0200
<b>2pm</b>	0,8123	0,0100	0,6736	0,0300
<b>4pm</b>	1,0699	0,0700	0,6736	0,0600
<b>6pm</b>	1,1173	0,0800	0,5310	0,0200
<b>8pm</b>	0,8108	0,0800	0,0795	0,0100
<b>10pm</b>	0,5044	0,0500	0,1148	0,0100
<b>12pm</b>	0,1749	0,0100	0,1743	0,0100
<b>2am</b>	1,0000	0,0800	1,0000	0,0500
<b>4am</b>	1,2262	0,0500	1,2834	0,1400
<b>6am</b>	0,9977	0,0400	1,1447	0,1800

## 8.3 Data from Figure 15 – Expression Analysis transgenic lines

<b><u>Overexpression</u></b>	<i>leaf</i>		<i>protoplast</i>	
	<b>ratio</b>	<b>SD</b>	<b>ratio</b>	<b>SD</b>
<b>WT</b>	1,0000	0,1125	2,7054	0,1700
<b>HXK1-10</b>	3,6998	0,7820	7,4513	1,9400
<b>HXK1-11</b>	3,1986	0,7195	6,9083	0,6250
<b>HXK1-15</b>	2,5793	0,1850	5,1934	0,3715
<b><u>RNAi</u></b>	<i>leaf</i>		<i>protoplast</i>	
	<b>ratio</b>	<b>SD</b>	<b>ratio</b>	<b>SD</b>
<b>WT</b>	1,0000	0,1125	2,7054	0,1700
<b>HXK1-19</b>	0,1200	0,0450	0,5368	0,1450
<b>HXK1-24</b>	0,2253	0,1250	0,7333	0,1250
<b>HXK1-64</b>	0,3010	0,2859	1,3472	0,3600

#### 8.4 Data from Figure 16 – Relative activity transgenic lines

<i>Overexpression</i>	<b>RA</b>	<b>SD</b>
<b>WT</b>	1,0000	0,1122
<b>HXK1-10</b>	14,9845	0,6115
<b>HXK1-11</b>	12,5155	0,4647
<b>HXK1-15</b>	15,7481	0,7725
<i>RNAi</i>	<b>RA</b>	<b>SD</b>
<b>WT</b>	1,0000	0,1122
<b>HXK1-19</b>	0,4729	0,0548
<b>HXK1-24</b>	0,5581	0,0548
<b>HXK1-64</b>	0,8915	0,0633

#### 8.5 Data from Figure 17 – qPCR NtHXK isoforms in WT and HXK1-19

	<u><i>WT</i></u>		<u><i>HXK1-19</i></u>	
	<b>ratio</b>	<b>SD</b>	<b>ratio</b>	<b>SD</b>
<b>HXK1</b>	1,0000	0,10	0,1286	0,01
<b>HXK2</b>	0,3943	0,02	0,5334	0,04
<b>HXK3</b>	0,1827	0,02	0,0459	0
<b>HXK4</b>	3,5532e-3	0	2,2675e-3	0
<b>HXK5</b>	0,6807	0,06	0,4179	0,0400
<b>HXK7</b>	4,3702e-4	0	2,1185e-40	

## 8.6 Data from Figure 21A – Photosynthetic activity

<b>PPFD</b> <b><math>\mu\text{E m}^{-2} \text{s}^{-1}</math></b>	<b>WT</b>		<b>HXK1-19</b>	
	<b>mmol / m<sup>2</sup> x s</b>	<b>SD</b>	<b>mmol / m<sup>2</sup> x s</b>	<b>SD</b>
0	0,0000	0,0000	0,0000	0,0000
50	2,2247	0,4815	0,6504	0,2079
100	4,5547	0,6979	1,3346	0,3972
250	9,2529	1,0761	2,4978	0,6714
500	11,8235	1,3451	3,1672	0,7847
1000	13,8529	2,1958	3,5133	0,7837
1500	14,9647	2,6718	3,7394	0,9423
2000	15,5941	3,1590	3,7750	0,9229

<b>PPFD</b> <b><math>\mu\text{E m}^{-2} \text{s}^{-1}</math></b>	<b>HXK1-24</b>		<b>HXK1-64</b>	
	<b>mmol / m<sup>2</sup> x s</b>	<b>SD</b>	<b>mmol / m<sup>2</sup> x s</b>	<b>SD</b>
0	0,0000	0,0000	0,0000	0,0000
50	0,6674	0,3745	2,3557	0,2548
100	1,5354	0,5270	4,5553	0,3168
250	2,9988	1,0008	8,3380	0,7009
500	3,8231	1,2472	10,1280	1,2612
1000	4,5488	1,4758	11,1410	1,5363
1500	4,8875	1,5906	11,5075	1,6517
2000	5,1419	1,6661	11,7804	1,6305

## 8.7 Data from Figure 21B and 21C – Chlorophyll content and respiration

<b>total chlorophyll</b>	<b>mg m<sup>-2</sup></b>	<b>SD</b>
<b>WT</b>	32,4920	1,8225
<b>HXK1-19</b>	13,5240	0,8418
<b>HXK1-24</b>	13,8560	1,4213
<b>HXK1-64</b>	29,0800	1,7963

<b>respiration</b>	<b>mmol / m<sup>2</sup> x s</b>	<b>SD</b>
<b>WT</b>	0,6612	0,1430
<b>HXK1-19</b>	0,3906	0,0849
<b>HXK1-24</b>	0,4493	0,1027
<b>HXK1-64</b>	0,4900	0,1070

## 8.8 Data from Figure 22 - Carbon and nitrogen content

	<b>C (%)</b>	<b>SD</b>	<b>N (%)</b>	<b>SD</b>
<b>WT</b>	40,3957	1,4732	5,8883	0,5035
<b>HXK1-19</b>	37,9619	2,4363	1,7259	0,5589
<b>HXK1-24</b>	40,5648	0,8290	2,0954	0,6779
<b>HXK1-19</b>	40,2800	1,6073	5,8487	0,3526

## 8.9 Data from Figure 24 – Changes in starch during day

	<i>WT</i>		<i>HXK1-19</i>	
	<b>μmol C<sub>6</sub> / g FW</b>	<b>SD</b>	<b>μmol C<sub>6</sub> / g FW</b>	<b>SD</b>
<b>6am</b>	3,9260	0,6360	5,2432	1,8584
<b>8am</b>	4,0931	0,8012	4,9294	1,1586
<b>10am</b>	4,2643	1,1205	4,8302	1,3002
<b>12pm</b>	4,2644	0,8209	5,0200	1,6537
<b>2pm</b>	4,4266	0,8226	4,9775	1,9883
<b>4pm</b>	4,7619	1,1199	4,7122	0,6743
<b>6pm</b>	5,1901	1,0087	4,6629	1,3583
<b>8pm</b>	5,4262	0,8938	4,4160	1,7929
<b>10pm</b>	5,6789	1,1310	4,4690	1,1095
	<i>HXK1- 24</i>		<i>HXK1-64</i>	
	<b>μmol C<sub>6</sub> / g FW</b>	<b>SD</b>	<b>μmol C<sub>6</sub> / g FW</b>	<b>SD</b>
<b>6am</b>	7,0154	0,9622	3,7152	0,5719
<b>8am</b>	6,7015	0,4990	3,7030	0,9297
<b>10am</b>	6,5811	1,0888	4,2114	0,8613
<b>12pm</b>	6,3209	2,3965	5,0361	0,7349
<b>2pm</b>	5,9549	1,1961	5,4242	1,2175
<b>4pm</b>	5,6169	2,1889	5,6934	1,1355
<b>6pm</b>	5,5651	2,1468	5,8757	0,8599
<b>8pm</b>	5,6468	1,5486	5,9194	1,5717
<b>10pm</b>	5,7023	2,1355	6,3684	1,2024

## 8.10 Data from Figure 25 – Soluble sugars in leaves of RNAi lines

	<i>glucose</i>		<i>fructose</i>	
	mmol/g	SD	mmol/g	SD
<b>WT</b>	0,0665	8,8778e <sup>-3</sup>	0,0768	0,0162
<b>HXK1-19</b>	2,8347	0,1321	2,1548	0,1152
<b>HXK1-24</b>	1,4373	0,0417	0,8780	0,0559
<b>HXK1-64</b>	0,4557	0,0473	0,5121	0,0247
	<i>sucrose</i>		<i>maltose</i>	
	mmol/g	SD	mmol/g	SD
<b>WT</b>	52,8583	7,0696	9,1683e <sup>-4</sup>	1,6691e <sup>-4</sup>
<b>HXK1-19</b>	490,7227	54,4300	2,5948	0,1084
<b>HXK1-24</b>	235,0439	6,9468	0,9844	0,0797
<b>HXK1-64</b>	57,3760	7,2820	2,5735e <sup>-3</sup>	1,9767e <sup>-4</sup>



## 9. Publikationsliste des Autors

**2007** – V. SCHUBERT, **Y.-M. KIM**, A. BERR, J. FUCHS, A. MEISTER, S. MARSCHNER & I. SCHUBERT - Random homologous pairing and incomplete sister chromatid alignment are common in angiosperm interphase nuclei. **Mol. Genet. Genomics** 278: 167-176

**2008-** V. SCHUBERT, **Y.-M. KIM** & I. SCHUBERT - *Arabidopsis* sister chromatids often show complete alignment or separation along a 1.2 Mb euchromatic region but no cohesion. **Chromosoma** 117: 261-266

**2013** - **Y.-M. KIM**, N. HEINZEL, J.O. GIESE, J. KOEBER, M. MELZER, T. RUTTEN, N. VON WIRÉN, U. SONNEWALD & M.-R. HAJIREZAEI - A dual Role of Tobacco Hexokinase 1 in Starch Primary Metabolism and Sugar Sensing. **Plant, Cell & Environment** 36: 1311-1327

## 10. Curriculum Vitae

### Young-Min Kim

#### Persönliche Daten

Geboren: 18. Januar 1979 in Lünen (NRW, Deutschland)  
Nationalität: Deutsch  
Familienstand: verheiratet  
Kinder: ein Sohn, Phillip Kim Plasun (geboren am 09.12.2010)

#### Berufliche Tätigkeit

---

*Seit September 2012* - Mitarbeiter in der Trinkwasseranalytik/-qualität des Trinkwasserzweckverband „Südharz“ (Standort Sangerhausen)

*2007 bis 2011*- Wissenschaftlicher Mitarbeiter am Leibniz-Institut für Pflanzengenetik und Kulturpflanzenforschung (**IPK**) in Gatersleben  
Abteilung Physiologie und Zellbiologie; Arbeitsgruppe Molekulare Pflanzenernährung (AG MPE)

#### Akademische Ausbildung

---

*2007 bis 2011* - Wissenschaftliche Arbeit zur Dissertation mit dem (ursprünglichen) Projektthema: „Molekularbiologische und biochemische Charakterisierung pflanzlicher Hexokinasen in Tabak“

*2006 bis 2007* - Bearbeitung der Diplomarbeit am IPK in der Arbeitsgruppe Karyotypevolution (Abteilung Cytogenetik und Genomanalyse) mit dem Thema „Untersuchungen zur Schwesterchromatiden-Kohäsion bei Pflanzen unter besonderer Berücksichtigung von *Arabidopsis thaliana*“ (Betreuer: Dr. Veit Schubert, Prof. Dr. Ingo Schubert)

*1998 bis 2007* - Studium Biologie auf Diplom an der Universität Kassel (Hessen);  
Schwerpunkte Genetik, Biochemie, Mikrobiologie, Ökologie, Tierphysiologie,  
Pflanzenphysiologie und Metallorganische Chemie.

### **Schulische Ausbildung**

---

*1985 bis 1989*      Kardinal-von-Galen-Schule (Grundschule) in Waltrop (NRW)

*1989 bis 1998*      Theodor-Heuss-Gymnasium in Waltrop (NRW)  
Abschluss: Allgemeine Hochschulreife / Abitur  
Leistungskurse: Biologie und Mathematik  
Grundkurse: Englisch und Geschichte

### **Ehrenamtliche Tätigkeiten und Vereine**

---

*2007 bis 2010*      Aktives Mitglied in der Doktorandenvertretung am IPK  
*2008*              Anteil an Planung und Ausführung der Plant Science  
Student Conference (PSSC) am IPK  
*seit 2012*        Mitglied bei Mensa in Deutschland e.V. (MinD)  
*seit 2013*        Aktiver Helfer beim Technischem Hilfswerk (OV  
Sangerhausen)

## **11. Eidesstattliche Erklärung**

Hiermit erkläre ich, dass diese Arbeit von mir bisher weder der Naturwissenschaftliche Fakultät I - Biowissenschaften der Martin-Luther-Universität Halle-Wittenberg noch einer anderen wissenschaftlichen Einrichtung zum Zweck der Promotion eingereicht wurde. Ich erkläre ferner, dass ich diese Arbeit selbständig und nur unter Zuhilfenahme der angegebenen Hilfsmittel und Literatur angefertigt habe.

Sangerhausen, den 17.11.2013

Young-Min Kim

